

Molecular adaptation mechanisms of phototrophic sulfur bacteria to different light conditions

Dissertation der Fakultät für Biologie
der Ludwig-Maximilian-Universität München



vorgelegt von

Ovidiu Ludwig Rücker

am 21.12.2011

1. Gutachter: Prof. Dr. Jörg Overmann

2. Gutachter: Prof. Dr. Dirk Schüler

Tag der mündlichen Prüfung: 09. Juli 2012

Contents

SUMMARY	- 1 -
INTRODUCTION	- 4 -
Adaptation of <i>Chromatiaceae</i> to specific wavelengths of light	- 6 -
Adaptation of <i>Chlorobiaceae</i> to low light conditions	- 11 -
MATERIAL AND METHODS	- 16 -
Adaptation of Chromatiaceae toward absorption of specific wavelengths of light	- 16 -
Cultivation and extraction of DNA	- 16 -
PCR amplification and cloning of photosynthesis genes	- 17 -
Transcriptional analysis	- 22 -
Cloning of environmental <i>puf</i> sequences.....	- 23 -
Sequence analyses	- 24 -
Modeling of three-dimensional structures	- 24 -
<i>Chlorobiaceae</i> and the adaptation to low light conditions.....	- 26 -
Cultivation of <i>Chlorobiaceae</i>	- 26 -
<i>In silico</i> subtractive hybridization analysis	- 27 -
Prokaryotic cDNA suppression subtractive hybridisation (cDNA-SSH).....	- 27 -
Illumina cDNA sequencing	- 29 -
Characterization of <i>Chlorobiaceae</i> from the chemocline of Lake Faro	- 30 -
Identification of carotenoids and fossil DNA in sediments.....	- 32 -
Distribution of <i>Chlorobiaceae</i> in the chemocline of Lake Sakinaw	- 34 -
RESULTS	- 36 -
Adaptation of <i>Chromatiaceae</i> toward absorption of specific wavelengths of light.....	- 36 -
Structure of the <i>puf</i> operon in strain 970	- 36 -
Structure of the <i>puf</i> operon in <i>Trv. winogradskyi</i> strains 06511 and DSM6702 ^T	- 43 -

Transcriptional analysis of the <i>puf</i> operon in strain 970	48 -
Comparative analysis of the Puf polypeptides	50 -
Structural models for the LHC1 polypeptides	53 -
Phylogenetic relationship of LHC1 and RC sequences	55 -
The adaptation of <i>Chlorobiaceae</i> to growth at low light conditions.....	59 -
Identification and classification of genes unique to the BS1 genome	59 -
Transcriptional analysis of cultures grown under different light conditions.....	60 -
Characterization of <i>Chlorobiaceae</i> from the chemocline of Lake Faro.....	67 -
Distribution of molecular markers in sediments.....	71 -
Distribution of <i>Chlorobiaceae</i> in the chemocline of Lake Sakinaw	76 -
DISCUSSION	78 -
Adaptation of <i>Chromatiaceae</i> toward absorption of specific wavelengths of light.....	78 -
Structure of the <i>puf</i> operons in strain 970 and <i>Trv. winogradskyi</i>	78 -
Transcriptional regulation of the <i>puf</i> operon in strain 970	79 -
Significance of amino-acid substitutions in the LHC1 polypeptides	80 -
Phylogeny of the unusual LHC1 in strain 970	82 -
The adaptation of <i>Chlorobiaceae</i> to growth at low light conditions.....	84 -
Genes up-regulated under high light condition	85 -
Genes up-regulated under low light condition	90 -
Distribution of <i>Chlorobiaceae</i> in different chemoclines and their molecular markers in marine sediments	94 -
Conclusions	98 -
APPENDIX.....	101 -
REFERENCES	119 -
Publications.....	130 -
Danksagung.....	131 -
Curriculum vitae	132 -

SUMMARY

The dependence on the simultaneous presence of light and sulfide typically restricts phototrophic sulfur bacteria to areas well below the surface of water or sediments. Various organisms compete for this main energy source, which led to the evolution of different strategies for the development of advantageous phenotypic traits.

Purple sulfur bacteria display various light absorption patterns, mainly due to the usage of different pigments integrated in their light harvesting complexes (LHC). Additionally, changes in the light absorption pattern can also occur, if the structure of proteins involved in the interaction with pigments is altered. The light harvesting complex 1 (LHC1) of strain 970 exhibits a unique absorption spectrum with an absorption peak at 963 nm. Its closest relatives, *Thiorhodovibrio (Trv.) winogradskyi* DSM6702^T and strain 06511 display a absorption peak at 867 nm, that is characteristic for most proteobacteria with an LHC 1 which is associated with BChl_a. As a first step toward the identification of the structural basis for this characteristic, the operon structure and the nucleotide sequences of the *puf* genes were determined and an analysis of their transcription in strain 970 was performed. The *puf* operons encoding the LHC1 and reaction center proteins were amplified, cloned and sequenced. For the *Trv. winogradskyi* strains they show the common *pufBALMC* gene arrangement, whereas strain 970 contains a second *pufBA* copy downstream of *pufC*. In strain 970 only *pufB₁A₁* is transcribed and the corresponding mRNA fragment had an increased stability. Candidate amino acids involved in the extreme red-shift of the Q_y absorption band in strain 970 were identified by comparing the inferred amino acid sequences of the LHC1 polypeptides with those of the two phylogenetically closest relatives, *Trv. winogradskyi* strains DSM6702^T and 06511, as well as with those of more distantly related purple sulfur bacteria. Alignments of the deduced protein sequences showed that the LHC1 polypeptides are closely related to those of *Thermochromatium (Tch.) tepidum*. A deletion between αHis⁰ and αTrp⁺¹¹, thought to be responsible for the red shifted Q_y absorption in *Tch. tepidum* was also detected in strain 970 and *Trv. winogradskyi*, whereas αLys⁺¹² is replaced by histidine only in strain 970. Based on our structural modeling, the side chain of this αHis is predicted to be in close proximity to the BChl_a, suggesting that it exerts a modulating effect on the spectral properties of the highly unusual LHC1 complex of strain 970. Since no

Summary

other *Chromatiaceae* with extremely red-shifted Q_Y absorption bands have been reported so far, the presence of bacteria related to strain 970 was assessed in a series of environmental samples from tidal sediments in the Little Sippewissett Saltmarsh. No *pufLM* sequences clustering together with strain 970 and the two *Trv. winogradskyi* sequences were detected.

The ability of *Chl. phaeobacteroides* BS1 to grow in the chemocline of the Black Sea where light intensities are very low compared to other habitats raises the question about the maintenance requirements and adaptational abilities of this bacterium. When compared to the 11 other green sulfur bacterial (GSB) genomes as a whole, a total of 331 ORFs were identified to be unique for the *Chl. phaeobacteroides* BS1 of which 222 ORFs code for hypothetical proteins with unknown functions. Employing different growth conditions regarding light availability to BS1 cultures as a model system, the present comparative genomic and transcriptomic study yielded a first inventory of genes with potential relevance to adaptation at low light intensities. Many of the 135 down regulated genes identified for low light condition, are part of major metabolic pathways like nitrogen fixation, molybdenum transport, molybdenum cofactor biosynthesis, phosphate transport or biotin synthesis. These operons code for enzymes involved in pathways with elevated energy requirement which seem not to be essential under conditions like low light availability. Additionally, some of the genes with multiple copies are also being down regulated which is expected to decrease maintenance energy requirements. Nevertheless, the transcriptome of *Chl. phaeobacteroides* BS1 still contains transcripts of a majority of the identified 2524 ORFs in the genome under low light condition. In comparison to cultures grown under higher light intensities, 76 genes involved in general stress response, transcription regulation and energy production are being up regulated inferring potential relevance for adaptation at low light intensities. But still most of the differentially regulated genes are coding for hypothetical proteins with unknown function. Through these investigations many of the genes belonging to this category could for the first time be affiliated to a physiological condition.

The identification of another *Chlorobi* strain adapted to low light intensities in the chemocline of Lake Sakinaw opens a new perspective in investigating this trait. Measurements of BChl *e* concentrations together with the concentration of ITS-RNA copies in the cell reflects the abundance and activity of this bacterium in different depths of the chemocline. A clear correlation with available light intensities in the chemocline has been observed.

In the chemocline of Lake Faro three different *Chlorobi* strains could be identified through GSB specific 16S rRNA PCR amplification and sequencing. One strain revealed 100% identical 16S rRNA nucleotide sequence information to *Chl. phaeobacteroides* BS1 present in the Black Sea chemocline. Further sequence analysis showed that the internal transcribed spacer (ITS) region of both strains differed in their nucleotide sequence composition. All strains were shown to persist over a longer period of time with slight shifts of distribution during the sampling period.

The investigation of sediment samples for fossil molecular markers specific for GSB like the carotenoid isorenieratene is often used as indicator of past water column anoxia (Passier et al., 1999; Menzel et al., 2002). The concentration of the carotenoid isorenieratene was measured in sediment samples from different locations in the Black Sea and Mediterranean Sea. In all investigated samples isorenieratene was detected, also in recently deposited sediments where the presence of an extended water anoxia reaching to the photic zone can definitely be excluded. This finding reconfirms the assumption that deposited isorenieratene can originate from allochthonous sources (Coolen and Overmann, 2007) and shows the importance of the usage of fossil DNA markers. Phylogenetic comparison of fossil DNA sequences of the ITS region with nucleotide sequences from recent bacterial populations of *Chl. phaeobacteroides* BS1 from the Black Sea and Lake Faro was also performed. It revealed a closer relationship between the extinct Mediterranean BS1 population and the green sulfur bacteria present now in the chemocline of the Black Sea. Therefore the BS1 strain found in Lake Faro represents a lineage which was geographically isolated much earlier from the Black Sea lineage, as the time of the sediment deposition 172.000 years ago.

INTRODUCTION

Sun light is the main source of energy present on our planet and its radiation is utilized by various forms of organisms capable of performing photosynthesis. On the way through the earth atmosphere, over 50% of the total amount of radiation is scattered or absorbed, and only an average of 160 W m^{-2} is reaching the earth surface (Gates, 1965; Dietrich et al., 1975). In order to make use of this energy, organisms have to capture electromagnetic energy and transform it into chemical energy, for the purpose of cellular maintenance and growth. Today, terrestrial higher plants represent the majority of photosynthetic active biomass, but marine phototrophs, although resembling much lower biomass, show a higher turnover thus contributing significantly to total primary productivity. Marine photoautotrophs are a diverse group with green, red, and brown seaweeds along coasts; diatoms, dinoflagellates, and coccolithophorids dominating shelf phytoplankton; and cyanobacterial and green picoplankton in oligotrophic mid-ocean environments. The latter represent prokaryotic organisms of which the unicellular cyanobacterial strains *Prochlorococcus* and *Synechococcus* may be responsible for the fixation of as much as 10-25% of the global primary productivity (Garcia-Pichel, 1999). *Cyanobacteria* are the only prokaryotes which are capable of oxygenic photosynthesis, in contrast to the group of various anoxygenic phototrophs. Under the present oxic atmosphere, anoxygenic phototrophs represent a less significant group when seen on global scale, mostly because they are constrained to specific anoxic habitats. But the diversity of this group leads to a scientific interest, which is based on the simple molecular architecture, the variety of their photosystems and their implication in the reconstruction of the evolution of photosynthesis.

Phototrophic bacteria are found in six of the currently recognized bacterial lineages: the *Chloroflexus* subgroup, the green sulfur bacteria (*Chlorobiaceae*), the *Proteobacteria*, the *Cyanobacteria*, the *Chloracidobacteria* and the *Heliobacteriaceae* (Fig. 1). With the exception of the *Cyanobacteria*, phototrophic bacteria perform anoxygenic photosynthesis. This light mediated form of energy acquisition uses various substrates, mainly H_2S , but also S^0 , $\text{S}_2\text{O}_3^{2-}$, Fe^{2+} or NO_2^- as external electron donors. Therefore it is not accompanied by photochemical cleavage of water and does not lead to the formation of molecular oxygen.

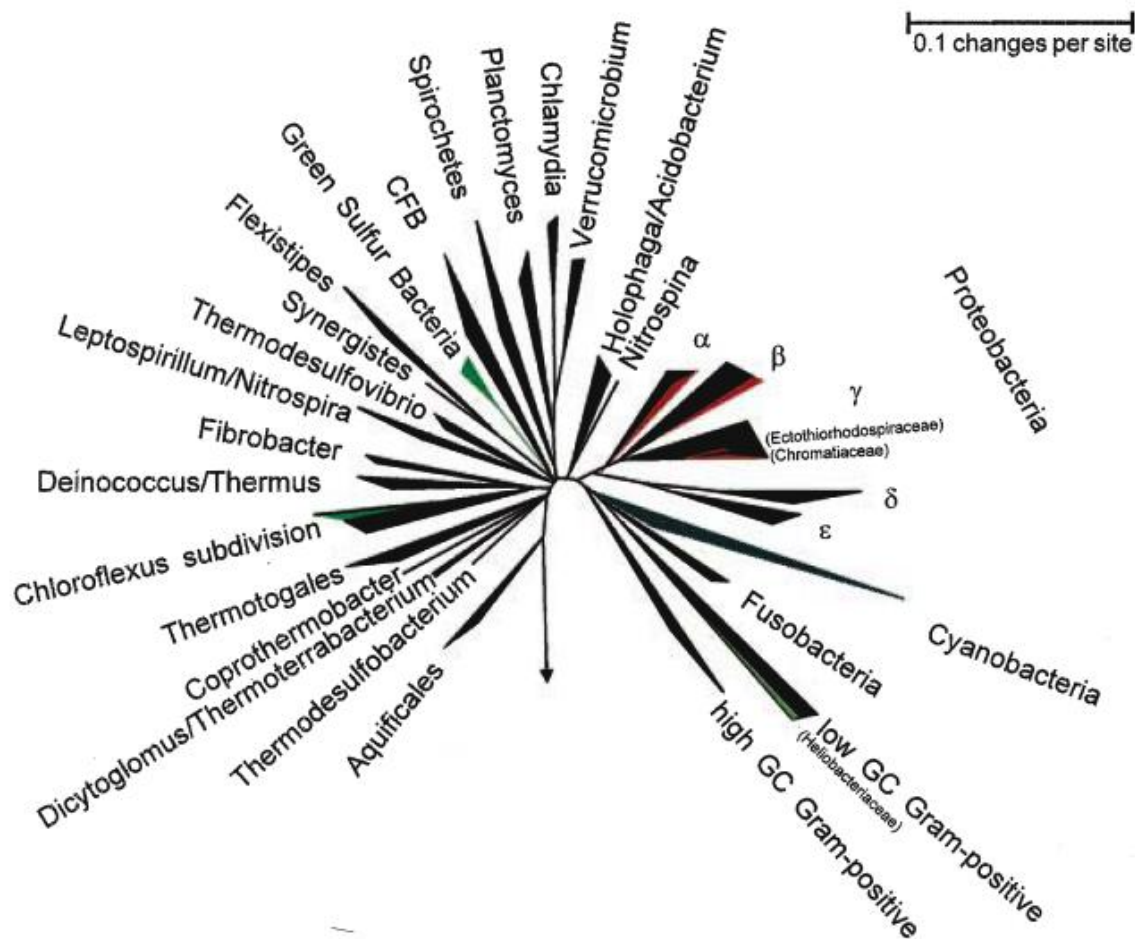


Fig.1. Phylogenetic tree based on 16S rRNA sequences. All bacterial divisions containing culturable representatives were included in the analyses so that the phototrophic nature of the bacterial strains could be confirmed. (light green) Bacteria containing chlorosomes as light-harvesting antenna. (red) Bacteria containing antenna complexes within the cytoplasmic membrane and quinone/pheophytin-type reaction centers. (medium green) Gram-positive phototrophic bacteria with FeS-type reaction centers. (dark green) Bacteria containing the two types of reaction centers. Width of colored wedges indicates the phylogenetic divergence. (Overmann and Garcia-Pichel, 2000)

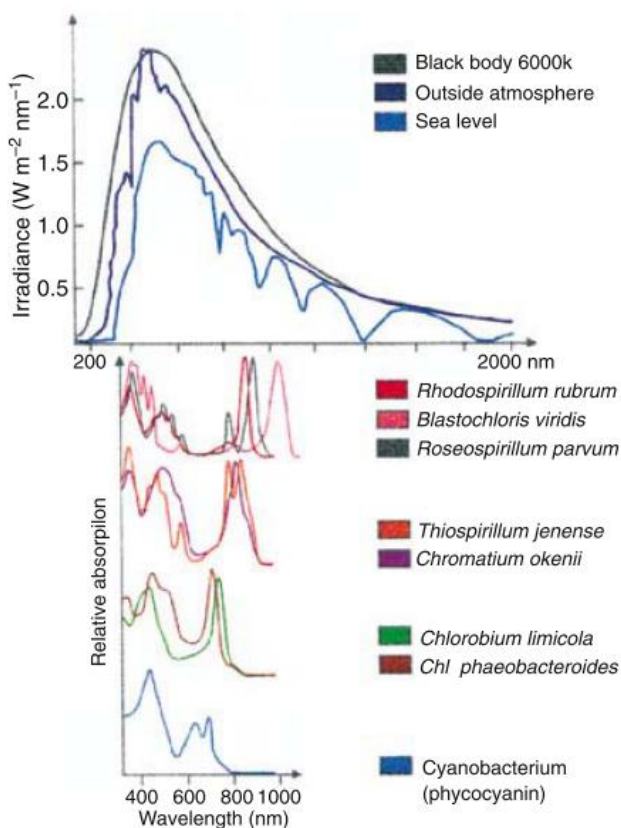
While the *Proteobacteria* and the *Chloroflexus*-subgroup both contain non-phototrophic representatives the use of light as an energy source for growth is not limited to phylogenetically coherent groups of bacteria. However, non-phototrophic representatives of the cyanobacterial lineage have not been isolated to date.

Adaptation of *Chromatiaceae* to specific wavelengths of light

Purple sulfur bacteria are anoxygenic phototrophs belonging to the phylum *Proteobacteria*, which occur primarily in stratified environments, where sufficient light reaches sulfide-containing water or sediment layers. In lakes harboring these bacteria, an average of 28.7% of primary production is anoxygenic (Overmann, 1997). The dependence of this pathway on reduced inorganic sulfur compounds which originate from the anaerobic degradation of organic carbon, previously fixed by oxygenic photosynthesis, has led to the term secondary primary production (Pfennig, 1978). Besides the limiting factors such as the availability of reduced sulfur compounds, organic carbon substrates, absence of oxygen, temperature and availability of nutrients, the availability and quality of light reaching these niches is another major determinant of the presence and composition of anoxygenic phototrophic communities. Depending on the position of these specific habitats, penetrating light lacks certain regions of its spectrum, due to scattering or absorption in the layers above. Being constrained to these anoxic environments, anoxygenic phototrophs had to adapt to performing photosynthesis with light that reaches their habitats. At sea level, light of the wavelength between 400 to 700 nm represents 50% of this irradiation (Fig. 2), mainly due to water vapor absorbing infrared light. In aquatic habitats, water is the major light-absorbing component only in very clear open ocean and inland lakes. Blue light is predominant, but between the wavelengths where water molecules absorb light (for example between 750 and 900nm) there are still niches available (Stomp et al., 2007). In many lacustrine and coastal habitats, light absorption by phytoplankton, or of other dissolved substances like gilvin and humic acids, exceeds that of water itself, leading to the prevalence of the long wavelength portion of the spectrum (Kirk, 1983).

This limited wavelength range available at great depth selects for species of anoxygenic phototrophic bacteria with complementary absorption spectra. The competition for light lead to the prevalence of species using different pigments and light harvesting antenna for the absorption of available light spectra (Fig. 2). Another habitat for anoxygenic phototrophs are intertidal marine sandy sediments, which harbor complex, fine-layered microbial mats that predominantly consist of a vertical sequence of different types of phototrophic microorganisms (Nicholson et al. 1987). The top layer is formed by a layer of diatoms, followed by a layer of cyanobacteria.

Fig.2. Spectral energy distribution of solar radiation outside the atmosphere and at sea level as compared to the absorption spectra of various phototrophic bacteria. Absorption spectra of the purple nonsulfur bacterium *Rhodospirillum rubrum* (containing BChl *a*, spirilloxanthin), *Blastochloris viridis* (BChl *b*, 1,2-dihydroneurosporene), and *Roseospirillum parvum* (BChl *a*, spirilloxanthin, lycopenal), of the Chromatiaceae species *Thiospirillum jenense* (BChl *a*, lycopene, rhodopin) and *Chromatium okenii* (BChl *a*, okenone), of the Chlorobiaceae species *Chlorobium limicola* (BChl *c*, chlorobactene) and *Chlorobium phaeobacteroides* (BChl *e*, isorenieratene) and of a cyanobacterium (Chl *a*, phycocyanin) are depicted. (Overmann and Garcia-Pichel, 2000)



Within the anoxic region below, purple sulfur bacteria (*Chromatiaceae*) containing bacteriochlorophyll (BChl) *a* [with a typical long-wavelength Q_y absorbance peak at 870-890 nm (Table 1)] overlie *Chromatiaceae* containing BChl *b* (Q_y at 1020 nm). The lowermost phototrophic layer contains green sulfur bacteria (*Chlorobiaceae*) that typically contain BChl *c* (Q_y at 735-775 nm). In contrast to pelagic systems, absorption of infrared radiation by the embedding matrix is very low within the euphotic zone of sandy sediments. As a consequence, mainly far-red and near-infrared light reaches the anoxygenic phototrophic bacteria in the anoxic layers of multilayered microbial mats. The vertical distribution of the different bacteria can therefore be related to their differential absorption of far-red and near-infrared radiation as well as their affinity for sulfide (Pierson et al., 1990).

Chlorin	Absorption maxima (nm)		Fluorescence maxima (nm)	
	Whole cells		Acetone extracts	Whole cells
Chl <i>a</i>	670–675		435, 663	680–685
Chl <i>b</i>	n.d		455, 645	(in acetone 652)
Chl <i>d</i>	714–718		400, 697	(in acetone 745)
BChl <i>a</i>	375, 590, 805, 830–911		358, 579, 771	907–915
BChl <i>b</i>	400, 605, 835–850, 986–1035		368, 407, 582, 795	1040
BChl <i>c</i>	457–460, 745–755		433, 663	775
BChl <i>d</i>	450, 715–745		425, 654	763
BChl <i>e</i>	460–462, 710–725		459, 648	738
BChl <i>g</i>	375, 419, 575, 788		365, 405, 566, 762	n.d.

Table 1. Major absorption maxima of chlorins in whole cells and in the dissolved state, and fluorescence maxima of whole cells of phototrophic prokaryotes (Overmann and Garcia-Pichel, 2000)

While most of the BChl *a*-containing anoxygenic phototrophs described so far exhibit long-wavelength absorption maxima between 800 and 900 nm, three proteobacteria possess Q_y absorption bands that are red-shifted to wavelengths above 900 nm. The alphaproteobacterium *Roseospirillum (Rss.) parvum* was isolated from a microbial mat (Glaeser and Overmann, 1999) and has a Q_y at 909 nm. The thermophilic *Tch. tepidum* is a member of the *Chromatiaceae* that was isolated from a hot spring (Madigan, 1984; Garcia et al., 1986) and has an absorption maximum at 915 nm. To date, the phototropic bacterium exhibiting the most extreme red shift for a BChl *a* containing LHC1 complex is strain 970. This photolithoautotrophic purple sulfur bacterium belongs to the *Gammaproteobacteria*, also originates from a marine microbial mat and absorbs light at a wavelength of 963 nm (Permentier et al., 2001).

The *in vivo* absorbance of bacteriochlorophylls is significantly influenced by their specific protein environment within the respective photosynthetic complexes (Zuber and Brunisholz, 1991). In the phototrophic proteobacteria, the photosynthetic reaction center (RC) is tightly surrounded by 15 or 16 light-harvesting complexes (LHC) I (Fig. 3). Each LHC I represents a heterodimer of α and β subunits that bind two BChl molecules as a dimer (Karrasch et al., 1995;

Roszak et al., 2003) via the highly conserved αHis^0 and βHis^0 histidine residues (Zuber and Cogdell, 1995). The van der Waals interaction of the BChl molecules has the largest impact on the red shift of the absorption band (Cogdell et al., 2002). Additionally, polar residues and point charges in the local pigment environment (Eccles and Honig, 1983), the deformation of the BChl macrocycle (Cogdell et al., 2002), and hydrogen bonding to the BChl macrocycle (Gudowska-Nowak et al., 1990) influence the position of the Q_y absorption.

The RC-LHC I core is encoded by the *puf* operon, which comprises the structural genes *pufBALM* that encode the surrounding antenna complex (β and α subunits of LHC I, encoded by *pufB* and *pufA*, respectively) as well as the reaction center L and M apoproteins. Downstream of *pufM*, several anoxygenic phototrophs contain an additional gene that encodes a RC-bound tetraheme cytochrome (*pufC*). In addition to LHC I, many phototrophic proteobacteria possess peripheral antenna complexes (LHC II and LHC III) that are formed by eight to nine $\alpha\beta$ heterodimers (Fig. 3).

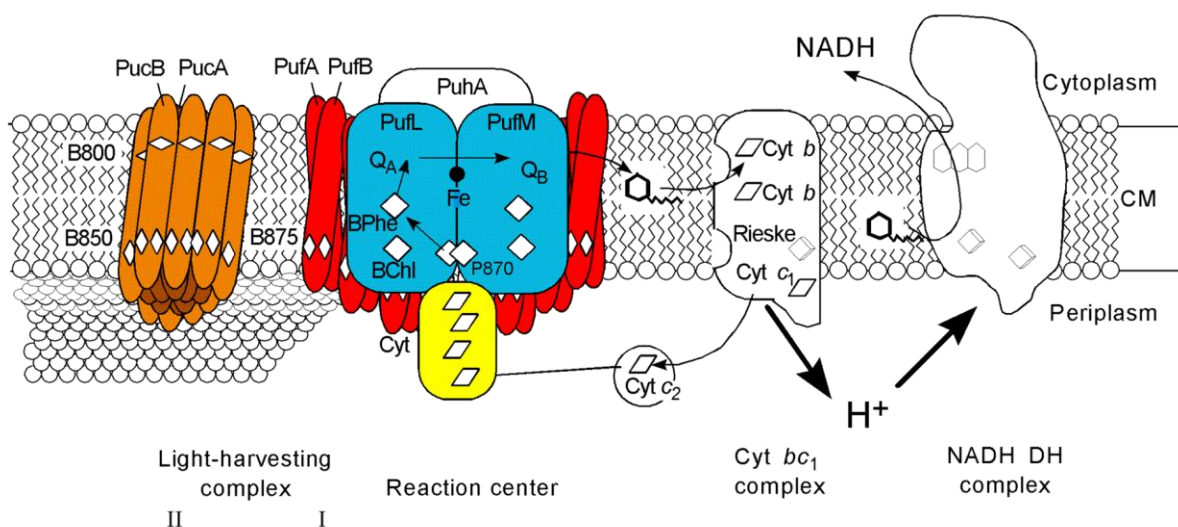


Fig.3. Localization and organization of the photosynthetic apparatus in purple nonsulfur bacteria and *Chromatiaceae*. CM = cytoplasmic membrane; Cyt = cytochrome; P870 reaction center special pair = primary electron donor; B800, B850, B875 = bacteriochlorophyll molecules bound to light-harvesting complexes II and I; QA, QB = ubiquinone (Overmann and Garcia-Pichel, 2000).

Introduction

The heterodimers in these peripheral complexes (β and α subunits of LHC II, encoded by *pucB* and *pucA*, respectively) contain one monomeric BChl molecule in addition to the BChl dimer (McLuskey et al., 2001). Whereas the monomeric BChl *a* in both complexes absorbs at 800 nm (Zuber and Brunisholz, 1991; Cogdell et al., 1999), the absorption maxima of the dimeric BChl *a* arrays in LHC II and LHC III are positioned at 850 and 820 nm, respectively, which enables an efficient funneling of excitation energy toward the photosynthetic reaction center (Zuber and Brunisholz, 1991; McLuskey et al., 2001).

Adaptation of *Chlorobiaceae* to low light conditions

Because phototrophic sulfur bacteria require the presence of light and sulfide for optimal growth, they are restricted to environments located well below the surface of water or sediments. Consequently, the light energy reaching these deeper layers represents a rather low percentage in the range of 0.02 and 10% of surface light intensity in pelagic environments (Van Gemerden and Mas, 1995). Selective pressure for efficient light harvesting and maximum quantum yield is therefore highly elevated when light represents the main variable controlling anoxygenic photosynthesis.

Green sulfur bacteria are well adapted to such low light habitats due to their large photosynthetic antennae (Fig. 4), their low maintenance energy requirements and higher sulfide tolerance (Overmann and Garcia-Pichel, 2000). The large light harvesting complexes of green sulfur bacteria are pigment carrying organelles, called chlorosomes (Olson, 1998). These contain bacteriochlorophylls *c*, *d* or *e* with carotenoids as antenna pigments and are attached to the inner cytoplasmic membrane via a baseplate consisting of trimeric proteins called Fenna-Matthews-Olson (FMO) protein. This FMO protein is an additional antenna complex containing BChl *a* which is mediating the energy transfer between the chlorosomes and the reaction center (Frigaard, 1997). Chlorosomes are exceptional in that proteins do not seem to be involved as ligands for most of the antenna bacteriochlorophyll molecules. Instead, interactions between the bacteriochlorophylls themselves determine the absorptive properties of the photosynthetic antenna in green sulfur bacteria (Blankenship and Matsuura, 2003). Recent investigation using bioimaging techniques revealed the assembly structure of bacteriochlorophylls inside the chlorosomes (Ganapathy et al., 2009). The assembly into coaxial cylinders in a new syn-anti stacking mode forms tubular shaped elements. Through this close packing of BChls a very efficient transmission of excitation energy is achieved, which is crucial for photosynthetic growth at very low light intensities. This suprastructure is also optimal for heterogenous side chains allowing an evolutionary optimization of light harvesting without the need of interacting proteins. This feature is critical in natural environments that are severely energy limited.

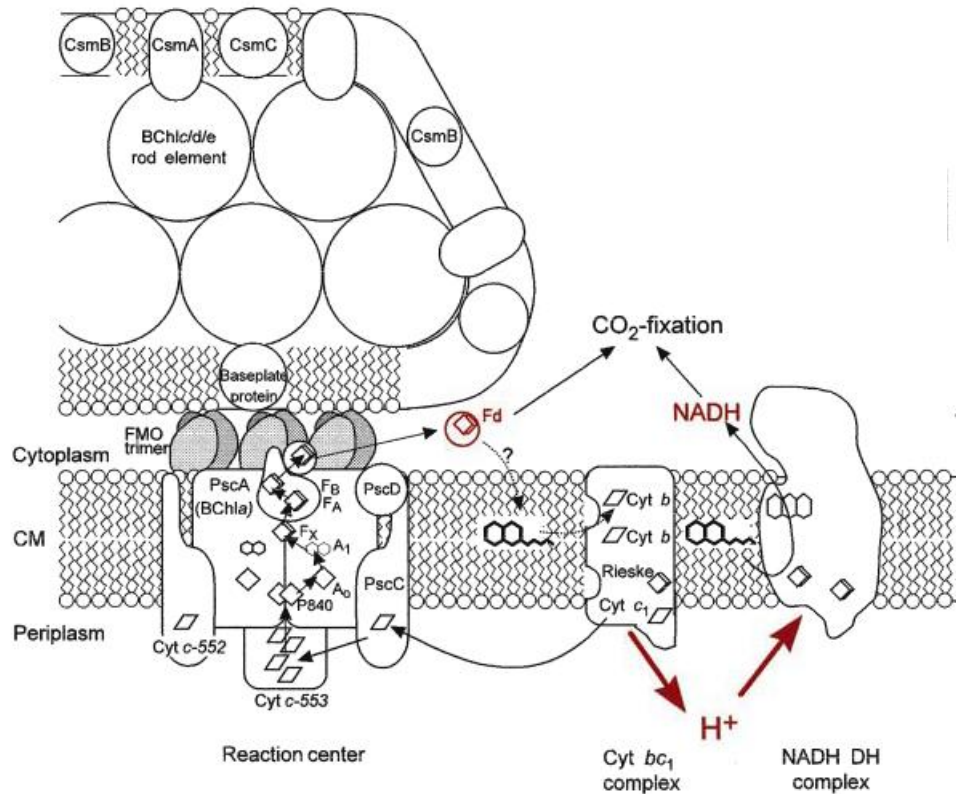


Fig.4. Localization and organization of the photosynthetic apparatus in green sulfur bacteria (*Chlorobiaceae*). CM = cytoplasmic membrane; Cyt = cytochrome; P840 reaction center special pair = primary electron donor; F_X , F_A , F_B = FeS-clusters bound to the reaction center; Fd = ferredoxin; FMO = Fenna-Matthews-Olson protein (Overmann and Garcia-Pichel, 2000)

The brown colored, BChl *e* containing species are better adapted to low light intensities than green colored BChl *c* or *d* containing species due to spectral properties and the high specific content of carotenoids (Montesinos et al., 1983; Overmann et al., 1992a; Manske et al., 2005). The intracellular content of bacteriochlorophyll is also higher in low light adapted species (Glaeser et al., 2002), which together with the low protein : bacteriochlorophyll mass ratio might explain the competitive advantage of green sulfur bacteria compared to their purple and cyanobacterial counterparts. Because the biosynthesis of proteins requires a major fraction of the energy expenditure of the bacterial cell (Gottschalk, 1986) a low protein : bacteriochlorophyll mass ratio therefore accounts for the low maintenance energy requirements. In purple bacteria, the size of the photosynthetic antenna is in the range of 20 - 200 BChl *a* per reaction center (Zuber and Cogdell, 1995), whereas chlorosomes contain about 5000 - 8000 bacteriochlorophyll

molecules connected to one reaction center (Frigaard et al., 2003). In addition, the theoretical quantum requirement for the CO₂-fixation of purple sulfur bacteria is 8 - 10.5 mol quanta (mol CO₂)⁻¹, but only 3.5 - 4.5 mol quanta (mol CO₂)⁻¹ for green sulfur bacteria (Brune, 1989).

In lacustrine habitats phototrophic sulfur bacteria are found in chemoclines usually situated at depths between 2 and 20 m, but not deeper than 30 m in pelagic environments (Van Gernerden and Mas, 1995). In the Black Sea, a green sulfur bacterium was isolated from the chemocline present at depths between 80 - 120 m (Overmann et al., 1992a). Further measurements revealed, that light intensity at this depth reaches only 0.0022 μmol quanta m⁻² s⁻¹ during winter, amounts which represent 0.0007% of surface light intensity (Manske et al., 2005). The incorporation of H¹⁴CO₃⁻ was experimentally measured and detected *in situ* at light intensities between 0.15 and 0.055 μmol quanta m⁻² s⁻¹ (Marschall et al., 2010). According to laboratory measurements, *Chlorobium* BS1 has a maintenance energy requirement of 1.6–4.9·10⁻¹⁵ kJ cell⁻¹ day⁻¹ which is the lowest value determined for any bacterial culture so far. This bacterium forms a stable population in the chemocline of the Black Sea, where no other photosynthetic sulfur bacteria could be detected. Therefore the phylotype *Chlorobium phaeobacteroides* BS1 represents the most extremely low light adapted bacterium isolated so far. Subsequent investigations with culture enrichments permitted first insights into its specific mechanisms of adaptation. While light saturation of photosynthesis occurs at 1 μmol quanta m⁻² s⁻¹, cells precultured at 3 μmol quanta m⁻² s⁻¹ also show decreased adaptation towards low light conditions if compared to cells grown at 0.1 μmol quanta m⁻² s⁻¹. Mutational investigation performed on the strain *Chlorobaculum tepidum* revealed some insight on the implication of the genes *bchQ*, *bchR* and *bchU* coding for the C-8, C-12 and C-20 methyltransferase respectively towards low light adaptation (Maresca et al., 2004; Chew et al., 2007). Through the methylation of Bchl_s at the mentioned positions, the Q_y absorption bands were broader and red shifted, and mutants lacking these methylations grew slower and had a lower BChl content than the wild type, especially at low light intensities. Nevertheless, these reports show the competitive advantage of BChl *c* containing strains over BChl *d* containing strains at light intensities as low as 8 μmol quanta m⁻² s⁻¹ and therefore represent a different adaptation model as observed in *Chlorobium phaeobacteroides* BS1. This latter bacterium therefore, provides a interesting model system for the study of adaptation towards low light intensities and low maintenance energy requirements.

Today, habitats of sulfur bacteria are scarce and the Black Sea represents the largest anoxic water body on earth. An oxic top layer of approximately 60 m is followed by a 40 m thick suboxic intermediate zone devoid of oxygen and sulfide, beneath which a 2000 m deep anoxic sulfidic bottom zone can be found (Murray et al., 1989). As a consequence, between 87 and 92% of the Black Sea water body remain permanently anoxic (Sorokin, 2002). In contrast to today's oxygenated oceans, the entire Proterozoic ocean may have consisted of sulfidic deep water covered by a possibly 100 m thick oxic surface layer (Anbar and Knoll, 2002), conditions which may have persisted over 1000 million years, and repeatedly occurred during later periods. Due to the fact that all known green sulfur bacteria are obligate anaerobic photolithoautotrophs, specific markers occurring only in these bacteria provide the opportunity to reconstruct past ecosystems. Numerous studies have used the presence of isorenieratene and its geochemical derivatives (Sinninghe Damste et al., 1993; Passier et al., 1999; Menzel et al., 2002) as evidence for extended water column anoxia of ancient oceans (Fig. 5). Since it represents a modern analogue of past water column anoxia, the development of anoxic conditions in the Black Sea has been studied extensively. Due to the intrusion of saltwater from the Mediterranean via the Bosphorus strait, bottom water anoxia started to develop between 7000 and 8000 years ago (Degens and Ross, 1972). Subfossil isorenieratene has been identified in up to 6000 year old sediment layers of the Black Sea (Sinninghe Damste et al., 1993) indicating the occurrence of GSB strains at that time. Recently, investigations using subfossil 16S rRNA gene sequences retrieved from sediments enabled a new approach for the reconstruction of past ecosystems. The occurrence of GSB specific sequences in sediments retrieved from the Black Sea (Manske et al., 2008) and the Mediterranean (Coolen and Overmann, 2007) was assessed. Fossil DNA could be retrieved and amplified from sediments up to 217,000 years old. Unexpectedly, however, recovered sequences grouped with freshwater or brackish, rather than truly marine, types of green sulfur bacteria indicating an allochthonous origin of these fossil biomarkers. The fact that carotenoids cannot enable such precise classification of the source of these fossil remnants, predisposes the use of fossil DNA for a much detailed reconstruction of past ecosystems. Further investigations using the Black Sea and *Chlorobium phaeobacteroides* BS1 as a modern analogue offer therefore a great potential for the evaluation of past water column anoxia.

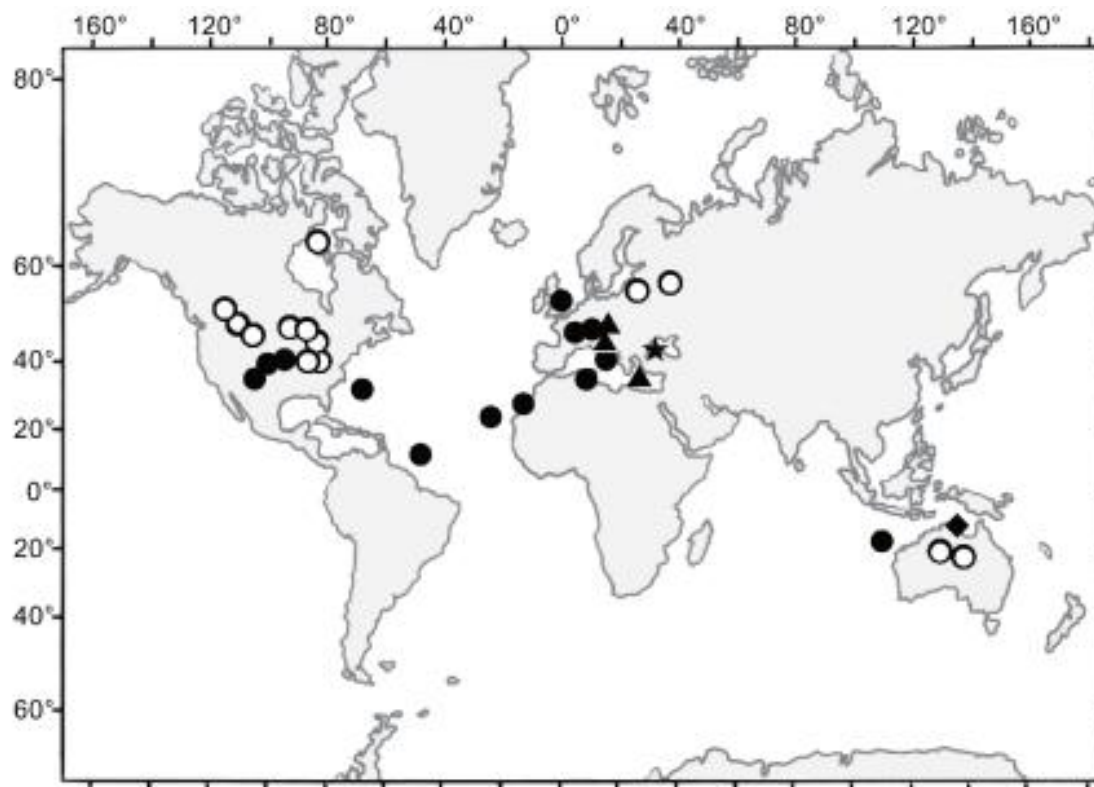


Fig. 5. Contemporary geographical location of fossil sediments and sedimentary rocks containing biomarkers of phototrophic sulfur bacterial as evidence for Oceanic Anoxic Events. Locations are distinguished according to their geological age (Overmann, 2008). ★ extant population of green sulfur bacteria in the chemochline and isorenieratene in the Black sea sediments. ▲ Cenozoic environments ● Mesozoic environments ○ Paleozoic environments and ◆ Proterozoic environments (1.64 Gyr old)

MATERIAL AND METHODS

Adaptation of Chromatiaceae toward absorption of specific wavelengths of light

Cultivation and extraction of DNA

The purple sulfur bacteria strain 970 and *Trv. winogradskyi* strain 06511 and DSM6702^T were grown under anaerobic conditions. Basal media contained KH₂PO₄, 1.84 mM; NH₄Cl, 6.36 mM; KCl, 4.56 mM; MgSO₄·7 H₂O, 14.2 mM; CaCl₂·2 H₂O, 1.7 mM and NaCl, 342.2 mM. After autoclaving, the following components were added: NaHCO₃, 60 mM; Na₂S, 1.25 mM; SL12, 1ml·l⁻¹ (Overmann et al., 1992b), and vitamin B₁₂, 20 µg·l⁻¹. The pH was adjusted to 7.3 and the medium distributed aseptically and anoxically in screw-cap bottles or tubes. Repeated addition of neutralized 100 mM sulfide solution (Siefert and Pfennig, 1984) and acetate (final concentration, 5 mM) was used to obtain higher cell yields. Stock cultures were grown photosynthetically at a light intensity of 100 µmol quanta·m⁻²·s⁻¹ of a 40 W-tungsten lamp bulb as determined with an LI-189 quantum meter plus an LI-200 pyranometer sensor (sensitivity range, 400–1,100 nm; LiCor, Lincoln, Neb., USA). The average light intensity (I_a) in the culture bottles was calculated from the light intensity measured at the front (I_1) and the back side (I_2) of bottles according to the equation below (Van Liere and Walsby 1982).

$$I_a = \frac{(I_1 - I_2)}{\ln\left(\frac{I_1}{I_2}\right)}$$

For extraction of chromosomal DNA, cells were harvested by centrifugation at 16,000 x g (Avanti J-25, rotor JA14; Beckman Coulter, Krefeld, Germany) for 10 min at 4°C and resuspended in lysis buffer (20 mM Na-acetate pH 5.5, 0.5% SDS, 1 mM EDTA, pH 8.0). Cells were lysed by addition of 300 µg of 0.1-mm-diameter siliconized zirconia beads (BioSpec Products, Bartlesville, USA) and disruption in a beadbeater (BioSpec Products, Bartlesville, USA) for 5 min. The homogenate was centrifuged again for 10 min at 16,000 x g and the

supernatant was treated further using the DNeasy[®] Blood and Tissue Kit (Quiagen, Hilden, Germany) according to the instructions of the manufacturer. In order to obtain DNA of sufficient purity for quantitative PCR amplifications an additional purification step was included. DNA was precipitated by adding 0.1 volumes of 3 M sodium acetate and 0.8 volumes ice cold 100% isopropanol followed by incubation at -20°C overnight. The DNA was sedimented by centrifugation at 18,000 x g for 30 minutes at 4°C (Eppendorf, 5417R), washed with ice cold 70% (v/v) ethanol, dried and resuspended in 50 to 100 µl of sterile Tris-buffer (2 mM Tris-HCl, pH 8.0) and stored at -20°C until further usage. The DNA concentrations were determined with the nanodrop ND-1000 (peqlab, Erlangen, Germany), and quality was assessed on a agarose gel (1%, w/v).

For cloning, *Escherichia (E.) coli* strain DH5α (Invitrogen, Carlsbad, CA, USA) was used. This strain was grown in Luria Bertani (LB) medium containing 1% Bacto-Tryptone, 1% NaCl and 0.5% yeast extract (Sambrook and Russell, 2001) and incubated at 37°C overnight. The pH was adjusted to 7 and ampicillin (100 µg·ml⁻¹) was supplemented as the selective antibiotic. Plasmid DNA was extracted with the NucleoSpin[®] Plasmid Kit (Macherey-Nagel, Düren, Germany) according to the instructions of the manufacturer.

PCR amplification and cloning of photosynthesis genes

Starting from fragments of *pufLM* genes, amplified with the *pufL*-f and *pufM*-r primers (Nagashima et al., 1997) (Table 2), similar amplification strategies was pursued for the three strains investigated. Polymerase chain reactions (PCR) were performed in a Veriti[®] 96-well thermal cycler (Applied Biosystems, Foster City, CA, USA) using the BD Advantage[™] 2PCR Kit (BD, Franklin Lakes, New Jersey, USA) that employs proofreading polymerase.

For strain 970, additional cloning steps were performed for the primary identification of fragments containing *pufLM* genes. For the fragment size identification Southern Blot analysis was performed. A total of 3 µg chromosomal DNA of strain 970 were digested with the restriction endonucleases *EcoR* I, *Sac* I, *Sph* I, *Pvu* I and *Xba* I (MBI Fermentas, St Leon-Rot, Germany) according to the instructions of the manufacturer. All of these endonucleases showed less than two recognition sites in the previously known sequence of *pufLM* genes. The resulting fragments were separated by gel electrophoresis and transferred by capillary blotting on a Hybond-N⁺ nylon membrane (Amersham Pharmacia, Freiburg, Germany) and crosslinked.

Material and Methods

Hybridization was performed with the Digoxigenin (DIG)-System (Roche, Basel, Switzerland) according to the instructions of the manufacturer. As a *pufLM* probe, a fragment of the *pufLM* gene was amplified using the primers PufLM-St970-f and PufLM-St970-r (MWG Eurofins, Ebersberg, Germany) (Table 2) and labeled via DIG incorporation during PCR. The amplification program included a 2 minutes denaturation step at 95°C followed by 10 cycles with 10 sec denaturation at 95°C, 30 sec annealing at 60°C, and 2 min elongation at 72°C additional 20 cycles with 10 sec denaturation at 95°C, 30 sec annealing at 60°C, and 2 min plus 20 sec (for each additional cycle) elongation at 72°C with an final 7 min elongation step at 72°C. Hybridisation with the *pufLM* probe was achieved at 50°C overnight. Detection procedure was performed using the chemoluminescent alkaline phosphatase substrate CSPD (Roche) and X-ray film (WICO Rex+; Linhardt Röntgenbedarf, Munich, Germany) according to the instructions of the manufacturer. Suitable fragments could be identified for the *EcoR* I digest and hence were chosen for further analysis. Digested genomic DNA was separated by gel electrophoresis and bands were excised according to the detected fragment length. DNA fragments were extracted using the Nucleospin Extract II Kit (Macherey-Nagel) according to the instructions of the manufacturer and eluted in 30 µl of sterile Tris-buffer (2 mM Tris-HCl, pH 8.0). For cloning, 6µl of genomic DNA fragments were ligated with *EcoRI*-digested pUC18 16h at 15°C in a volume of 100 µl using 10 U of T4 DNA ligase (MBI Fermentas). Ligase inactivation was achieved through incubation at 65°C for 15 min. Resulting plasmids were cloned in chemocompetent *E. coli* DH5α cells. For this, the whole ligation reaction was added to 100 µl chemocompetent cells and incubated at 4°C for 30 min. A heat shock was performed at 42°C for 2 min followed by cooling down on ice for 2 min. After the addition of 600 µl LB medium and incubation at 37°C for 1 h, cells were spread on LB plates with added ampicillin as the selective antibiotic. Clones containing fragments with *pufLM* genes were identified via PCR using PufLM-St970-f and PufLM-St970-r primers and a program including a 2 minutes denaturation step at 95°C followed by 35 cycles with 30 sec denaturation at 95°C, 30 sec annealing at 58°C, and 1 min elongation at 72°C. The initial cloned fragment was sequenced using primers M13-forward, M13-reverse, St970-seq-rev1, st970-IrevB103, PufLM-St970-f, PufLM-St970-r, st970-IfwA891 and St970-seq-fw1. Sequencing was performed on a ABI 3730 capillary sequencer (Applied Biosystems) using the BigDye Terminator v3.1 cycle sequencing kit (Applied Biosystems) according to the protocol of the manufacturer.

Additional sequence information for the *puf* operons was obtained by an inverse PCR (iPCR) approach (Ochman et al., 1993). Based on the sequence information obtained by the cloning experiment outlined above, restriction sites suitable for iPCR were identified and 1 µg of chromosomal DNA was used for digestion following the protocols of the manufacturer (MBI Fermentas). Digested fragments were then ligated for 16 h at 15°C in a volume of 100 µl using 10 U of T4 DNA ligase (MBI Fermentas). For the genomic region upstream of *pufLM* iPCRs with primers st970-IfwA891 and st970-IrevA127 amplifying unknown flanking regions (Table 1) were performed on 100 ng ligated fragments which were previously digested with *Pvu* I. A PCR protocol that comprised a hot start at 95°C for 5 min, followed by 30 cycles with denaturation at 95°C for 30 sec as well as a combined annealing and extension step at 68°C for 4 min was employed. Amplification products were sequenced using nested primers st970-IfwB910 and st970-IrevB103 from known regions and missing sequence stretches were obtained by primer walking with the primers St970-seq-rev1 and St970-seq-rev2. For the genomic region downstream of *pufC* iPCR with primers St970-IfwPufC and St970-IrevPufC amplifying unknown flanking regions (Table 1) was performed on 100 ng ligated fragments which were previously digested with *Pvu* I. A PCR protocol that comprised a hot start at 95°C for 5 min, followed by 30 cycles with denaturation at 95°C for 30 sec as well as a combined annealing and extension step at 68°C for 4 min was employed. Amplification products were cloned and sequenced using the primers M13-forward, M13-reverse, St970-IfwPufC and St970-IrevPufC from known regions and missing sequence stretches were obtained by primer walking with the primer St970-seq-fw2. In order to identify a putative third copy of *pufBA* genes, genomic DNA was digested with *Hind* III and self-ligated as described above. This experiment was performed by Anne Köhler. iPCR with primers St970-seq-fw2 and St970-IrevBA3 was applied for amplification of unknown flanking regions. A PCR protocol that comprised a hot start at 95°C for 5 min, followed by 30 cycles with denaturation at 95°C for 30 sec as well as a combined annealing and extension step at 68°C for 4 min was employed. Amplification products were cloned and sequenced using the primers M13-forward and M13-reverse.

The *pufLM* genes from *Trv. winogradskyi* strain 06511 were amplified using the *pufL*-f and *pufM*-r primers (Nagashima et al., 1997). For the genomic region upstream of *pufLM* iPCRs with primers Wino-Ipcr-fw2 and Wino-Ipcr-rev2 amplifying unknown flanking regions (Table 1) were performed on 100 ng ligated fragments which were previously digested with *EcoR* I. A

Material and Methods

PCR protocol that comprised a hot start at 95°C for 5 min, followed by 30 cycles with denaturation at 95°C for 30 sec annealing at 63°C and extension step at 72°C for 3 min was employed. Amplification products were cloned and sequenced using the same primers and Wino-Ipcr-fw1 from known regions. The genomic region further upstream of *pufA* was amplified via iPCR using the primers Wino-Ipcr-fw3 and Wino-Ipcr-rev4 (Table 2) on 100 ng ligated fragments which were previously digested with *Sac* I. A PCR protocol that comprised a hot start at 95°C for 5 min, followed by 30 cycles with denaturation at 95°C for 30 sec annealing at 60°C and extension step at 72°C for 3 min was employed. Amplification products were cloned and sequenced using the primers M13-forward and M13-reverse.

For *Trv. winogradskyi* strain DSM6702^T the information gained from strain 06511 was used for the design of a forward primer in the conserved site of the *bchZ* gene. The genetic region containing the *pufBA* genes was amplified using this forward primer (W6702-BChlZ-f) and a reverse primer (W6702-r; Table 2) targeting the known *pufLM* sequence. A PCR protocol that comprised a hot start at 95°C for 5 min, followed by 30 cycles with denaturation at 95°C for 30 sec annealing at 58°C and extension step at 72°C for 90 sec was employed. Amplification products were cloned and sequenced using the primers M13-forward and M13-reverse.

Table 2 Oligonucleotides used for PCR and sequencing

Primer	Sequence (5' → 3')	Source
PufLM-St970-fw1	GGAGCGGCAATTGGGCCG	this study
PufLM-St970-rev1	CCTCAAGAGCGATAAAGCCG	this study
st970-IrevA127	CCACAAACCGCCTTCCCTG	this study
st970-IrevB103	CGCAAATCCAAGACCAACG	this study
st970-IfwB910	CGGCTTTATCGCTCTTGAGG	this study
st970-IfwA891	GCATCGCCTCACTGATCTCC	this study
St970-IfwPufC	GACAGAACCTACAGCACCTCCG	this study
St970-IrevPufC	CAACAGGAAGGGCGTGAATGG	this study
St970-seq-fw1	GCGTTCATCACAGGTTGCG	this study
St970-seq-rev1	CAACCAAACCAAACCAAAGGG	this study
St970-seq-fw2	ATCCTCGTAGTCGTTCTCGGTCG	this study
St970-seq-rev2	TCGGGAATCGCTGTCACTGG	this study
St970-IrevBA3	GCCAAGATCCGACGCACCC	this study
Wino-Ipcr-fw2	GTGTTGCTTGGTGCTTGGG	this study
Wino-Ipcr-rev2	GCAAACGAAAAGGCGAAGGG	this study
Wino-Ipcr-fw3	TCAAGATGAACGAAAGCCTGC	this study
Wino-Ipcr-rev3	GGAGCGGATTACAGCCAGG	this study
Wino-Ipcr-fw4	CTGTAATCCGCTCCTTCAGC	this study
Wino-Ipcr-rev4	CGATACATCCAAGCCAGCAG	this study
PulLM-qPCR-fw1	ACCCTTTGCCTTCTCGTTCG	this study
PulLM-qPCR-rev1	CACCTTTCTGCGGATTCACC	this study
pufB1+2-qPCR-fw1	GTTTGGTTGTTCTTGCTCAC	this study
pufA1+2-qPCR-rev1	AGCACAATCATGTGGATCAG	this study
pufA2-qPCR-rev	TTGTAGTTGCGAGCCTGAG	this study
W6702-BChlZ-fw	CGGCACGCCCTTCATGG	this study
W6702-rev	GCGAAGGCGAAAGGCACA	this study
pufL-f	CTKTTCGACTTCTGGGTS GG	Nagashima et al. 1997
pufM-R	CCCATSGTCCAGCGCCAGAA	Nagashima et al. 1997
Uni-8f	AGAGTTTGATCCTGGCTCAG	Lane 1991
341-mod-f	CCTACGGGWGGCWGCAG	Muyzer et al. 1998
uni-515-r	CCGCGGCTGCTGGCAC	Lane 1991
907r	CCGTCAATTCCTTTGAGTTT	Lane 1991
L1-r	CAAGGCATCCACCGT	(Jensen et al., 1993)
GSB822r	ATGACCAACATCTAGTATT	Overmann et al., 1999
BS1-ITS38f	GCTCAAAGAGTAATGGTCC	Marschall et al., 2010
BS1-ITS518r	GCATTTCAATCTTACCAGCT	Marschall et al., 2010

Transcriptional analysis

For RNA extraction, cells growing in culture were mixed with 12.5% ice-cold ethanol/phenol stop solution (5% phenol pH 4.5-5.5 in 100% ethanol) to avoid RNA degradation. After centrifugation at 10,000 \times g for 10 min at 4°C, pellets were frozen in liquid nitrogen and stored at -80°C. Extraction was started by resuspending cells in lysis buffer (20 mM Na-acetate pH 5.5, 0.5% SDS, 1 mM EDTA, pH 8.0) supplemented with one volume of phenol (pH 4.5-5.5), and using bead beating with the addition of 300 μ g of 0.1-mm-diameter siliconized zirconia beads (BioSpec Products) for 1 min. Total RNA was isolated using phenol-chloroform (Chomczynski and Sacchi, 1987) and subsequently purified with the RNeasy Mini Kit (Quiagen) according to the protocol of the manufacturer. The RNA was treated with Turbo DNA free (Applied Biosystems) to remove all remaining DNA contamination. For this purpose the rigorous treatment was chosen and additional 2 U of Turbo DNase was added after 30 min of incubation and incubation lasted another 30 min. Another purification step using the RNeasy Mini Kit (Quiagen) followed subsequently. RNA concentrations were determined with the nanodrop ND-1000 (peqlab, Erlangen, Germany), and quality was assessed on a formaldehyde gel (3.1%, w/v).

Reverse transcription was performed with RevertAid™ First strand cDNA Synthesis Kit (Fermentas) using 1 μ g of RNA according to the protocol of the manufacturer. Negative controls were prepared by omitting the reverse transcriptase and served to verify the absence of contaminating genomic DNA. Quantitative real-time PCR (RT-qPCR) with custom designed gene specific primers (pufB1+2-qPCR-f, pufA1+2-qPCR-r, pufA2-qPCR-r, PulLM-qPCR-fw1 and PulLM-qPCR-rev1 Table 2) was performed using 20 μ l reactions, the LightCycler 480 SYBR Green I Master and 1 μ l of cDNA solution in a LightCycler 480 (Roche). The RT-qPCR reaction protocol comprised a hot start at 95°C for 5 min, followed by 35 cycles with denaturation at 95°C for 10 sec annealing at 56°C for 15 sec and an extension step at 72°C for 16 sec was employed. Melting curve was measured continuously between 65-97°C at a ramp rate of 0.11°C/s. For standardization, the copy number of 16S rRNA gene transcripts was quantified in parallel for all samples using the eubacterial primer set 341-mod-f and Uni-515-r (Lane, 1991; Muyzer and Smalla, 1998). A linearized plasmid containing the cloned fragment from the *puf* operon of strain 970 was used for calibration. Each quantification was performed in three parallels. cDNA samples for determination of 16S rRNA concentrations were diluted before qPCR. For the measurement of transcript half-lives, cultures of strain 970 were grown to a total

cell density of 2×10^7 cells ml^{-1} at $100 \mu\text{mol quanta m}^{-2} \text{s}^{-1}$ and cells from 50 ml culture were harvested for RNA isolation at consecutive time points. Additionally cultures were grown under limiting light intensities of $2 \mu\text{mol quanta} \cdot \text{m}^{-2} \cdot \text{s}^{-1}$. Transcription initiation was inhibited by the addition of rifampicin ($200 \mu\text{g} \cdot \text{ml}^{-1}$) (Campbell et al., 2001). The data obtained after 15 min of incubation were used for the calculation of transcript half-lives.

Cloning of environmental *puf* sequences

Several layered microbial mats and sediments containing purple bacteria were collected from Little Sippewissett Saltmarsh, Falmouth, MA, USA. The samples comprised (i) the sandy, pink-colored bottom sediment of a small puddle (Sipp1), (ii) pink cell aggregates from a tidal pond (Sipp2), (iii) sandy, pink to orange-colored bottom sediment of a tidal channel (Sipp3), (iv) a layered microbial mat (Sipp4), and (v) a cyanobacterial mat (Sipp5). Samples were stored in 50 ml screw cap tubes at 4°C . Genomic DNA was extracted from 2 g of sample using the UltraClean® Mega Soil DNA Isolation Kit (MoBio Laboratories, Inc. Carlsbad, CA, USA) and following the protocol of the manufacturer. The genomic region containing *pufLM* was amplified with conserved primers PufL-f and PufM-r (Nagashima et al., 1997) using 10 μg of DNA as template. The PCR reaction protocol comprised a hot start at 95°C for 5 min, followed by 40 cycles with denaturation at 95°C for 15 sec annealing at 62°C for 15 sec extension step at 72°C for 1.5 min and a final extension step was employed for 7 min. The amplification products with a size of 1.4 kb were excised from an agarose gel (1%, w/v) cleaned using the Nucleospin® Extract II Kit (Macherey-Nagel) according to the instructions of the manufacturer and eluted in 30 μl of sterile Tris-buffer (2 mM Tris-HCl, pH 8.0). Further on, 4 μl cleaned PCR product was cloned using the TopoTA cloning kit (Invitrogen) according to the protocol of the manufacturer. A total of 60 clones were picked and grown in LB medium with 100 μM ampicillin added as selective antibiotic. Plasmids were extracted using the Nucleospin® Plasmid Kit (Macherey-Nagel) according to the instructions of the manufacturer and eluted in 30 μl of sterile Tris-buffer (2 mM Tris-HCl, pH 8.0). The insertion of cloned PCR products were tested by digesting 1 μl of plasmid DNA with the restriction endonuclease *EcoR* I and separation with electrophoresis on an agarose gel (1 %, w/v). Positive clones were subsequently sequenced using the primers M13-forward and M13-reverse.

Sequence analyses

Sequences were analyzed by comparative database searches employing the BLAST X program (Altschul et al., 1997), ORF Finder (<http://www.ncbi.nlm.nih.gov/gorf/gorf.html>) and processed with Vector NTI version 11.0 (Invitrogen). Open reading frames (ORFs) were identified using the NCBI ORF Finder graphical analysis tool (<http://www.ncbi.nlm.nih.gov/gorf/gorf.html>). Stem loop structures were predicted and free energy for stabilities of secondary structures were calculated with the Mfold web server (Zuker, 2003). For comparison, related sequences of photosynthesis genes and proteins were retrieved from the GenBank database (Benson et al., 2008). Raw sequence data were aligned with Clustal X version 2.0.11 (Larkin et al., 2007) and imported into the ARB program package (Ludwig et al., 2004). Phylogenetic trees were constructed using the RAxML maximum likelihood algorithm for proteins and with FastDNAML for 16S rRNA, followed by bootstrap analyses for 100 datasets. The nucleotide sequences obtained in this study have been deposited in the GenBank database under accession numbers JF523526 (*puf* operon strain 970), JF523525 (*puf* operon *Trv. winogradskyi* strain 06511), JF523524 (*puf* operon *Trv. winogradskyi* DSM6702^T), JF523527 (SIPP-1-1), JF523528 (SIPP-1-2), JF523529 (SIPP-1-4), JF523530 (SIPP-1-6), JF523531 (SIPP-2-2), JF523532 (SIPP-2-7), JF523533 (SIPP-2-8), JF523534 (SIPP-3-1), JF523535 (SIPP-4-7), JF523536 (SIPP-4-8) and JF523537 (SIPP-5-8).

Modeling of three-dimensional structures

In order to identify potential polypeptide BChl interactions in the antenna complex of strain 970, three-dimensional (3-D) models were constructed. The RCSB protein data bank (www.pdb.org) (Berman et al., 2000) was used for the identification and acquisition of appropriate modeling templates. The SWISS-Model workspace (Arnold et al., 2006) was then employed for modeling via the alignment mode using the chosen templates. Visualization of 3-D models was achieved with the program Deep View – Swiss-Pdb Viewer version 4.0.1 (Guex and Peitsch, 1997).

To date only few entries of 3-D structures of purple bacterial LH1 are available in the Protein Data Bank (PDB) and comprise the solution structures of *Rhodobacter (Rbc.) sphaeroides* LH1 β (1dx7) and of LH1 β (1wrg) and LH1 α (1xrd) from *Rhodospirillum (Rsp.) rubrum*, respectively. While the crystal structure of the RC-LH1 core complex from *Rhodopseudomonas (Rps.) palustris* is available at a 4.8 Å resolution, this structure does not contain the information about

the exact location of the LHC1 polypeptide residues. Detailed information is available for two LH2 crystal structures, including *Rhodoblastus (Rbl.) acidophila* (1nkz) at 2.0 Å resolution and *Phaeospirillum (Phs.) molischianum* (1lgh) at 2.4 Å resolution. The latter structures include also information about pigment coordination inside the complex. Therefore, the structural models of LH2 complexes were also used for the modeling of the polypeptides of strain 970 in order to provide additional information about protein-pigment interactions.

***Chlorobiaceae* and the adaptation to low light conditions**

Cultivation of *Chlorobiaceae*

The bacterial strain *Chl. phaeobacteroides* BS1 previously isolated from the chemocline of the Black Sea was cultivated in artificial seawater medium as an enrichment culture where it constitutes $\geq 80\%$ of cells in culture (Manske et al., 2005). Artificial seawater medium (Coolen and Overmann, 2000) was adjusted to the ionic strength of the Black Sea chemocline. The medium contained (per liter) 14.1 g NaCl, 2.9 g $\text{MgCl}_2 \cdot 6 \text{H}_2\text{O}$, 0.6 g $\text{CaCl}_2 \cdot 2 \text{H}_2\text{O}$, 0.4 g KCl, 2.3 g Na_2SO_4 , 2.4 g HEPES, 0.2 ml selenite-tungstate solution (58), 100 mg KBr, 24.7 mg H_3BO_3 , 23.8 mg SrCl_2 , 21.4 mg NH_4Cl , 5.4 mg KH_2PO_4 and 2.9 mg NaF. After autoclaving, 1.4 mM NaHCO_3 , 1 mM $\text{Na}_2\text{S} \cdot 9 \text{H}_2\text{O}$, 1 ml of trace element solution SL10 (75 mM g/l $\text{Fe(II)Cl}_2 \cdot 4 \text{H}_2\text{O}$, 92 mM $\text{CoCl}_2 \cdot 6 \text{H}_2\text{O}$, 618 mM $\text{MnCl}_2 \cdot 2 \text{H}_2\text{O}$, 514 mM ZnCl_2 , 100 mM $\text{NiCl}_2 \cdot 6 \text{H}_2\text{O}$, 149 mM $\text{Na}_2\text{MoO}_4 \cdot 2 \text{H}_2\text{O}$, 97 mM H_3BO_3 , 12 mM $\text{CuCl}_2 \cdot 2 \text{H}_2\text{O}$) (Widdel et al., 1983), 0.1 ml of a solution of 10 vitamins (Balch et al., 1979), and 200 μM dithionite were added. The pH was adjusted to 7.2 and the medium was distributed into 500-ml screw cap bottles. Cultures were incubated under low light ($0.15 \mu\text{mol quanta} \cdot \text{m}^{-2} \cdot \text{s}^{-1}$) and high light ($3 \mu\text{mol quanta} \cdot \text{m}^{-2} \cdot \text{s}^{-1}$) conditions using a 40 W-tungsten lamp bulb. Light intensities were determined with an LI-189 quantum meter plus an LI-200 pyranometer sensor (sensitivity range, 400–1,100 nm; LiCor, Lincoln, Neb., USA). The average light intensity (I_a) in the culture bottles was calculated from the light intensity measured at the front (I_1) and the back side (I_2) of bottles according to the equation described in the previous chapter (Van Liere and Walsby 1982).

Enrichments from Sakinaw Lake were cultivated in SL10 medium containing 2.5 mM KH_2PO_4 , 6.4 mM NH_4Cl , 4.6 mM KCl, 2.0 mM $\text{MgSO}_4 \cdot 7 \text{H}_2\text{O}$ and 2.0 mM $\text{CaCl}_2 \cdot 2 \text{H}_2\text{O}$. After autoclaving, 18.0 mM NaHCO_3 , 2.5 mM $\text{Na}_2\text{S} \cdot 9 \text{H}_2\text{O}$, 1 ml of trace element solution SL10, 0.1 ml of a solution of 10 vitamins and 20 $\mu\text{g/l}$ Vitamin B_{12} were also added. The pH was adjusted to 6.7 and the medium was distributed into 50-ml screw cap bottles. Cultures were incubated under the low light ($0.15 \mu\text{mol quanta} \cdot \text{m}^{-2} \cdot \text{s}^{-1}$) and high light ($3 \mu\text{mol quanta} \cdot \text{m}^{-2} \cdot \text{s}^{-1}$) conditions.

Enrichment cultures from Faro Lake were cultivated in SL10 medium and artificial seawater medium at low light intensities as described above.

***In silico* subtractive hybridization analysis**

In silico subtractive hybridization was conducted with the Phylogenetic Profiler available at the DOE Joint genome Institute website (<http://img.jgi.doe.gov>). The *Chl. phaeobacteroides* BS1 genome (<http://genome.jgi-psf.org/chlpb/chlpb.home.html>) was screened for single genes which had no homologs based on BLASTP alignments against the other 11 publicly available genome sequences of the green sulfur bacteria *Chlorobaculum parvum* NCIB 8327, *Cba. tepidum* ATCC 49652^T, *Chl. ferrooxidans* DSM 13031^T, *Chl. limicola* DSM 245^T, *Chl. luteolum* DSM 273^T, *Chl. phaeobacteroides* BS1, *Chl. phaeobacteroides* DSM 266^T, *Chl. phaeovibrioides* DSM 265, *Chl. clathratiforme* DSM 5477^T, *Chloroherpeton thalassium* ATCC 35110^T and *Prosthecochloris aestuarii* DSM 271^T (<http://img.jgi.doe.gov/cgi-bin/geba/main.cgi?section=TaxonListandpage=taxonListPhyloandpidt=14955.1250667420>). A maximum e-value of 10⁻⁵ and a minimum identity of 30% were applied for identification of homologs.

Prokaryotic cDNA suppression subtractive hybridisation (cDNA-SSH)

Cultures of *Chl. phaeobacteroides* BS1 grown under low light (0.15 $\mu\text{mol quanta}\cdot\text{m}^{-2}\cdot\text{s}^{-1}$) and high light (3 $\mu\text{mol quanta}\cdot\text{m}^{-2}\cdot\text{s}^{-1}$) were used for determination of differentially expressed genes under changed light conditions. For RNA extraction, cells exponentially growing in culture were mixed with 12.5% ice-cold ethanol/phenol stop solution (5% phenol pH 4.5-5.5 in 100% ethanol) to avoid RNA degradation. After centrifugation at 10,000 x *g* for 10 min at 4°C pellets were frozen in liquid nitrogen and stored at -80°C. Total RNA was isolated using phenol-chloroform (Chomczynski and Sacchi, 1987) and subsequently purified with the RNeasy Mini Kit (Quiagen) according to the protocol of the manufacturer. The RNA was treated with Turbo DNA free (Applied Biosystems) to remove all remaining DNA contamination. As a test for the absence of genomic DNA, a step-down PCR was inferred, using a specific pair of primers BS1-Sig70-94fw (5'-ACGGCGGAAGATGAGGTGAA-3') and BS1-Sig70-252rev (5'-CTGATTCTGGTATTGTTTGGCGA-3') targeting the *rpoD*-gene (Cpham1_2035) which codes for the RNA polymerase sigma factor A. The test was conducted using 200 ng of the total RNA preparation. RNA concentrations were determined with the nanodrop ND-1000 (peqlab, Erlangen, Germany), and quality was assessed on a formaldehyde gel (3.1%, w/v).

Material and Methods

The separation of the mRNA from 40 µg of total RNA was performed with the MICROBExpress bacterial mRNA enrichment kit (Applied Biosystems) according to the instructions of the manufacturer. Multiple preparations were pooled and concentrated with the RNeasy MinElute Cleanup Kit (Qiagen). The efficiency of rRNA depletion in the mRNA extract was analyzed using an Agilent 2100 bioanalyzer with a RNA LabChip (Agilent Technologies, Santa Clara, USA). First strand cDNA synthesis was done with Superscript III Reverse Transcriptase (Invitrogen) as described by the manufacturer, using 2 µg of mRNA 0.5 µl of 10 µM PCS primer (De Long et al., 2008) and 400 U reverse transcriptase. After 90 min of incubation, additional 400 U of the enzyme were added and the incubation continued for another 90 min. Two first strand synthesis reactions were pooled and the second strand cDNA synthesis performed with the PCR-Select™ cDNA subtraction kit (Clontech Laboratories, Mountain View, USA) according to the instructions of the manufacturer. One microliter of DNase-free RNase (500 µg·ml⁻¹) (AppliChem, Darmstadt, Germany) was added and the samples incubated for 30 min at 37°C. The cDNA was purified with a QIAquick PCR purification kit (Qiagen) and yields were quantified by absorbance at 260 nm. Tester and driver were digested with RsaI and purified using the MinElute reaction cleanup kit (Qiagen). Successful digestion of the cDNA was verified by gel electrophoresis on a 1% agarose gel stained with ethidium bromide. Adaptor ligation was performed according to the manual for the PCR-Select™ cDNA subtraction kit (Clontech). Afterwards the ligation efficiency was tested using the primer pair targeting the *rpoD*-gene described above. The first and second hybridisations were done following the instructions of the kit with the exception that 3 µl denaturated driver and 1 µl 4x hybridisation buffer were used during the second hybridization for high light cDNA as driver and 0.5 µl denaturated driver and 0.5 µl 4x hybridisation buffer were used during the second hybridization for low light cDNA as driver. Primary and secondary nested suppression PCRs were run in a GeneAmp 9700 Thermal Cycler (Applied Biosystems) with Advantage 2 polymerase mix (Clontech) according to the PCR-Select™ cDNA subtraction kit (Clontech) protocol using 50 nM of nested-PCR primer 2R in the secondary PCR. Amplification products of this secondary PCR were cloned using the TOPO TA cloning kit (Invitrogen). Plasmids were isolated from selected clones and inserts were sequenced with M13 forward and reverse primers (Invitrogen). Sequence analysis was performed on basis of the annotated genome sequence of *Chl. phaeobacteroides* BS1.

Illumina cDNA sequencing

Total RNA from cultures of *Chl. phaeobacteroides* BS1 grown at different light conditions were extracted as described above. Library preparation and sequencing were performed at the University of Delaware by Brian Eddie and Prof. Thomas Hanson.

cDNA library preparation and sequencing. RNA samples were partially depleted of rRNA using the MicroExpress kit (Ambion, Austin, TX, USA) following the instructions of the manufacturer. cDNA was generated from 25 ng of RNA using the Ovation mRNA-seq kit (Nugen, San Carlos, CA, USA), fragmented by the recommended protocol using an S2 Adaptive Focused Acoustic Disruptor (Covaris, Woburn, MA, USA). Fragmented cDNA was end repaired, ligated to sequencing adapters and prepared for sequencing using the Encore library generation kit (Nugen). Sequencing was carried out on the Illumina Genome Analyzer Iix (Illumina, San Diego, CA, USA). Sequences of 42 bp long were aligned to the *Chl. phaeobacteroides* BS-1 genome (NC_010831) by the Eland software package allowing for up to two mismatched bases, which yielded 2,792,174 uniquely matching sequences for the STRG sample and 3,280,048 uniquely matching sequences for the SLK sample.

Gene expression calculation and analysis. The mean coverage depth for every annotated feature was calculated from the Eland alignment output using custom Perl scripts. The coverage depth per gene was Log_2 transformed and normalized between the two samples using the quantile normalization procedure using the mean of expression for each gene as the reference distribution (Bullard et al., 2010). Statistical significance thresholds were determined by calculating the standard deviation from a null expectation of a 1:1 expression ratio for each ORF, over a sliding window of 101 genes centered on the gene of interest. The resulting set of standard deviations was fitted to the equation $\sigma = 0.35/(0.8+(e^{m^{1.5}})/2)+0.45$, where m is the mean of expression for each ORF. ORFs that had a difference of expression greater than 2σ were considered differentially expressed.

Characterization of *Chlorobiaceae* from the chemocline of Lake Faro

Isolation of DNA, PCR amplification and cloning. Samples of 100 ml from different depths of the chemocline in Lake Faro (Sicily, Italy) were taken in May, June and July 2008 (sampling was performed by Dr. Alessandro Sacca, University of Messina). Cell material was concentrated on polycarbonate filters (0.22 μm pore size Millipore, Bedford, MA) and stored at -20°C . For extraction of chromosomal DNA, cells on filters were lysed by addition of 600 μl lysis buffer (20 mM Na-acetate pH 5.5, 0.5% SDS, 1 mM EDTA, pH 8.0), 300 μg of 0.1-mm-diameter siliconized zirconia beads (BioSpec Products, Bartlesville, USA) and disruption in a beadbeater (BioSpec Products, Bartlesville, USA) for 5 min. The homogenate was centrifuged for 10 min at $16,000 \times g$ and the supernatant was treated further using the DNeasy[®] Blood and Tissue Kit (Quiagen, Hilden, Germany) according to the instructions of the manufacturer.

The 16S rRNA gene fragments and 16S to 23S rRNA intergenic transcribed spacer regions (ITS) were amplified using the primer combination 8f/L1R. The PCR reaction protocol comprised a hot start at 95°C for 5 min, followed by 10 cycles with denaturation at 95°C for 15 sec annealing at 55°C for 15 sec extension step at 72°C for 2 min, then 15 cycles with changed annealing temperature of 50°C and a final extension step for 7 min. The amplification products with a size of 2 kb were excised from an agarose gel (1%, w/v) cleaned using the Nucleospin[®] Extract II Kit (Macherey-Nagel) according to the instructions of the manufacturer and eluted in 30 μl of sterile Tris-buffer (2 mM Tris-HCl, pH 8.0). Further on, 4 μl cleaned PCR product was cloned using the pGEM Easy cloning kit (Promega, Madison, WI) according to the protocol of the manufacturer. A total of 110 clones were picked and grown in LB medium with 100 μM ampicillin added as selective antibiotic. Plasmids were extracted using the Nucleospin[®] Plasmid Kit (Macherey-Nagel) according to the instructions of the manufacturer and eluted in 30 μl of sterile Tris-buffer (2 mM Tris-HCl, pH 8.0). A fragment of the cloned PCR products were amplified using the primer. The variable region of 16S rRNA genes was amplified using the universal bacterial primer GC341f and 907r. To ensure stable melting behavior of PCR-generated DNA fragments primer 341f contained a 40 bp-long GC-clamp at its 5' end. Cycling conditions were as followed. A hot start at 96°C for 4 min was followed by a step-down PCR protocol: 10 cycles with denaturation at 94°C for 30 sec, primer annealing at 58°C for 45 sec and elongation at 72°C for 1 min were followed by 20 cycles with denaturation at 94°C for 30 sec,

primer annealing 53°C for 45 sec and elongation 72 °C for 1 min. A final extension at 72°C for 7 min was included to ensure maximum amount of correct-sized PCR products. For specific PCR amplification of green sulfur bacterial sequences primer 341f in combination with GSB822r was used (Overmann et al., 1999). Standard conditions for PCR comprised 20 ng DNA, 10 µM of each primer, 5 µl of 10x PCR buffer, 0.2 mM of each deoxynucleoside triphosphate, 3.5 mM MgCl₂ and 2.5 U Taq DNA polymerase (Qiagen) in a total volume of 50 µl. All reactions were run in a Veriti 96 well thermocycler (Applied Biosystems). Amplification products were analyzed by standard agarose gel electrophoresis.

Denaturing gradient gel electrophoresis and sequencing. PCR products were loaded onto 6% (wt/vol) polyacrylamide gels in 1x TAE (40 mM Tris-acetate, 1 mM EDTA, pH 7.4) containing a urea/formamide gradient from 70% to 30% where 100% denaturant is defined as 7M urea and 40% (v/v) formamide, were used (Muyzer et al., 1995). Electrophoresis was performed in an Ingeny phoU system (Ingeny International BV, Goes, The Netherlands). Electrophoresis buffer was preheated to 60°C. Electrophoresis was run at 150 V for 16 h. Gels were subsequently stained in a rotating buffer bath containing 1 in 10000 diluted SYBRgold (MoBiTec, Göttingen, Germany) for 45 min. Bands were visualized on a UV transilluminator (LTF Labortechnik, Wasserburg, Germany) and gels were then photographed (Visitron Systems GmbH, Puchheim, Germany). For sequence analyses gel bands were excised with a sterile scalpel and immediately transferred to 1.5 ml reaction tubes each containing, 40 µl of 10 mM Tris-HCl (pH 8.5) and eluted at 65°C for 45 min. For initial identification of different bands and subsequent sequencing, 1 µl of the eluate was reamplified using the same primer set without GC-clamp and the same PCR cycling conditions. The reamplification products were purified with the Nucleospin Extract II Kit (Macherey-Nagel). For sequencing of 16S rRNA gene amplicates from DGGE fragments and cloned fragments, primers M13, 8f, 341f, 907r, L1R and M13r were used. Sequencing was performed on a ABI 3730 capillary sequencer (Applied Biosystems) using the BigDye Terminator v3.1 cycle sequencing kit (Applied Biosystems) according to the protocol of the manufacturer. DGGE, 16S rRNA amplification and cloning experiments were partially performed by the student Roland Schmitz under the supervision of Ovidiu Rucker during a laboratory internship.

Identification of carotenoids and fossil DNA in sediments

Isolation of isorenieratene. The carotenoid isorenieratene was extracted from several samples taken from the Black Sea and the Mediterranean Sea using 2.5 g of sediment (sediment samples were taken by Prof. Jörg Overmann and Evelyn Marschall). Carotenoids from the sediment were dissolved using following solvents: (i) 20 ml methanol/acetone (2/7 v/v), (ii) 20 ml acetone, (iii) 20 ml dichlormethane and (iv) 30 ml methanol/KOH (6% KOH v/v). During all extraction steps samples were sonicated 10 min in an ultrasonic bath in the dark at room temperature except the extraction with methanol/KOH where extraction was performed at 60°C for 20 min. After each extraction step sediment samples were centrifuged for 15 min at 15.000 x g and supernatants were collected and stored in the dark. Pooled extracts were transferred in a separatory funnel and the organic phase was collected after the addition of 30 ml of dichlormethane and 30 ml H₂O. The water phase was washed again twice with the addition of 30 ml of dichlormethane. All organic supernatants were pooled and evaporated using a rotary evaporator at 35°C. Remaining solvent containing carotenoids was transferred to brown glass tubes, dried via a constant nitrogen flow and stored under nitrogen at -20°C until use. Prior to chromatography samples were purified through filtration (0.22 µm pore size). One third of the filter was dissected into small pieces and extracted three times with 2.5 ml methanol/acetone (80:20 v/v). The combined supernatants were centrifuged (10 min, 14000 x g, 4°C), and the supernatant was evaporated to dryness with a rotary evaporator. The sample is stored under nitrogen atmosphere at -20°C until use for further usage.

Chromatography and mass spectrometry. Further enrichment of carotenoids was achieved by a RP18 chromatography (Waters, Milford, Massachusetts, USA), which was suspended in methanol and filled in a column with 2.5cm diameter and length of 15 cm. Then the column was equilibrated with 60% acetone for several hours. The pigments were diluted in 1 ml acetone and applied on the column. The separation was carried out with the following step gradient: 60% acetone; 70% acetone; 80% acetone; 85% acetone; 90% acetone and 100% acetone. The isorenieratene containing fraction (90% and 100% acetone) was collected and diluted with 15ml water, 100 µl of saturated NaCl solution and 15 ml hexane. The hexane phase was separated, washed twice with water and dried by addition of Na₂SO₄. The absorption of the isorenieratene containing fractions were recorded and employing the molar extinction coefficient of 107 mM⁻¹

cm^{-1} at 450 nm the absolute concentration was calculated (Borrego et al., 1999). The samples were dissolved in 500 μl acetone, and frozen for 2 hours at -20°C . Afterwards the samples were centrifuged (15 min, 14,000 \times g, 4°C), dried via a constant nitrogen flow and stored under nitrogen at -20°C until use. Prior to the measurement samples were dissolved in 100 μl methanol/dimethylsulfoxide (1:1, v/v). LC-MS data were acquired on a LTQ-Orbitrap mass spectrometer (Thermo Fisher Scientific Inc., Waltham, MA, US). From each sample 2 μl was injected on a 3 μm C18 ACE capillary column (Bischoff, Leonberg, Germany) with 10 cm to 100 μm ID and separated with $\text{CH}_3\text{CN}/\text{MeOH}/\text{THF}$ (5.8/3.5/0.7, v/v/v) under isocratic conditions for 120 min at 25°C . MS run time was 120 min, which included three scan events. First scan event (1): Fourier transform mass spectrometry (FTMS) resolution was set to 60000 with a detected mass range of 528.0-532.0 and a surface-induced dissociation (SID) achieved at 35.0V. Second scan event (2): ion trap mass spectrometry (ITMS) for the most intense ion from (1) MS/MS activation type: collision-induced dissociation (CID), minimum signal required: 20.0, isolation width: 3.00; normalized collected energy: 15.0, default charge state: 1, activation Q: 0.250, activation time: 30,000. Third scan event: ITMS for the most intense ion from parent list in (2) MS3 activation type: CID, minimum signal required: 20.0, isolation width: 3.00, normalized collected energy: 20.0, default charge state: 1, activation Q: 0.250, activation time: 30,000 (chromatography and LC-MS measurements were performed by Ulrike Oster, from the working group of Prof. Soll at the Department of Botany, LMU Munich).

Examination of fossil DNA. Genomic DNA from sediment samples was extracted using the Ultra Clean Soil™ DNA Kit (Mobio Laboratories, Solana Beach, CA) according to the instructions of the manufacturer, using 0.4 ml aliquots of each sample. For the detection of BS-1 genomic DNA in sediments a set of specific primers was employed BS1-ITS38f and BS1-ITS518r (Marschall et al., 2010). For specific amplification of green sulfur bacterial sequences primer 341f in combination with GSB822r was used (Overmann et al., 1999). Quantitative real-time PCR (RT-qPCR) reactions were performed in 25 μl of reactions using the iQ SYBR GreenSupermix (Biorad) and a Biorad iCycler. To each reaction, bovine serum albumine was added at a concentration of 0.4 mg ml^{-1} . Each reaction contained between 0.5 and 5 ng of DNA extract or the cDNA equivalent to 9 ng of RNA. PCR conditions were 95°C for 5 min, 45 cycles consisting of 94°C for 30 sec, melting at 63°C for 45 sec, and extension at 72°C for 1 min, and a final step of 10 min at 72°C . In the sediment samples, the copy numbers of ITS-DNA were

Material and Methods

determined using 20 ng of DNA per assay. A linearized plasmid containing the cloned fragment from the 16S and 23S rRNA operon of *Chlorobium phaeobacteroides* BS1 was used for calibration. An inhibition test containing 10^5 copies of this plasmid was performed for each sample. When inhibition was observed a sample dilution of 1:10 was employed for further measurements. Each quantification was performed in three parallels. (DNA was extracted by Evelyn Marschall and RT-qPCR were performed by Evelyn Marschall and Ovidiu Rucker)

Distribution of *Chlorobiaceae* in the chemocline of Lake Sakinaw

Pigment analysis. Samples from different depths of the chemocline in Lake Sakinaw (Canada) were taken in May 2008 (500 ml) and July 2009 (2 l) (sampling was performed by Prof. Tom Beatty, University of British Columbia). Cell material was concentrated on GF/F filters (Whatman, Maidstone, UK) and stored at -20°C . For pigment extraction 4 ml methanol/acetone (2:7, v/v) were added to each filter and after 15 min of sonication in an ultrasonic bath extraction was performed in the dark at 4°C over night. The resulting extracts were purified through filtration (0.22 μm pore size), the solvent evaporated by a nitrogen flow and dried samples were stored at -20°C upon usage. For standardization of BChl *e* contents pigment extracts from *Chl. phaeobacteroides* BS1 were used. Total standard BChl *e* was quantified photometrically at a wavelength of 650 nm (Lambda 25 spectrophotometer, Perkin Elmer), after redissolving the pigments in acetone, employing the molar extinction coefficient of $48.9 \text{ mM}^{-1} \text{ cm}^{-1}$ ($58.6 \text{ l g}^{-1} \text{ cm}^{-1}$) (Borrego et al., 1999).

For separation of different homologs, pigments were redissolved in 135 μl methanol/acetonitrile (1:5, v/v) and 15 μl of a ammonium acetate solution as ion pairing agent were added. Reversed-phase HPLC was accomplished using a Dionex system equipped with a P580 pump, an STH585 column oven, a PDA-100 photo diode array detector and a RF2000 online fluorescence detector (Dionex Softron, Sunnyvale, CA). For separation, a Spherisorb ODS2 column (3 μm , 250 mm by 4.6mm) in-line with a precolumn packed with the same material (CS Chromatographie Service, Langerwehe, Germany) was employed. The mobile phase consisted of a linear gradient of a mixture of acetonitrile, methanol, 0.01M ammonium acetate and ethyl acetate at a flow rate of 0.7 ml min^{-1} as described previously (Airs et al., 2001). Fluorimetric detection was carried out at an excitation wavelength of 476 nm and an emission at

676 nm. For samples from 2009 measurements were performed by Anne Köhler under supervision of O. Rucker.

RNA extraction and RT-qPCR. Samples from different depths of the chemocline in Lake Sakinaw were taken July 2009 (2 l). Cell material was concentrated on filters in sterivex and 1 ml RNAlater solution was added. Cells from filters were lysed by addition of 600 µl lysis buffer (50 mM Na-acetate, 1% SDS, 10 mM EDTA, pH 4.2), 600 µl phenol (pH 4.5-5.5) and 1 g of 0.1-mm-diameter siliconized zirconia beads (BioSpec Products, Bartlesville, USA) followed by disruption in a beadbeater (BioSpec Products, Bartlesville, USA) for 5 min. The RNAlater solution was concentrated using Amicon Ultra – 0.5 ml 50K centricons (Millipore, Bedford, MA) and 0.7 ml lysis buffer (20 mM Na-acetate pH 5.5, 0.5% SDS, 1 mM EDTA, pH 8.0) were added. Cells were lysed by mechanical disruption using a syringe needle with 0.6 µm diameter. Total RNA from filter and liquid fractions was isolated using phenol-chloroform (Chomczynski and Sacchi, 1987) and subsequently pooled and purified with the RNeasy MiniElute Cleanup Kit (Qiagen, Hilden, Germany) according to the protocol of the manufacturer. The RNA was treated with Turbo DNA free (Applied Biosystems, Foster City, CA) to remove all remaining DNA contamination. RNA concentrations were determined with the nanodrop ND-1000 (peqlab, Erlangen, Germany), and quality was assessed on a formaldehyde gel (3.1%, w/v).

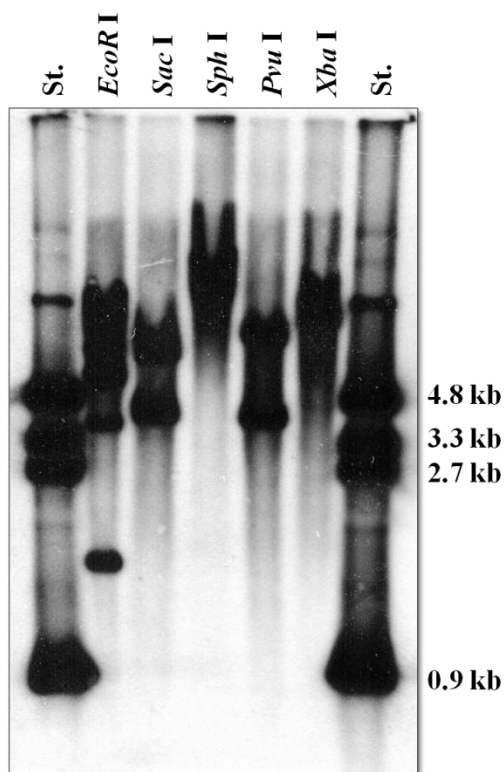
Reverse transcription was performed with the ImProm II Kit (Promega) using 4.5 µl of RNA samples (total 16 µl) according to the protocol of the manufacturer. Negative controls were prepared by omitting the reverse transcriptase and served to verify the absence of contaminating genomic DNA. Quantitative real-time PCR (RT-qPCR) reactions with custom designed gene specific primers were performed using 25 µl reactions with iQ SYBR Green Supermix and 4 µl of cDNA solution and at optimized PCR conditions in a iCycler (Bio-Rad, Hercules, CA). For standardization, the copy number of 16S rRNA gene transcripts was quantified in parallel for all samples using a plasmid containing the cloned fragment from the 16S rRNA and ITS region of the investigated bacterium. Each quantification was performed in three parallels. This experiment was performed by Anne Köhler under the supervision of O. Rucker.

RESULTS

Adaptation of *Chromatiaceae* toward absorption of specific wavelengths of light

Structure of the *puf* operon in strain 970

Using genomic DNA of strain 970, fragments containing the *puf* operon were obtained by the combination of several cloning and iPCR strategies. As a first approach, a southern blot analysis lead to the identification of several fragments containing the main core of the LHC1 genes (Fig. 6). The hybridization probe which was complementary to a 0.85 kb span of *pufLM* showed feasible fragments containing *puf* genes for the *EcoR* I, *Sac* I and *Pvu* I restricted genomic DNA. For the first approach, the 1.5 and 3.7 kb fragments resulting from the *EcoR* I digestion were used for cloning. The screening of 170 clones containing 1.5 kb fragments showed no positive



result and the screening of 360 clones containing the 3.7 kb fragments lead to the identification of one positive clone. While this cloned and sequenced fragment contained only the incomplete information of the *puf* operon (Fig. 7A), two additional fragments resulting from an *Pvu* I restriction were amplified through iPCR.

Fig.6. Southern blot analysis of genomic DNA isolated from strain 970, digested with five different restriction endonucleases and separated by gel electrophoresis. Fragments containing *puf* genes were detected using a hybridization probe complementary to *pufLM*

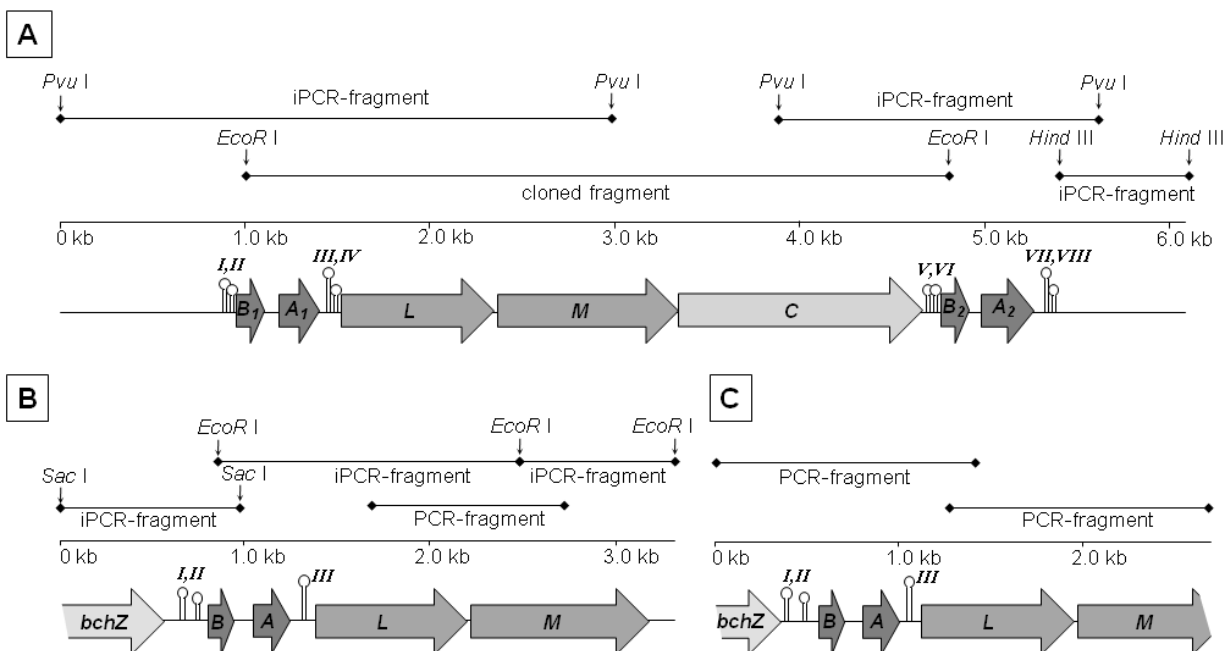


Fig.7. Organization of the *puf* operons in strain 970 and two strains of *Trv. winogradskyi*. **A** Genetic map of a 6048 bp-long section of the chromosome of strain 970 containing the *puf* operon. **B** Genetic map of a 3324 bp-long section of the *puf* operon in *Trv. winogradskyi* strain 06511. The cloned *pufLM* fragment was generated with primers *pufL-f* and *pufM-r* (Suppl. Table 1). **C.** Genetic map of the 2688 bp-long section of the *puf* operon in *Trv. winogradskyi* strain DSM6702^T resembling the partial *puf* operon. The restriction sites and the fragments obtained by cloning, PCR or iPCR are shown. The *puf* genes identified are indicated by filled horizontal arrows. Predicted hairpin structures in intergenic regions are depicted and distinguished according to their roman numerals (see text).

These fragments contained the additional information of sequences flanking the main core of LHC1 genes. The 3 kb long fragment revealed the complete sequences of both genes coding for the light harvesting antenna (*pufBA*) upstream of the core *puf* genes. Another 1.7 kb long fragment showed the presence of additional *pufBA* genes downstream of the core *puf* genes. In order to identify a putative third copy of *pufBA* genes similar to the *puf* operons found in *Allochrochromatium (Alc.) vinosum* and *Lamprocystis (Lpc.) purpurea* (Tuschak et al., 2005; Yutin and Béjà, 2005) a third fragment was amplified through iPCR (experiment performed by Anne Köhler). For this purpose a 0.8 kb long fragment originating from a *HindIII* restriction was amplified and sequenced.

Results

A 6084 nucleotides (nt)-long genome fragment containing the *puf* operon was obtained by the combined cloning and iPCR strategy (Fig. 7A, Fig. 8). Seven ORFs with high similarity to *pufBALMC* genes of other proteobacterial species were comprised within this whole fragment. Two copies of the genes encoding the β and α subunits of the LHC1 (*pufB₁A₁* and *pufB₂A₂*) are flanking the three genes coding for the L and M subunits (*pufLM*) and for the RC-bound tetraheme cytochrome (*pufC*) of the photosynthetic reaction center. The individual *puf* genes were 141 nt (*pufB₁*), 222 nt (*pufA₁*), 822 nt (*pufL*), 975 nt (*pufM*), 1329 nt (*pufC*), 141 nt (*pufB₂*), and 261 nt (*pufA₂*) long. An additional ORF was detected 3' of *pufA₂* and represents a putative fragment of a radical SAM domain protein (not shown in Fig. 7A). This sequence is most closely related to the *Rps. palustris* BisA53 radical SAM domain-containing protein (accession no. YP_781910.1), a protein that usually is not located in the proximity of the *puf* operon. ORFs detected upstream of *pufB₁* encode putative peptides with no significant similarity to known protein functions. In addition, no fragments of *bchZ* could be found.

Several secondary structures flanking the *pufBA* genes were detected (Fig. 7A, Fig. 8) and their stabilities calculated with Mfold. Two predicted hairpin structures were found upstream of *pufB₁* (**I**: $\delta G = -17.3 \text{ kcal mol}^{-1}$, **II**: $\delta G = -12.5 \text{ kcal mol}^{-1}$; compare Fig. 7A) and two more stable secondary structures in the intergenic region between *pufA₁* and *pufL* (**III**: $\delta G = -38.3 \text{ kcal mol}^{-1}$, **IV**: $\delta G = -16.0 \text{ kcal mol}^{-1}$). Similarly, stable hairpins are present between *pufC* and *pufB₂* (**V**: $\delta G = -10.8 \text{ kcal mol}^{-1}$, **VI**: $\delta G = -11.5 \text{ kcal mol}^{-1}$) and downstream of *pufA₂* (**VII**: $\delta G = -34.9 \text{ kcal mol}^{-1}$, **VIII**: $\delta G = -13.7 \text{ kcal mol}^{-1}$).

Fig.8. Nucleotide sequence and deduced amino acid sequences of predicted *puf* genes of strain 970. Gene names were depicted at the codon start and stop codons are marked with an asterisk. Predicted hairpin-loop structures are underlined and numbered on the left side of the sequence from I to VIII. Recognition sites for *Escherichia coli* RNase E (GAUUU) found in the sequence of *puf A₂* are shaded in grey.

```

1      CCCGTATCACAGTCAGGGCAAATCTGTTCTGAGCAGACAGCGCGAGAGCCGGCCNGGCCG
61     GCGCGTGGCGTCAGTTGTCAGTGAGACGGAGCTAGTCAAAGACCAGACGGGCAAGCGAG
121    CCAGACGTTGAATGGCCGCGGCCAGGGTGCCATCCGAGATGAGCTTAATCACGCCGATGG
181    CGAAGCATTGCAAGGCATTCATGCTCTCCGGTCTGCGCTCCGTGCGGATGGTTGAGCGAT
241    CCTCATCCCAGCTTCGAGCCCACCTTGGATCCATGCGCCAGTGACAGCGATTCCCGATCA
301    CCTAGTGTGCAATAAAGGCTAGCAGGCGCTCGGGGTCAGGCTTCCCGGAGGATGGCTTG
361    TGCCCCAATGGATTTCAGGAATTGCTGGGTGCTTAAGGGTTCATCTGGTAGAGGTGTA
421    TCGGACTTGACATGTTTCATCAGTCAGGCTAGACTTACACCTAGTTTCCCGAGCCGGCC
481    CGAGGCGGGCTCTGTTCATCCTGGTTCTTCGCGACTAGACCCATTGCACAAATGCCCACTG
541    ACAGCCTGACTAATAACATAAGCACATCCCCGGTGGCTGCTCTTGTGCAACGTTTCGCCCA
601    GGCAACCCTCTCTCAGCGGGTTGGATCTGACCCCGTTGGGGGAGGCTGACAGTGTGGTGG
661    ATATTCGCAATAGCATTCAATCAGGAGGCTGTGGATTGGCCAGGTGCCACAACGGGGAAA
721    CAGTTTCGTGGTTGGTTGCCGGAGCAAGAGTTGCTGCGGGAACCGACTCGTTTAGAGCTT
781    CAGTGGTGCCTGTCGATTTGTCATGCACCAAGAAGCGCATGGCCGCCGGNTCGTACGG
841    I, II GCACTTGGTCCGTTGGGGCAGTTTTGTCCCAACAAACAAGATGGTGCTTGCAAGCGCGC
901    CGAAAACCTAAGCCGCAAGGCTCAACTCACTCTCTAGAGAGGATTTTCATCATGGCTGAAA
                                           pufB1  M A E
961    AATCAACCACCGGTCTGACTGAAGCAGAATCAAAGAATTCCACGGAATTTTCATGGCCA
K S T T G L T E A E S K E F H G I F M A
1021   GCATGACCCTTTGGTTTGGTTTGGTTGTTCTTGCTCACATTCTGTCTTGGTTGTACCGCC
S M T L W F G L V V L A H I L S W L Y R
1081   CCTGGCTGTAAGCCCTTCGAGCTAGTCCGACCGACCTTTCTTTATTAGCAGATGCCGATG
P W L *
1141   TTCGGCACTGTGACACGCACTTGGAGATGACACAATGAACGCAAAAAGCTTCGACGGTAT
                                           pufA1  M N A K S F D G M
1201   GCACAAACTGTGGATGATCATGAACCCGGTTTTCCACACTTTGGGCCATCTTTATTTTCCA
H K L W M I M N P V S T L W A I F I F Q
1261   GATCTTCCTGGGTCTGCTGATCCACATGGTTGTGCTGAGCTCTGACCTGAACTGGCATGA
I F L G L L I H M V V L S S D L N W H D
1321   TGATCAGATTCCCTGTGCGTTATCAGCTGCAGGGCGAGACGTTGCCTGTCAACCTCGAAAT
D Q I P V G Y Q L Q G E T L P V N L E M
1381   III GAAAGCCGCCAATAAATCGGCCCAACGGTCTTTTCGGATGGTGCTGACCGGGGCGTAC
K A A Q *
1441   IV TCGCCCCCGGGTTTTGCGCGTCGGTCAGCATCCGAATTGCTATGTGGAGGCAGCAGGTCA
1501   TGGTGTCTCCCCAGCAGAGGAAATTACGATGGCCTTGCTAAATTTTGAGAAAAAATACCG
                                           pufL  M A L L N F E K K Y R
1561   CGTACGCGGTGGGACGTTGGTCGGGGGAGACCTGTTTGACTTTTGGGTGGGGCCGTTTTA
V R G G T L V G G D L F D F W V G P F Y
1621   TGTCGGCTTCTTCGGAGTCTCGGCGGTCTTCTTCGCGACCCTCGGTACCATGCTGATCTT
V G F F G V S A V F F A T L G T M L I L
1681   ATTTGGAGCGGCAATTGGGCCGACATTAACATCTGGCAAATCAGTATTGCCCGCCTGA
F G A A I G P T L N I W Q I S I A P P D
1741   TCTAAGCGTTGGTCTTGGATTTGCGCCGATCAGGGAAGGCGGTTTTGTGGCAGGTAATCAC
L S V G L G F A P I R E G G L W Q V I T

```

Results

Fig.8 continued

1801 CATTGTGTCAGTTGGGGCCTTTGTGTCCTGGGCGCTGCGGCAAGTTGAGATTGCCCGCAA
I C A V G A F V S W A L R Q V E I A R K
1861 GTTGGGCATGGGGCTGCATGTACCCTTTGCCTTCTCGTTCGCGATTTTGGCGTACCTCAC
L G M G L H V P F A F S F A I L A Y L T
1921 CCTGGTGTTCCTCCGCCCGGTGTTACTGGGTGCGTGGGGACATGCTTTCCCATACGGATT
L V F F R P V L L G A W G H A F P Y G L
1981 GTTCAGTCACCTTGACTGGGTTTTCCAATGTCGGCTACCAGACCCTACACTTCCACTACAA
F S H L D W V S N V G Y Q T L H F H Y N
2041 CCCAGCGCACATGCTGGCGATCAGTTTCTTCTTCATTAACACGCTGGCGCTGGCAATGCA
P A H M L A I S F F F I N T L A L A M H
2101 CGGTTCTCTGATCCTGTCCGTGGTGAATCCGCAGAAAAGGTGAGGAAGTGAAGACCGCTGA
G S L I L S V V N P Q K G E E V K T A E
2161 GCACGAGAACACGGTTTTCCGTGACATCGTGGGTTACTCCATTGGAGCCTTGGCTATCCA
H E N T V F R D I V G Y S I G A L A I H
2221 TCGCCTGGGTCTGTTTCTGGCGATCAACGCGGCTTTCTGGAGTGCGGTCTGCATGATTCT
R L G L F L A I N A A F W S A V C M I L
2281 GACCGGTCCCTTCTGGACGCGCGGTTGGCCAGAATGGTGGATGTGGTGGCCCAACCTTCC
T G P F W T R G W P E W W M W W P N L P
2341 AATCTGGTAACCTGAGGACACCAAAATGCCTGAATATCAAAATATCTTTAACAAGGTACA
I W * *pufM* M P E Y Q N I F N K V Q
2401 GGTTTCGGAACCTGCTTACCCTGGTGTGCAACTCCCAGAAAGGCAGTCTGCCACGCGTCGG
V R E P A Y P G V E L P K G S L P R V G
2461 CAAGCCGATTTTTCAGTTACTGGCTTGGAAAGATTGGCGATGCGCAGATTGGACCGTTGTA
K P I F S Y W L G K I G D A Q I G P L Y
2521 CCTTGGGGGTTGGGGCATCGCCTCACTGATCTCCGGCTTTATCGCTCTTGAGGTTATCGG
L G G W G I A S L I S G F I A L E V I G
2581 TCTGAACATGCTGGCATCGGTGCGCTGGGACCCGCGGCTTTTCTCAAGGAATTCTTCTG
L N M L A S V G W D P R L F L K E F F W
2641 GTTGGGTCTGGAGCCGCCCGCCTGCATACGGCCTGAGCATCCCGCCCTGGCAGAAGG
L G L E P P P P A Y G L S I P P L A E G
2701 TGGCTGGTGGTTAATCGCTGGTTTATTTCTGACCATGTCCCTCCTGCTGTGGTGGGTGCG
G W W L I A G L F L T M S L L L W W V R
2761 AGTCTACAAGCGGGCGAAAGATCTTGGCATGGGTACCCACCTGTCTGGGCCTTTGCTGT
V Y K R A K D L G M G T H L S W A F A V
2821 CGCGATCCTGTTTTTCTGACACTCGGCTTTATCCGCCCGGTGCTCATGGGAAGCTGGGG
A I L F F L T L G F I R P V L M G S W G
2881 AGAGGCACCACCGTTTGGCATCTTCCCAGCATCTTGACTGGACAGCGGCGATTTTCGATTCTG
E A P P F G I F P H L D W T A A I S I R
2941 CTACGGGAACCTTCTACTACAATCCCTTCCACGGGTTGTCGATCGCCTTTATGTACGGTTC
Y G N F Y Y N P F H G L S I A F M Y G S
3001 AGCCGTTCTGTTTCGCGATGCACGGTGGCACCATTTTGGCCGTCTCTCGTTACGGTGGTGA
A V L F A M H G G T I L A V S R Y G G D
3061 TCGCGAGATCGATCAGATCACGGATCGCGTACTGCAGCTGAGCGGCCATGTTGTTCTG
R E I D Q I T D R G T A A E R A M L F W
3121 GCGCTGGTGCATGGGCTTCAATGCCAGCATGGAATCCATCCATCGCTGGGCCTGGTGGTT
R W C M G F N A S M E S I H R W A W W F
3181 CGCAGTCTTCTGCATCATTAACTCCATACTGGGTATTATCTTGACCGGCACCGTCTGTAGA
A V F C I I N S I L G I I L T G T V V D

Results

Fig. 8 continued

4681 **VI** AGGCGAAAACCGCCGAAACTTATCGACATATGACAAGGCCCTCGGGCCTATCGTGAAACA
4741 AAGAGGAAATTATCATGGCTGAAAAACCAAGTACTGGCCTTACAGAAAGCGAAGCCAAAG
pufB₂ M A E K P S T G L T E S E A K
4801 AATTCCACGGACTTTTCATGGCTAGCATGACCCTTTGGTTTGGTTTGGTTGTTCTTGCTC
E F H G L F M A S M T L W F G L V V L A
4861 ACATTTTGTCTGGATGTACCGCCCCTGGCTGTAATGTCCC GGATGATCTGAAGCAAACG
H I L S W M Y R P W L *
4921 CAAACGTGTAATCTAGCGGTTTCGATAGACGCTTTAAACCGCGTCTATCACCGCTAATATG
4981 GGGGCAATATAATGAATAGTGACAAATTCGCCGGAATGTACAAACTGTGGACTTTTCATCG
pufA₂ M N S D K F A G M Y K L W T F I
5041 ATCCGCGTAGGACGTTGATTTTCATCGTGGCATTCCAGATTATGCTGGGTATTCTGATCC
D P R R T L I F I V A F Q I M L G I L I
5101 ACATGATTGTGCTCGGGTCTGATTTGAACTGGCACAATGACGGGATTCCCAGGTTTTACA
H M I V L G S D L N W H N D G I P R F Y
5161 GCCCGCGCCCTGTTGATGTTGCCGTAGGTCCC GCAGGAATCCCCTTGAAATTCTGGGT
S P R P V D V A V G P A G I P L E I P G
5221 **VII** CGCCGATGCCTCAGGCTCGCAACTACA ACTGATTGCCCTTTGGTGGGCACGGTCGGGCCG
S P M P Q A R N Y N *
5281 **VIII** CGACAGTGAGTCAATTGGACTCGCTGTCGCGGCTTTTTTCGTTGTAGGCGGTCAACACTT
5341 GCTGCCACTGCAGCTAGAGTGCGGCTAAAGCGGTTTACAAGCTTTAGCCGGAGAGAGAGC
5401 TTTTCCGAAATCCTCTAGGAAAGTGCTGCAGAGATTTTGCGGGGGGGGCTCAAGCGGCAG
5461 GTCGGCGATGGGTGCGTCGGATCTTGGCCTGTGCCGTGGCCCGCGGGCTGCACTGGCCA
5521 CGGCCCGCTTGCCGCCGCGTGTGTCTGGTAGAGACCGAGATCCTCGTAGTCGTTCTCGG
5581 TCGCCGTTGTGATGGCTGGGTGCGGTA CTGAGCCGATCGGGATCGGCAGCGATGGCCG
5641 CATCAATGGCGCGTAAGCGGCGCACGACGCGCCAGAAAGTGAAGATGTCACGAATCTCGC
5701 GGTAAAGGTAGCGCGGTTAGAAGATTAGCGGATTTTTCGCGGGGAGCCCTGGTCGGCGTT
5761 GGGTGCGCGCTGGTAGCCGAGCAAGCCTCCCTCGACGGGGTGGATGCCGAGGTTGACCG
5821 GAAAGTGGTGGTACCAGCCAACGTAGGTGCGTGTCA TTTTCGATATCGCCCGGAGTGCCT
5881 GAACGCGCTTGAGGATAGTGGTCATGTGATCCCAGGAGTAATAGCTGTGCCACATGTGCA
5941 GATATCCCTCGTCCCAGTCTTCGTCCGACATCACCGGGT GATGGGTGACGCGGTAGTTGG
6001 TGTTGTAGCGGTTGAAGTCCGGGTCCAGCCAGGCACCTGAGGTGTAGAGACGGGCGTGAT
6061 CGGCCGAGCCAGGTAGCGGGGTCA

Structure of the *puf* operon in *Trv. winogradskyi* strains 06511 and DSM6702^T

The analysis of the *puf* operon from *Trv. winogradskyi* strain 06511 was based on a 1.4 kb fragment of *pufLM* genes, amplified with the conserved primers *pufL*-f and *pufM*-r. Starting from this sequence information, two fragments retrieved from a *EcoR* I digestion were amplified in an iPCR approach. One fragment contained sequence information of the *pufA* gene and partial information of the *pufB* gene located upstream of *pufLM*, while the second fragment completed the *pufM* nucleotide sequence information. In order to gain the complete sequence of *pufB*, another iPCR amplification on fragments digested with *Sac* I was performed.

In total a 3324 nt-long sequence was assembled with these additional three fragments generated by inverse PCR of *EcoR* I and *Sac* I restriction fragments (Fig 7B, Fig. 9). Four ORFs resembling the *pufBALM* genes were identified. Individual *puf* genes were 141 nt (*pufB*), 204 nt (*pufA*), 822 nt (*pufL*) and 975 nt (*pufM*) long. In addition, the partial sequence of the *bchZ* gene that encodes a chlorine reductase subunit was detected 5' of *pufB* and the *pufC* gene is present 3' of *pufM*. Similar to strain 970, two predicted hairpin structures were localized between *bchZ* and *pufB* in strains DSM6702^T (**I**: $\delta G = -23.2$ kcal mol⁻¹, **II**: $\delta G = -18.8$ kcal mol⁻¹). But only one additional stable hairpin was present in the non-coding region between *pufA* and *pufL* (**III**: $\delta G = -36.7$ kcal mol⁻¹).

Fig. 9. Nucleotide sequence and deduced amino acid sequences of predicted *puf* genes of *Trv. winogradskyi* DSM6702^T. Gene names were depicted at the codon start and stop codons are marked with an asterisk. Predicted hairpin-loop structures are underlined and numbered on the left side of the sequence from I to III.

```

1      TCTGGTGCAGAGTTTGCACGCGCTTTTCGACGCGCTGTTCAATATCCTGCCGCTGGGCAC
bchZ L V Q S L H A L F D A L F N I L P L G T
61      GGATCTCGACCGGGTCGAAGCAACACTCGCGCGCGAGTGGCAACGAGCATCGCGAGCT
      D L D R V E A T L A R A S G N E H R E L
121     TCCCTGGGAGGGCGCCGCAAACACTCAAGCTTGATGAGCTGCTTGAGTCAGCGCCGGTGCT
      P W E G A A K L K L D E L L E S A P V L
181     GGTGCGCATCTCCGCCGCAAGCGCTTGCGCGATGCCGCCGAGCGCGCCGCGCGCCGAGC
      V R I S A A K R L R D A A E R A A R R A
241     GGGGGCGGATCGGGTCACGGCCGAGCACGTGCGCCAAGCAGGCTCGGCAATGAATCAGGA
      G A D R V T A E H V G Q A G S A M N Q E
301     I  GGCCGTGGCATGAATGTCCGCGGCAGCACGAGAGGTTTCGTGGTTCGGTGACCAAGGCAGTC
      A V A *
361     GATGTCTTCGGCGTCGCCGCTTTCAAGCTTCAGAGGTGCCAGTCGAGTTGTCTTGCACC

```

Results

Fig. 9 continued

421 **II** CAGGAAGCGCATGGCCGCCGGGTGCGAACGGGCGCTAAATCTGTAAGGGGTCTTTTAACC
481 CTCGGCAGAATGGATGGTGCCTCTCTGGCGCGCTGAAAGACAGCCGCAAGGCTTCACTCA
541 CTTTATTTGAGGATTGAATCATGGCAGAGAAATCAATGACCGGCTTGACTGATGCTGAAG
pufB M A E K S M T G L T D A E
601 CAAAAGAATTCCACGGTATCTTCATGTCCAGCATGACCGCCTATTTTGGTCTGGTTGTAT
A K E F H G I F M S S M T A Y F G L V V
661 TCGCGCATCTGTTGGCTTGGATGTATCGCCCCTGGCTGTAATCCGCCATTGGCCTTAAGC
F A H L L A W M Y R P W L *
721 CAATCGCCCCGTATTGACCAATCATTTTTTTAGCAGATGCCGTTGCTAGGCATTGCTCGCC
781 AAACCTGGAGAATTTACAAATGAACGACAGCATGCAAAACCTGCACAAAATCTGGCAGAT
pufA M N D S M Q N L H K I W Q I
841 CATCAACCCAGCTCAGACCCTGGTGGCACTGGGCGTTTTCCAGATCGTTCTGGGTCTGGG
I N P A Q T L V A L G V F Q I V L G L G
901 TATTCACATGATCCTGCTGAGCACCGACCTGAACTGGCTCGACGACGGCATTCCGGTCAC
I H M I L L S T D L N W L D D G I P V T
961 **III** CTATCAGGACCAGGCTGCCGCTCGGTGCCGAAAATCAATAAGAAGGCCTTTTCGGATG
Y Q D Q A A A S V P Q N Q *
1021 GTGCTGACCGGCGCGTACTCGCCCCCGGGTTTTGCGCGTCGGCCAGCATCCGAGTTGCTA
1081 TGTGGAGGCAGCAGGTCATGGTGTCTCCCCAGCAGAGGATTTAACGATGGCCATGCTGAG
pufL M A M L S
1141 TTTTGAAAAAATAACCGCGTACGCGGTGGGACGCTGGTTCGGGGGAGACCTGTTTCGACTT
F E K K Y R V R G G T L V G G D L F D F
1201 CTGGGTGGGGCCGTTTTATGTCGGCTTCTTCGGAGTCTCCGCGGTCTTCTTCGCGACCCT
W V G P F Y V G F F G V S A V F F A T L
1261 CGGTACCCTACTAATCATTTTTAGGAGCGGCTCTCGGGCCGACTTGGAATATCTGGCAAAT
G T L L I I L G A A L G P T W N I W Q I
1321 CAGTATCGCTCCGCCCCGATCTGGATGTTGGTCTGGGTGTCGCGCCACTGAAAGAGGGAGG
S I A P P D L D V G L G V A P L K E G G
1381 TTTGTGGCAGTTCATCACCATCTGCGCATCGGGCCTTTGTGTCTGGGCGCTCAGACA
L W Q F I T I C A I G A F V S W A L R Q
1441 GGTTGAGATTGCTCGCAAACCTGGGCATGGGGCTCCATGTGCCTTTCGCCTTCGCCTTCGC
V E I A R K L G M G L H V P F A F A F A
1501 GATTCTGGCCTATATCACGCTGGTGGTCATCCGCCCGGTGCTCATGGGTGCTTGGGGGCA
I L A Y I T L V V I R P V L M G A W G H
1561 TGGCTTTCCCTATGGAATTTTCAGTCACCTCGACTGGGTTTTCCAACGTGGGTTACCAGAC
G F P Y G I F S H L D W V S N V G Y Q T
1621 GCTTCACTTCCATTACAACCCGGCGCACATGCTGGCGATCAGCTTCTTCTTCCACCAACTG
L H F H Y N P A H M L A I S F F F T N C
1681 TCTGGCGCTGGCGATGCATGGCTCACTGATTTTGTCCGTGACCAACCCGCGTGACGGCGA
L A L A M H G S L I L S V T N P R D G E
1741 GGCGGTGAAGACGGATGAGCACGAGAACACCGTCTTCCGTGACATCGTGGGGTATTCCAT
A V K T D E H E N T V F R D I V G Y S I
1801 CGGTGCCCTGGGCATCCATCGCCTGGGCGTCTTCCCTGGCAATCAACGCGGCTTTCTGGAG
G A L G I H R L G V F L A I N A A F W S
1861 TGCGGTCTGTATCCTGCTGACCGGTCCCTTCTGGACGCGCGGATGGCCAGAATGGTGGAT
A V C I L L T G P F W T R G W P E W W M
1921 GTGGTGGCCCAACCTCCCAATCTGGTAATCTGAGGACACCAAATGCCTGAATATCAAAA
W W P N L P I W * **pufM** M P E Y Q N

Fig. 9 continued

```

1981   CATTTCACGAGGGTCCAGGTTTCGCGAACCGGGCTACCCTGGTGTGCGAGCTCCCAAGGGG
      I F T R V Q V R E P G Y P G V E L P R G
2041   CAGTCTGCCTCGCCTTGGCAAGCCGATCTTCAATTACTGGATCGGCAAGATTGGCGATGC
      S L P R L G K P I F N Y W I G K I G D A
2101   GCAGATTGGTCCGCTGTATCTTGGGGGTTGGGGCATCGCTTCCCTGATCGCTGGCTTCAT
      Q I G P L Y L G G W G I A S L I A G F I
2161   CGCCATCGAGATCATGGGGGCTCAACATGCTGGCCTCGGTCGACTGGAACCCGATCTTGT
      A I E I M G L N M L A S V D W N P I L F
2221   CGTCAAGAACTTTTTCTGGTTGGCTCTGGAGCCACCACCGCCCGCTTATGGCCTAAGCTT
      V K N F F W L A L E P P P P A Y G L S F
2281   CCCACCGCTTGCTGAAGGCGGCTGGTGGCTCATCGCCGGGTTCTTTTTGACCCTCTCCAT
      P P L A E G G W W L I A G F F L T L S I
2341   CCTGCTGTGGTGGGTCCGGGTCTACAAGCGCGGTCGATCTCGGCATGAGCACCCATCT
      L L W W V R V Y K R A V D L G M S T H L
2401   CGCGTGGGCCTTCGCGGCCCATCTTTTTCTACCTCACGCTTGGGTTTATCCGCCGAT
      A W A F A A A I F F Y L T L G F I R P I
2461   TCTCATGGGTAGTTGGGGTGAGGCACCGCCTTTCGGCATCTTCCCGCATCTTGACTGGAC
      L M G S W G E A P P F G I F P H L D W T
2521   GGCTGCTATTTTCGATCCGCTATGGGAATTTCTACTATAATCCCTTCCATGCGTTGTCGAT
      A A I S I R Y G N F Y Y N P F H A L S I
2581   TGCCTTCCCTGTACGGCTCCGCGGTGCTCTTCGCCATGCACGGCGGCACCATCCTGGCTGT
      A F L Y G S A V L F A M H G G T I L A V
2641   TTCGCGCTACGGCGGTGATCGCGAGATCGATCAGATTACCGATCGCGG
      S R Y G G D R E I D Q I T D R

```

Using the sequence information of a conserved site in the *bchZ* gene of strain 06511 the primer W6702-BChZ-fw, (Table 2) was used together with primer W6702-rev which binds in the *pufL* region. With this approach the LHC1 genes of *Trv. winogradskyi* strain DSM6702^T could be amplified through conventional PCR. Additional sequence information for the *pufLM* genes was obtained previously through amplification with primers *pufL*-f and *pufM*-r (Table 1). The resulting genetic map of the *puf* operon from *Trv. winogradskyi* strain DSM6702^T revealed the canonical gene order (Fig. 7C, Fig. 10). The lengths of the individual *pufB*, *pufA*, and *pufL* genes were identical to that in *Trv. winogradskyi* strain 06511. The sequences of the *pufM* and *bchZ* genes identified at the 3' and 5' ends respectively were incomplete. Similar to the intercistronic regions in strain 970, mRNA secondary structures were also identified in the *puf* operon of the two *Thiorhodovibrio* strains. Two predicted hairpin structures were localized between *bchZ* and *pufB* (**I**: $\delta G = -27.6 \text{ kcal mol}^{-1}$, **II**: $\delta G = -16.7 \text{ kcal mol}^{-1}$). One additional stable hairpin was present in the non-coding region between *pufA* and *pufL* (**III**: $\delta G = -38.4 \text{ kcal mol}^{-1}$).

Results

Fig.10. Nucleotide sequence and deduced amino acid sequences of predicted *puf* genes of *Trv. winogradskyi* strain 06511. Gene names were depicted at the codon start and stop codons are marked with an asterisk. Predicted hairpin-loop structures are underlined and numbered on the left side of the sequence from I to III.

```
1      GAGCTCGGCATGCCCTGTCATTTTCGCCATCGCGCGTTCGCCCCGGGGTCAAGACCGATAAC
bchZ E L G M P C H F A I A R R P G V K T D N
61     GCTGCCACGCGCGAGGCGGTGCGTGGCAAGACTCCGCTGGTGGTCTTCGGCGGCTACAAC
      A A T R E A V R G K T P L V V F G G Y N
121    GAGCGCATGTATCTGGCCGAGGCCGGCGGACGCGCGGCTTTCATCCCAGCCTCGCTGCC
      E R M Y L A E A G G R A A F I P A S L P
181    GGCACCCTGGTGCGCCGCCACCCGGCACGCCCTTCATGGGCTTCTCGGGCGCGACCTAT
      G T L V R R H T G T P F M G F S G A T Y
241    CTAGTGCAGGAAGTCTGCAACGCGCTCTTTGATGCGCTCTTTAATATTTTGGCCCTGGGT
      L V Q E V C N A L F D A L F N I L P L G
301    ACGGACCTTGACCGGGTCGAAGGGACTCTTGCCCGCGCCGGCAGCGAGCGCCACCGCGAG
      T D L D R V E G T L A R A G S E R H R E
361    CTGCCGTGGGAGAGCGATGCCAAGCGCAAGCTCGACGAGATGCTGGAATCAGCGCCCGTT
      L P W E S D A K R K L D E M L E S A P V
421    CTGGTGCGCATCTCCGCTGCCAAGCGGCTGCGCGACGCGCCGAGCGCGCAGCGCGCAGC
      L V R I S A A K R L R D A A E R A A R S
481    GCGGGTGAAGATCGAGTAACAGCCGAGCATGTTCGCACAAGCGGGCTCGGCGATGAATCAG
      A G E D R V T A E H V A Q A G S A M N Q
541    GAGCCGTGGCATGAAAAAGCCGCGAGCCAGCTAAAAGCTTTGTGTTCGGTTTTTCGGGA
      E A V A *
601    I CTTCGTATGTCCGGGGTGCCGACGCATTTTCGCGCTTCAGAGGTGCTAGTCGCGTTTTTGT
661    II GCACCCAGGAAGCACATAGTCGTCCGGGCAACCGGACCTCTGGTCTGTTGGGGCATCTGC
721    TTGCCCTCGACGCCCGTTATGGTGCGCCGCGGGCGCGCTGACAGCCGAAGGCTTAACACT
781    TAAATCTCTTCGGAGGATTTACTCATGGCTGAAAAATCAATGACCGGTCTGACCGACGCT
      pufB M A E K S M T G L T D A
841    GAAGCAAAAGAATTCCATGGCATCTTCATGGCTAGCATGAGCGCTACTTCGGCTTGGTG
      E A K E F H G I F M A S M S A Y F G L V
901    GTTTTTCGCCCATCTGCTGGCTTGGATGTATCGCCCCCTGGCTGTAATCCGCTCCTTCAGCA
      V F A H L L A W M Y R P W L *
961    TAACGGGAGCTCATCGCGAGCCCGCGGACCTTTTTTCTGATGCTGCTTCTAGGCAGCGC
1021   CTTACACCAAATTTGGAGATATCAAGATGAACGAAAGCCTGCAAAACCTGCACAAAGTTT
      pufA M N E S L Q N L H K V
1081   GGCTGCTGATCAATCCTGCTCAGGTCCTGGTTCGCTCTTGGCGTTTTTCAGATCGTTTTGG
      W L L I N P A Q V L V A L G V F Q I V L
1141   GTCTTGGGATCCACATGATCCTGCTCAGCACCGACCTCAACTGGCTGGACGACGGCGTGC
      G L G I H M I L L S T D L N W L D D G V
1201   CTGTGACTTATCAGGCACAGGCTGCATCGGCAGCGCCCCAGAACAAATAAGAAGGCCTTT
      P V T Y Q A Q A A S A A P Q N K *
1261   III TCGGATGGTGTGACCCGCGCGGGCTCGCCCCCGGGCCACGTGCCGGTCAGCATCCGA
1321   GTTGCTATGTGGAGGCAGCAGGTCATGGTGTCTCCCCAGCAGAGGAATTAACGATGGCCA
      pufL M A
1381   TGCTGAGTTTTGAAAAAATACCGGTACGCGGTGGGACGCTGGTTCGGGGGAGATCTGT
      M L S F E K K Y R V R G G T L V G G D L
1441   TCGACTTCTGGGTGGGGCCGTTTTATGTTCGGCTTCTTCGGTGTGTGCGACGGTTTTCTTCG
      F D F W V G P F Y V G F F G V S T V F F
```

Fig.10 continued

1501 CGACCCTCGGTACCCTGCTTATCATTACGGTGC GGCTCTTGGGCCGACCTGGAATCTCT
 A T L G T L L I I Y G A A L G P T W N L
 1561 GGGCAATCAGTATTGCTCCGCCGAACCTGGATGTTGGGTTAGGTGTTGCACCACTGAGAG
 W A I S I A P P N L D V G L G V A P L R
 1621 AAGGTGGTCTCTGGCAGTTTATTACCATCTGTGCAATCGGGGCCTTTGTGTCTGGGCGC
 E G G L W Q F I T I C A I G A F V S W A
 1681 TCAGACAAGTTGAGATTTGCCGGAAGCTGGGCATTGGGCTCCATGTACCCTTCGCCCTTTT
 L R Q V E I C R K L G I G L H V P F A F
 1741 CGTTTGGCATCCTGGCCTATGTCACCCTGGTTGTGATTGTCAGTGTTGCTTGGTGCTT
 S F A I L A Y V T L V V I R P V L L G A
 1801 GGGGACATGGTTTCCCTTACGGAATCTTCAGTCACCTCGATTGGGTTTCCAATATCGGCT
 W G H G F P Y G I F S H L D W V S N I G
 1861 ACCAAACGCTGCACTTCCATTACAACCCGGCGCATATGCTGGCGATCAGCTTCTTCTTCA
 Y Q T L H F H Y N P A H M L A I S F F F
 1921 CCAACTGCCTGGCGCTGGCGATGCACGGATCTTTGATCCTTTCCGTGGTCAACCCGCGCG
 T N C L A L A M H G S L I L S V V N P R
 1981 ACGGCGAGCCGGTGAAGACAGGCGAGCATGAAAACACCGTCTTCCGGGACATCGTTGGTT
 D G E P V K T G E H E N T V F R D I V G
 2041 ATTCCATCGGTGCGTTGGGCATCCATCGCCTCGGTCTGTTTCTTGGCATCAACGCTGCTT
 Y S I G A L G I H R L G L F L A I N A A
 2101 TCTGGAGCGCGGTCTGCATCGTGCTGACCGGTCCCTTCTGGACGCGCGGATGGCCGGAAT
 F W S A V C I V L T G P F W T R G W P E
 2161 GGTGGATGTGGTGGCCTAACCCCCCAATTTGGTAATCTGAGGACACCAAATGCCTGAAT
 W W M W W P N P P I W * *pufL* M P E
 2221 ATCAAAACATTTTACGAGGGTGCAGTTTCGCGAACCTGGCTACCCTGGTGTGCGAGCTCC
 Y Q N I F T R V Q V R E P G Y P G V E L
 2281 CGAGAGGCAGTCTGCCTCGCCTTGGCAAGCCGATCTTCAATTACTGGATCGGCAAGATTG
 P R G S L P R L G K P I F N Y W I G K I
 2341 GCGACGCGCAGATTGGTCCGCTCTATCTCGGGGGCTGGGGCATCGCTTCGCTGATCGCGG
 G D A Q I G P L Y L G G W G I A S L I A
 2401 GCTTTATCGCCATTGAGATCATGGGTCTCAATATGCTGGCGTGGTTCGACTGGAGTCCAA
 G F I A I E I M G L N M L A S V D W S P
 2461 TTCTTTTCCTTAAAGAATTCTTCTGGTTAGCCCTGGAGCCACCACCGCCGCTTACGGCC
 I L F L K E F F W L A L E P P P P A Y G
 2521 TGAGCTTCCCACCCTTGGTGAAGGTGGCTGGTGGCTGATCGCCGGGTTCTTCTGACTC
 L S F P P L A E G G W W L I A G F F L T
 2581 TCTCCATCCTCTTGTGGTGGGTGCGGGTCTACAAGCGTGC GGTTGATCTTGGCATGGGTA
 L S I L L W W V R V Y K R A V D L G M G
 2641 CCCATCTGGCATGGGCCTTTGCTGCGGCGATCTTCTTCTACCTGACGCTGGGCTTCATTC
 T H L A W A F A A A I F F Y L T L G F I
 2701 GCCCAATCCTGATGGGTAGCTGGGGTGAGGCTCCTCCGTTTGGCATCTTCCC GCATCTTG
 R P I L M G S W G E A P P F G I F P H L
 2761 ACTGGACAGCGGCTATTTGATTCGCTACGGGAACTTCTACTACAACCCGTTCCATGCGC
 D W T A A I S I R Y G N F Y Y N P F H A
 2821 TGTCGATCGCCTTCTGTACGGCTCAGCGGTGCTCTTTGCGATGCACGGTGGGACCATTC
 L S I A F L Y G S A V L F A M H G G T I
 2881 TGGCCGTGTGCGTTACGGCGGCGACCGGAGATCGATCAGATCACTGATCGCGGTACCG
 L A V S R Y G G D R E I D Q I T D R G T

Results

Fig.10 continued

```
2941      CGGCCGAGCGTGCAATGCTGCTGTGGCGCTGGTGCATGGGCTTCAACGCCAGCATGGAGT
          A A E R A M L L W R W C M G F N A S M E
3001      CTATCCATCGCTGGGCCTGGTGGTTCGCGGTCTTTACGGTCATAACCGCTGGTCTGGGTA
          S I H R W A W W F A V F T V I T A G L G
3061      TCCTGCTGACCGGCACCGTGGTCGAGAACTGGTACCTTTGGGCCGTCAAGCACGGATTCCG
          I L L T G T V V E N W Y L W A V K H G F
3121      CGCCGACCTACCCGTCGGAGCTGTCCATCGAGAATCCCTATCTGACGCAGGGGGTGTCCG
          A P T Y P S E L S I E N P Y L T Q G V S
3181      AATGAAGATGCGTAACCGCAATGCGCTGGCGCTCCTGAGCCTGGGGGCGACCGCGTTTCAT
          Q *
      pufC M K M R N R N A L A L L S L G A T A F I
3241      CGTCGGCTGCGAGGCACCGCCACCCGAGATTGTCCAAAACGGCTATCGTGGCTTGGCCAT
          V G C E A P P P E I V Q N G Y R G L A M
3301      GCAGCAGAACTACAACCCGGACC
          Q Q N Y N P D
```

Transcriptional analysis of the *puf* operon in strain 970

The stoichiometry of the *pufL* and *pufBA* transcripts was determined through a RT-qPCR approach. To quantify transcripts of the two different gene copies for light harvesting polypeptides (*pufB_{1A1}* and *pufB_{2A2}*), two different primer sets were constructed that amplified both gene pairs (*pufB1+2-qPCR-f* with *pufA1+2-qPCR-r*, Suppl. Table 1) or *pufB_{2A2}* separately (*pufB1+2-qPCR-f* with *pufA2-qPCR-r*). This primer design took advantage of the fact that the sequence of *pufA₂* exceeded that of *pufA₁* by 39 nucleotides (see above), thus providing a specific target sequence for the *pufA₂*-specific primer. However, *pufB_{2A2}* transcripts could only be detected in cultures grown under light saturated conditions where they still were 1030-fold less abundant than *pufB_{1A1}* transcripts. No *pufB_{2A2}* transcripts were found in cells grown under light limitation.

When cells were grown under light saturation, *pufB_{1A1}* transcripts were 9.9 fold more abundant than the *pufL* transcript. This stoichiometry changed to 18.7 fold (*pufA* to *pufL*) when cultures were grown under limiting light intensities of 2 $\mu\text{mol quanta}\cdot\text{m}^{-2}\cdot\text{s}^{-1}$. Under the latter conditions, the overall abundance of *puf* transcripts decreased.

The stability of the *pufB₁A₁* transcripts and the *pufL* transcript was determined following inhibition of transcription with rifampicin and employing cultures grown under saturating light conditions. Samples were taken at various time intervals and the abundance of the respective transcripts was quantified by RT-qPCR as described above. An exponential decline of *pufB₁A₁* and *pufL* transcripts was observed 15 min after the addition of rifampicin (Fig. 11). The transcript of the LHC-I structural genes showed a half-life of (27.5 ± 8.1) min, whereas the corresponding value for the *pufL* transcript was smaller and reached (14.3 ± 2.1) min.

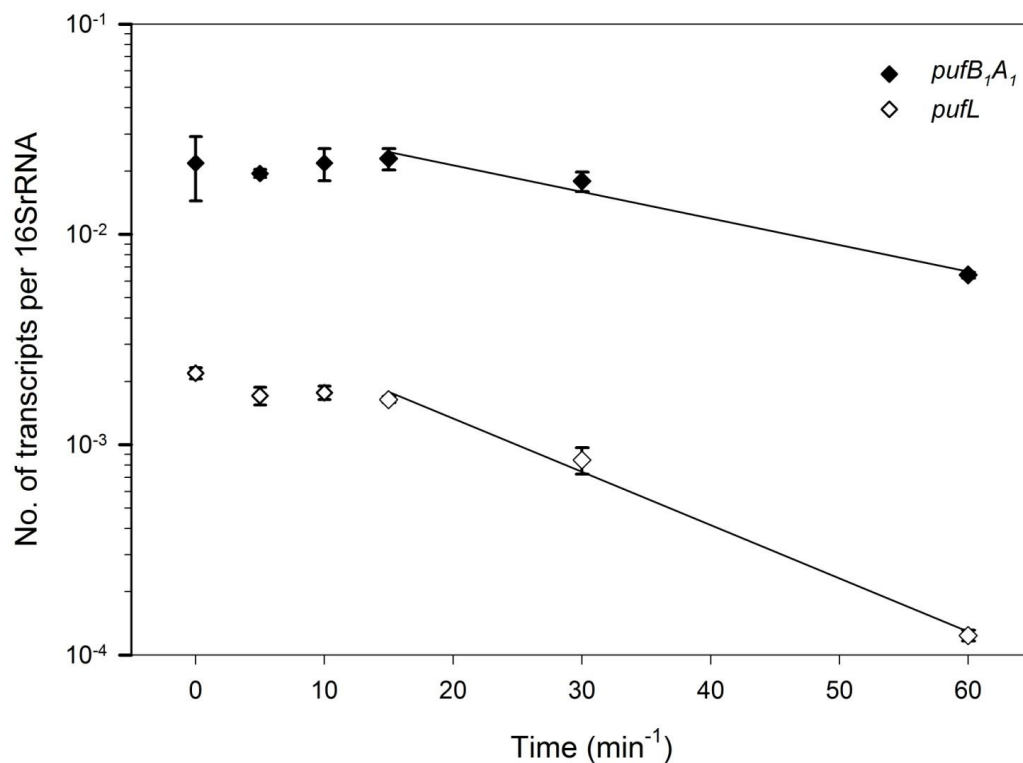


Fig. 11 Kinetics of mRNA decay of *pufB₁A₁* and *pufL* transcripts in strain 970 grown under light saturation. Transcripts were quantified by qRT-PCR after addition of rifampicin and normalized to the amounts of 16S rRNA amounts in each sample. Vertical bars indicate one standard deviation. The regression lines for the determination of the *pufB₁A₁* and *pufL* transcripts half lives (between the sampling points at 15 and 60 min) are depicted

Comparative analysis of the Puf polypeptides

Typically, the LHC1 α - and β -polypeptides are between 40 and 70 amino acid residues long. Comparable lengths of amino acid (aa) sequences can be inferred for LHC1 β of strain 970 and the two *Trv. winogradskyi* strains (46 aa) and for LHC1 α of the two *Trv. winogradskyi* strains (67 aa). In contrast, the two LHC1 α polypeptides of strain 970 display an unusual length of 73 aa and 86 aa, respectively. An alignment of the sequences of all LHC1 α and β polypeptides obtained in the present study against all available LHC1 sequences confirmed the three domain structure of the polypeptides including polar N- and C-terminal domains that frame a hydrophobic transmembrane α -helix (Bullough et al., 2008).

A detailed comparison of amino acid sequences of the LHC1 α - and β -polypeptides was conducted with 73 sequences retrieved from 65 different microbial strains. After omitting redundant sequence information, a total of 33 other LHC1 polypeptide sequences encompassing the conserved region and the transmembrane region were analysed (Fig. 12). The LHC1 α polypeptides of all three investigated *puf* operons show a deletion between α His⁰ and α Trp⁺¹¹ in a region with close interactions with BChla. This deletion can also be found in LHC1 α chains of *Tch. tepidum* ATCC 43061^T, *Roseobacter denitrificans* ATCC33940^T, *Roseobacter litoralis* Och149 and *Jannaschia sp.* CCS1. Our analysis also revealed the presence of two conspicuous amino acid replacements that clearly distinguish *PufBA* sequences of strain 970 from all other known sequences or all other sequences except (in one case) that of *Thermochromatium tepidum* ATCC 43061^T (highlighted in black in Fig. 12). In strain 970, histidine replaces the α Lys⁺¹². This change together with the deletion is positioned in the vicinity of the acetyl carbonyl of the BChla macrocycle and represents a unique feature of strain 970 LHC1 α polypeptides. Another significant change is the occurrence of β Trp⁻⁸ in both LHC1 β sequences of strain 970, a feature that is also observed in the LHC1 β chain of *Tch. tepidum* ATCC 43061^T, and not in LHC1 β from both *Trv. winogradskyi* strains or any other anoxygenic phototrophic proteobacterium. While more conserved than the LHC1 α , the LHC1 β polypeptides of strain 970 harbors an uncharged polar β Ser⁺³ residue instead of the more commonly found apolar β Val⁺³ or β Ala⁺³ residues. Another LHC1 β chains harbouring an β Ser⁺³ can only be found in *Rhodomicrobium vannielii* ATCC 17100^T.

In addition, the polarity of the N- and C-terminal domains framing the membrane spanning α -helices of both LHC1 polypeptides varies between the different strains. Instead of three acidic side chains, only two appear in the N-terminal domain of LHC1 β in strain 970 and both strains of *Trv. winogradskyi*. This feature is shared with several other sequences, however (Fig. 12). Similarly, the N-terminal domain of LHC1 α lacks some charged polar side chains in strain 970 (PufA₁) and *Trv. winogradskyi*. The conserved positions α Asp⁻²⁰, α Arg⁻¹⁸ and α Arg⁻¹⁷ are substituted with α Asn⁻²⁰, α Val⁻¹⁸ and α Ser⁻¹⁷ in strain 970 and α Asn⁻²⁰, α Ala⁻¹⁸ and α Gln⁻¹⁷ in *Trv. winogradskyi*. A similar decrease in the number of charged polar side chains was only detected in *Chloroflexus (Cfl.) aurantiacus* and the LHC1 α protein of *Lpc. purpurea*.

Structural models for the LHC1 polypeptides

The LHC1 polypeptide sequences of strain 970 display considerable changes in amino acid residues that are located at positions that might interact with bound BChl molecules. Therefore the three dimensional orientation of the unusual amino acids in the α - and β -polypeptides of strain 970 was evaluated using 3-D structural modeling (Fig. 13). Two structural models were constructed based on the structure from LHC2 of *Phaeospirillum molischianum* ATCC14031^T (1lgh) (Koepke et al., 1996) (Fig. 13A) and of *Rhodoblastus acidophilus* DSM137^T (1nkz) (Papiz et al., 2003) (Fig. 13B). Additional structural data are available for LHC1 of *Rhodospirillum rubrum* (Wang et al., 2005) or *Rhodobacter sphaeroides* (Conroy et al., 2000), but were not suitable as templates as they were determined exclusively in solution and cannot provide sufficient structural details on the orientation of BChl *a* molecules and the loop domain at the C-terminus of the pigment-binding polypeptides.

Modeling based on β polypeptide templates suggests that β Trp⁻⁸ is in close proximity (3.03 Å or 1.34 Å depending on the template; Fig. 13A, B) to BChl *a* in the antenna polypeptide of strain 970. In the β polypeptides of *Rbl. acidophilus* DSM137^T and *Phs. molischianum* ATCC14031^T, this residue is a phenylalanine (Phe), which cannot form a hydrogen bond with the acetyl group. The conserved β Trp⁺⁹ displays the expected proximity to the C3¹ acetyl group of BChl*a* in both models calculated (3.60 Å and 4.87 Å; Fig. 13A,B). The models based on the α -polypeptide templates differ with regard to the position of α His⁺¹¹. The model derived from the LHC2 α of *Rbl. acidophilus* DSM137^T as template displays clearly the proximity to the BChl C3¹ acetyl group with a calculated distance of 3.54 Å (Fig. 13A). This distance differs when LHC2 α of *Phs. molischianum* ATCC14031^T serves as a template (6.63 Å; Fig. 13B). Both LHC2 α sequences used for modeling do not display a deletion in this region. The models also differ in the structure predicted for this periplasmic region, with the model derived from the LHC2 α of *Phs. molischianum* ATCC14031^T displaying a short α -helical structure, which is not present in the other model.

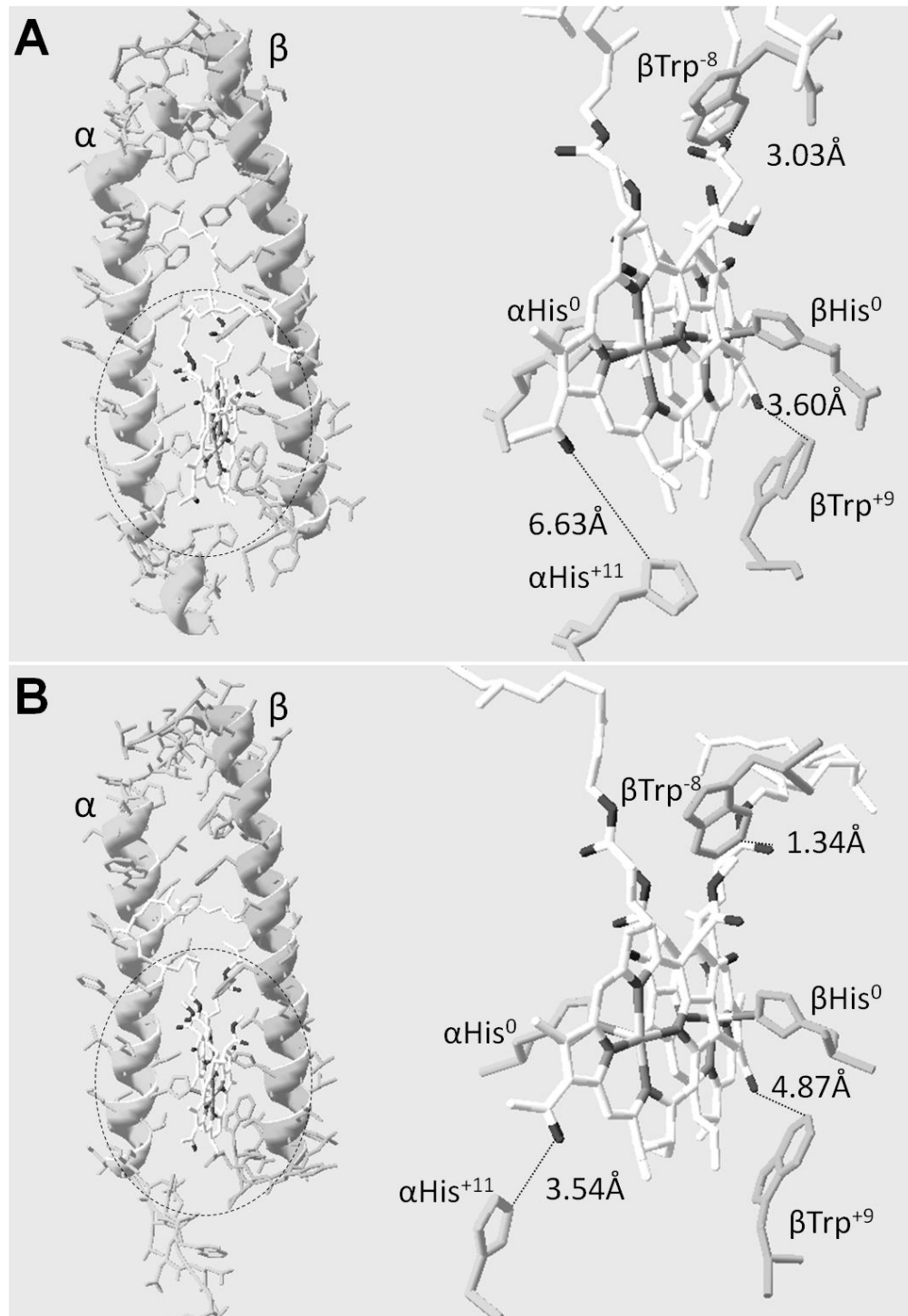


Fig. 13 Comparative 3-D models of the LHC1 polypeptides of strain 970 calculated based on the crystallographic structures of LHC2 from **A** *Rhodoblastus acidophilus* DSM137^T and **B** *Phaeospirillum molischianum* ATCC14031^T as templates. On the right, the region around the BChl *a* macrocycle is depicted at higher magnification. Residues with close proximity to bound BChl are colored in light grey, backbone C-atoms of BChl in white and O-atoms and N-atoms of BChl in dark grey. The distances calculated for hydrogen bonds are displayed as dotted lines.

Phylogenetic relationship of LHC1 and RC sequences

Some of the peculiarities of LHC1 polypeptides of strain 970 and *Trv. winogradskyi* strains were also detected in a few sequences of other proteobacteria (Fig. 13). Therefore, the phylogenetic relationships of LHC1 polypeptides of strain 970 and *Trv. winogradskyi* strains with those found in other bacteria were evaluated (Fig. 14). Since previous investigations (Tuschak et al., 2004) had shown that the phylogenetic relationships of α and β LH1 polypeptides are very similar, amino acid sequences of the two polypeptides were concatenated in these analyses. The LHC1 sequences from strain 970 and both *Trv. winogradskyi* strains are most closely related to those of *Tch. tepidum* ATCC43061^T and cluster together with polypeptides from the other *Gammaproteobacteria*. Most notably, LHC1 sequences of strain 970 are very closely related to those of *Tch. tepidum* ATCC43061^T. In contrast, the phylogenetic analysis of the 16S rRNA gene sequences placed strain 970 among the *Thiorhodovibrio* strains and at a larger distance to *Tch. tepidum* ATCC43061^T, the latter falling into a cluster with *Alc. vinosum* DSM180^T and *Lpc. purpurea* DSM4197^T (Fig. 14). Similarly, the phylogenetic analysis of concatenated *pufLM* gene sequences placed strain 970 and both *Trv. winogradskyi* strains in one subcluster that was only distantly related to *Tch. tepidum* ATCC43061^T, *Alc. vinosum* DSM180^T and *Lpc. purpurea* DSM4197^T (Fig. 15).

Since no other *Chromatiaceae* with extremely red-shifted Q_Y absorption bands have been reported so far, the presence of bacteria related to strain 970 was assessed in a series of environmental samples from tidal sediments that were visibly colonized by anoxygenic phototrophs. Because *pufLM* sequences are more conserved than *pufBA* sequences, only primers are available that permit a selective amplification of *pufLM* sequences from all known sequence types. Sequence analysis of clone libraries prepared with the amplification products of five different types of samples revealed that most of the retrieved sequences were closely related to *Roseobacter* species, whereas only three sequences were related to those of known *Gammaproteobacteria* (Fig. 15). No sequences clustering together with strain 970 and the two *Trv. winogradskyi* sequences were detected.

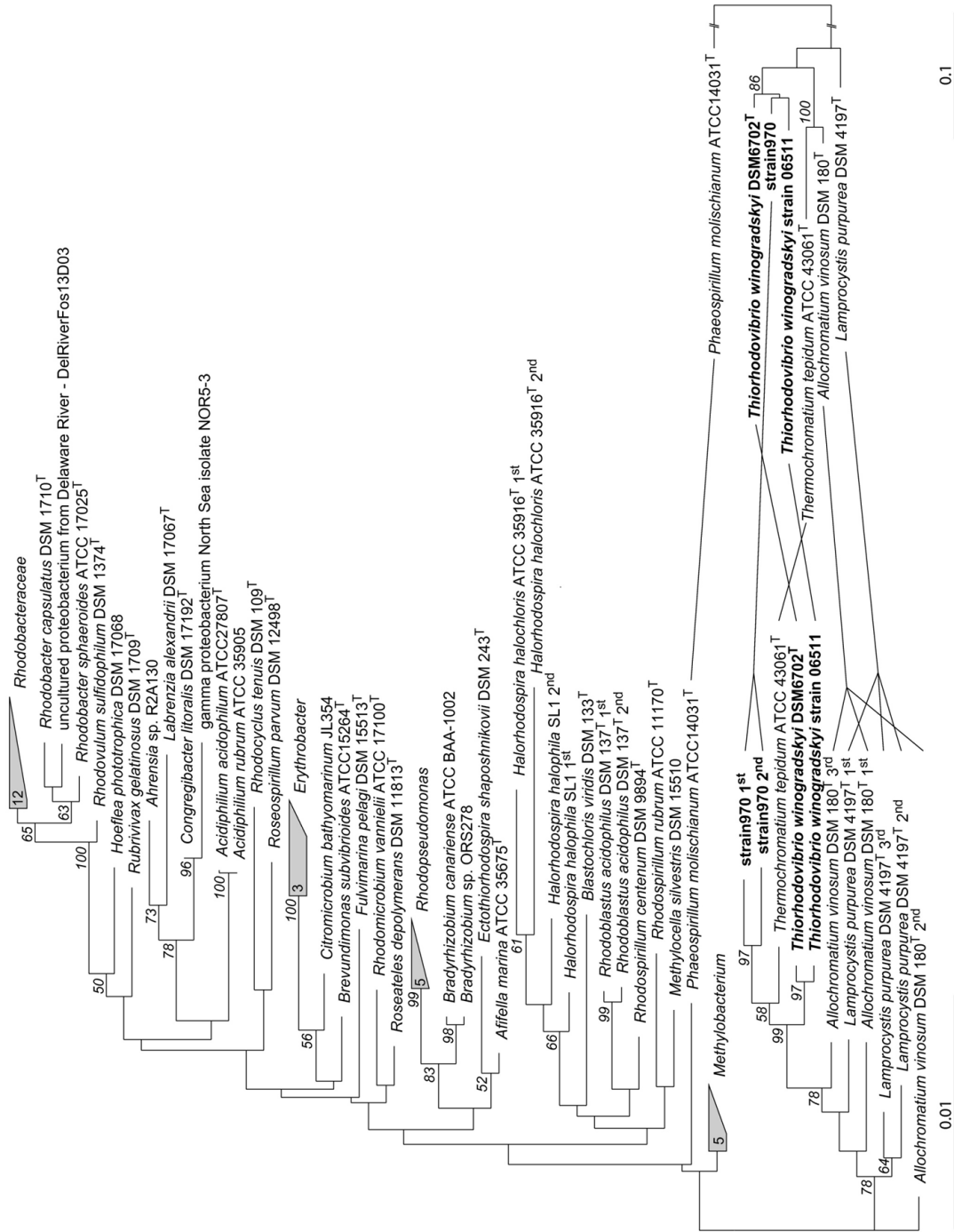
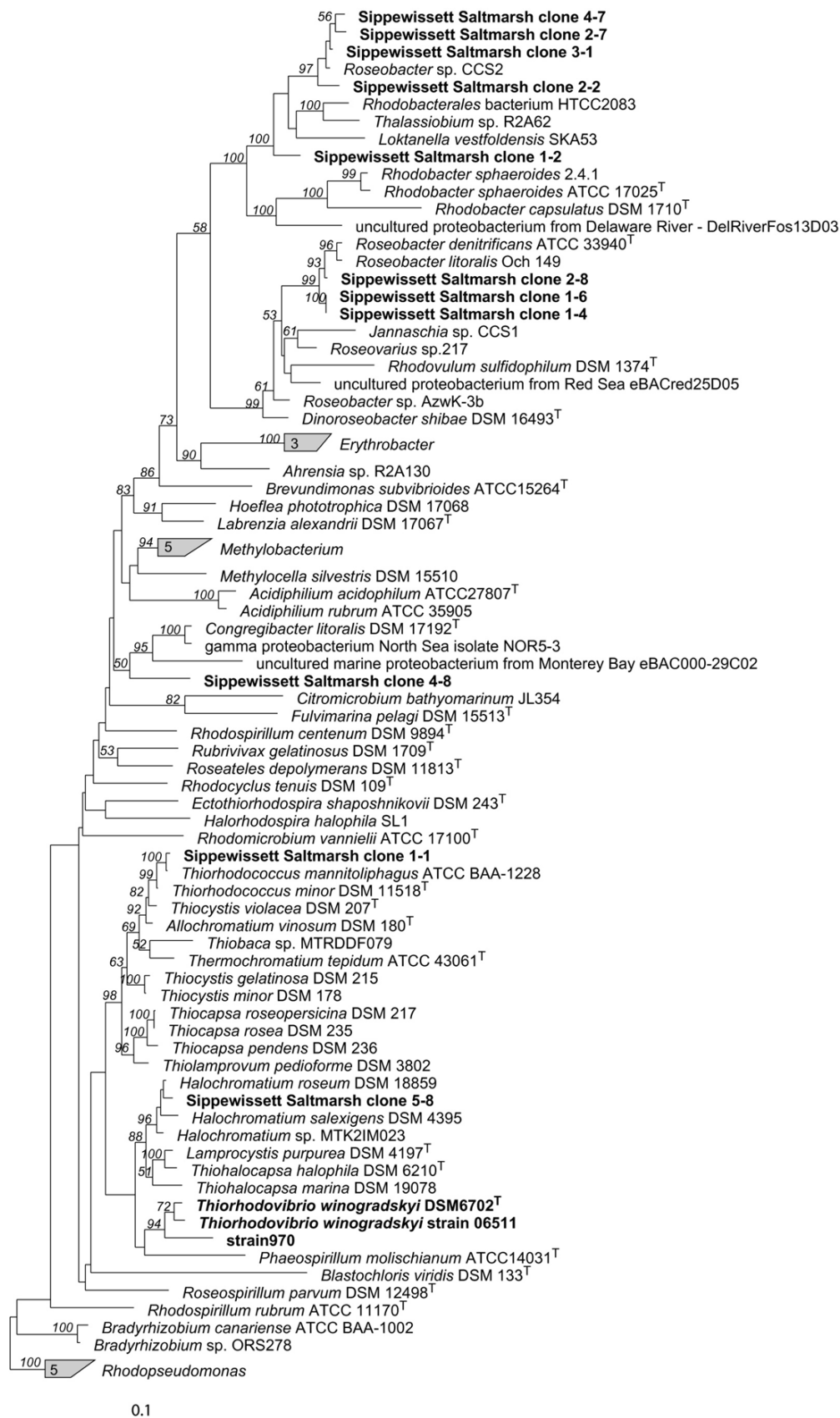


Fig. 14 Phylogenetic tree based on amino acid sequences of LHC1 antenna polypeptides of anoxygenic phototrophic proteobacteria (left) compared to the phylogeny inferred from 16S rRNA gene sequences for the closest relatives of strain 970 (right). Both trees were determined by maximum likelihood analysis. Bootstrap values of 50% or higher are given at the nodes. Bars represent substitutions per site. Strains present in both trees are interconnected with continuous lines, strains investigated in the present paper are shown in boldface. 1st, 2nd, 3rd, denote phylogenetic positions of *pufBA* gene sequences of strains with multiple gene copies.



Results

Fig. 15 (depicted on previous page) Maximum likelihood phylogenetic *pufLM* tree of amino acid sequences from 74 different anoxygenic phototrophic proteobacteria, as well as 11 environmental sequences and 3 cultured sequence types from the present study. Bootstrap values of 50% or higher are given at the nodes. Bars represent substitutions per site. Sequences originating from strains or environmental clone libraries investigated in the present paper are shown in boldface.

The adaptation of *Chlorobiaceae* to growth at low light conditions

Identification and classification of genes unique to the BS1 genome

There are 12 available genome sequences of green sulfur bacteria covering the phylogenetic diversity of this group (Eisen et al., 2002). Therefore, a comparison of the *Chl. phaeobacteroides* BS1 genome to the 11 genomes of the free living relatives was used in order to identify ORFs which are unique to this green sulfur bacterium. Such genes could potentially be involved in the low light adaptation of *Chl. phaeobacteroides* BS1. Pairwise comparisons by *in silico* subtractive hybridization analysis revealed that the BS1 genome contained 740 (compared to *Chl. phaeobacteroides* DSM 266^T) to 1201 (compared to *Chloroherpeton thalassium* ATCC 35110^T) unique genes. When compared to the 11 other green sulfur bacterial genomes as a whole, a total of 331 ORFs were identified to be unique for the *Chl. phaeobacteroides* BS1 (Fig.16, Appendix Table 1).

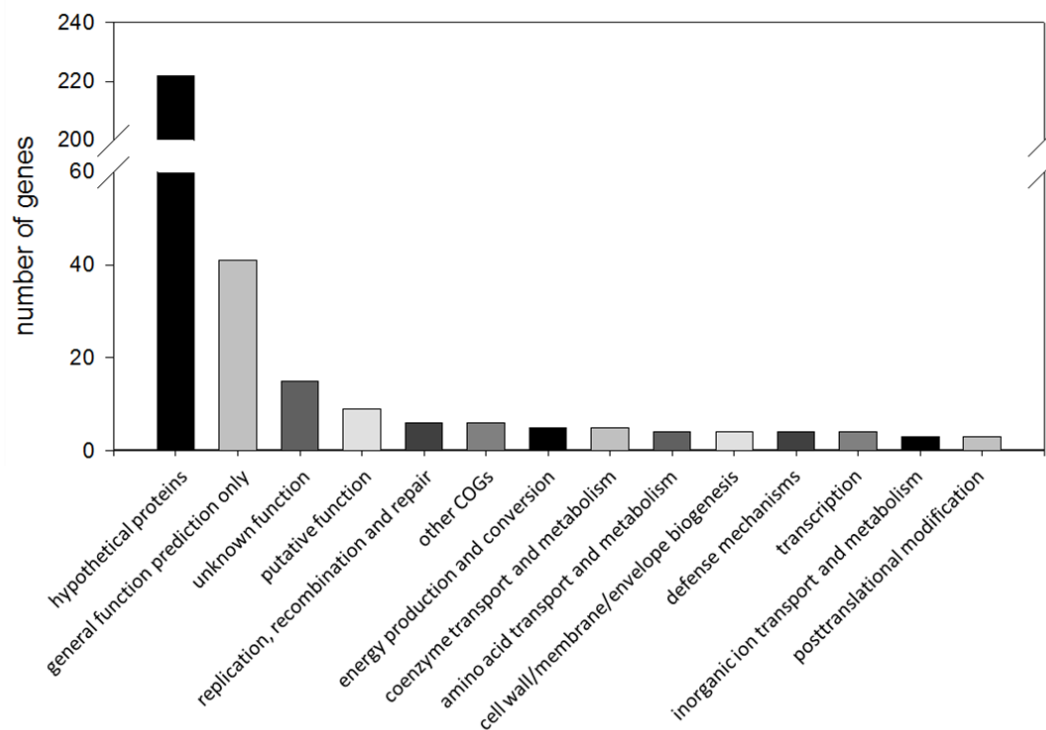


Fig. 16 Distribution of function for the 331 ORFs identified to be unique to *Chl. phaeobacteroides* BS1 when compared to the other 11 green sulfur bacterial genomes

Results

Of these, 222 ORFs code for hypothetical proteins with unknown functions, 41 have general function prediction only, 15 unknown function, 9 putative function, 6 are involved in replication, recombination and repair, 5 in energy production and conversion, 5 in coenzyme transport and metabolism, 4 in amino acid transport and metabolism, 4 in cell wall/membrane/envelope biogenesis, 4 in defense mechanisms, 4 in transcription, 3 in inorganic ion transport and metabolism, 3 in posttranslational modification and 6 fall in other COGs. Among all identified hypothetical proteins there are 69 which are unique in the whole IMG database.

Transcriptional analysis of cultures grown under different light conditions

The differences in the transcriptomes of cultures of *Chl. phaeobacteroides* BS1 grown under low light ($0.15 \mu\text{mol quanta}\cdot\text{m}^{-2}\cdot\text{s}^{-1}$) and high light ($3 \mu\text{mol quanta}\cdot\text{m}^{-2}\cdot\text{s}^{-1}$) conditions were investigated using (i) a prokaryotic cDNA suppression subtractive hybridization (cDNA-SSH) technique and (ii) whole transcriptome analyses based on Illumina sequencing.

Suppression subtraction hybridization.

Through the analysis by cDNA-SSH, differentially expressed transcripts in the investigated sample called “tester” are detected through specific amplification. Transcripts which show no regulation are suppressed through the addition of an excess of cDNA from the second condition called “driver”. Two experiments were conducted where cDNA from high light cultures (tester) were subtracted from cDNA from low light cultures (driver) and vice versa. Amplificates resulting from both experiments were tested against unsubtracted amplificates by gel electrophoresis (Fig. 17).

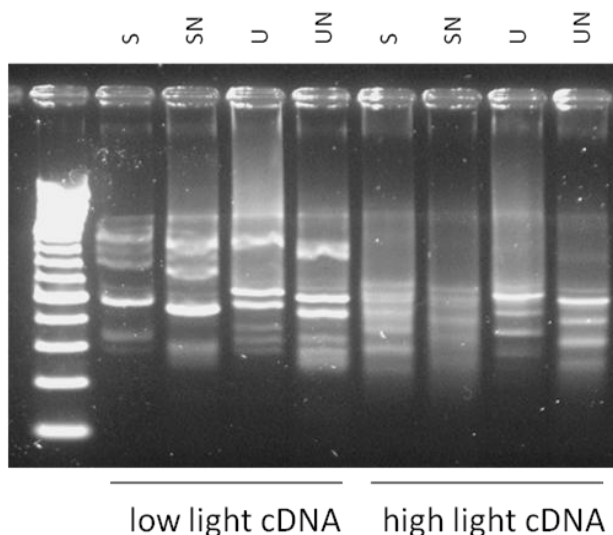


Fig. 17 Amplificates generated by cDNA suppression subtractive hybridization separated through gel electrophoresis. Amplificates from subtracted cDNA are marked with S, amplificates with nested primers are denoted with N and unsubtracted test amplificates are denoted with U. cDNA from the culture which served as “tester” in the SSH experiment are depicted at the bottom.

For subsequent cloning, amplicates from low light cDNA as tester, amplified with nested primers (SN, Fig. 17) and the first amplicates from high light cDNA as tester (S, Fig. 17) were chosen.

A total of 116 clones generated by the subtraction reaction were isolated and their inserts sequenced, of which 58 clones each originated from SSH reactions where cDNA from low light or high light cultures were used as tester, respectively. Eleven of these clones where cDNA from high light cultures served as tester were affiliated with *Chl. phaeobacteroides* BS1 non-ribosomal transcripts (Table 3), whereas all other, including all clones with cDNA from low light cultures, contained 16S and mainly 23S rRNA gene fragments of the different bacteria present in the BS1 enrichment cultures. The eleven non-ribosomal transcripts originated from 10 different ORFs and one intergenic region and represent transcripts up regulated under high light conditions. Eight of these genes code for proteins involved in various central metabolic function.

Gene ID	Protein/Product	Function prediction
Cphamn1_0009	Cytochrome c553, sulfite dehydrogenase cytochrome subunit	Electron carrier activity Sulfide oxidation
Cphamn1_0020	dapD, 2,3,4,5-tetrahydropyridine-2,6-carboxylate N-succinyltransferase	Lysine biosynthesis
Cphamn1_0326	korA, 2-oxoglutarate ferredoxin oxidoreductase subunit beta	rTCA cycle/CO ₂ Fixation
Cphamn1_0841	FMO - Protein	LH-complex / Photosynthesis
Cphamn1_1091	Fer4 / 4Fe-4S ferredoxin	Electron carrier activity rTCA cycle/CO ₂ Fixation
Cphamn1_1138	Amt/MEP/RH family protein	Ammonium transporter
Cphamn1_1228	Hypothetical protein	
Cphamn1_2207	chlH / magnesium chelatase subunit H	Bacteriochlorophyll biosynthesis
Cphamn1_2363	Hypothetical protein	
Cphamn1_R0045	tmRNA	Ribosome arrest remediation
Intergenic region	5' to XhoI restriction endonuclease	

Table 3. Differentially transcribed ORFs identified by cDNA subtractive hybridization using cDNA from high light cultures as tester.

Results

Proteins involved in photosynthesis and related pathways are coded by five of the detected genes. While the FMO-protein (Cphamn1_0841) is directly involved in the photosynthetic apparatus another gene, the magnesium chelatase subunit H (Cphamn1_2207) codes for a protein involved in the bacteriochlorophyll biosynthesis. Two other proteins, the oxoglutarate ferredoxin oxidoreductase (Cphamn1_0326, subunit beta) and ferredoxin (Cphamn1_1091) are involved in the reductive citric acid (rTCA) cycle. One cytochrome which is involved in sulfide oxidation (Cphamn1_0009), thus providing the electron donors for photosynthesis is also being up regulated. Other genes being up regulated under high light conditions are involved in the lysine biosynthesis (Cphamn1_0020), ammonium transport (Cphamn1_1138) or in ribosome arrest remediation (Cphamn1_R0045). Two ORFs were identified to code for hypothetical proteins, with Cphamn1_2363 being unique to *Chl. phaeobacteroides* BS1.

Transcriptome sequencing

A first comparative analysis of global transcriptomes of BS1 cultures grown under low light and high light conditions was achieved by Illumina sequencing of cDNA libraries. After removing sequence tags that matched to rRNA, a total of 2,792,174 uniquely matching sequences originating from the high light sample and 3,280,048 uniquely matching sequences from the low light sample were mapped to the *Chl. phaeobacteroides* BS1 genome. Additionally out of 2524 total number of genes (excluding pseudogenes), 81 genes from cultures grown under high light and 85 under low light conditions had zero reads, out of which 70 genes showed no reads in cultures from both conditions of growth. ORFs that had a difference of expression greater than 2σ were considered differentially expressed ($\sigma = 0.35/(0.8+(e^{m^{1.5}})/2)+0.45$, where m is the mean of expression for each ORF). A total of 211 genes were determined to be differentially expressed between cultures grown under high light and low light conditions (Fig.18, Appendix Table 3). Of these, transcripts of 11 genes were only found in low light cultures, whereas transcripts of 12 genes were only detected in the library from high light cultures. These genes were found to code mainly for hypothetical proteins, 5 expressed only in low light together with 6 expressed only in high light and represent extreme examples of differential detection. Other 8 ORF code for several tRNAs (Val, Ser, Pro tRNA in high light and Thr, Leu tRNA in low light) two IS5 family transposases and one non coding RNAs like the ffs signal recognition particle (Cphamn1_R0055).

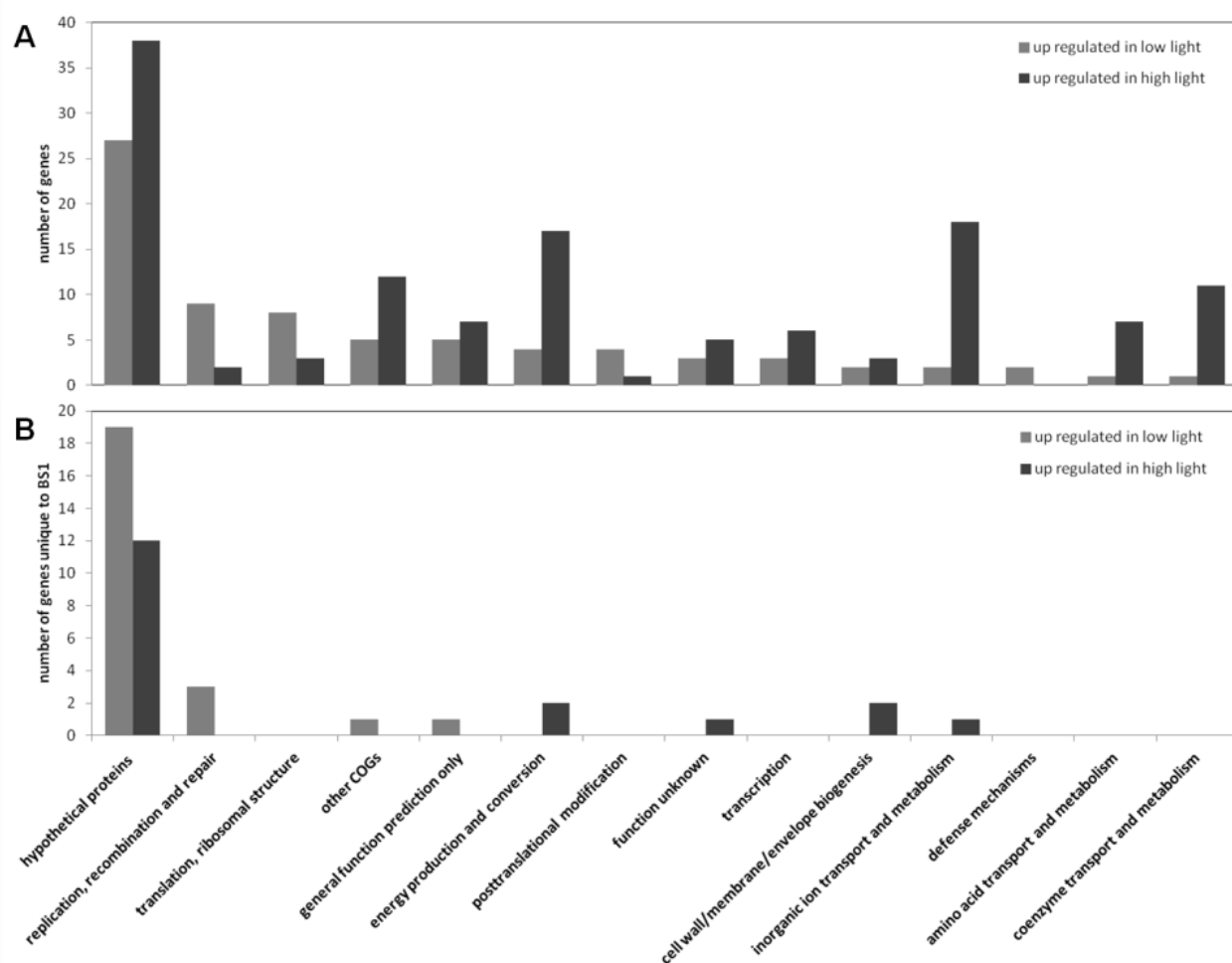


Fig 18. Distribution and function of 211 genes found to be differentially expressed by comparative analysis of global transcriptomes of BS1 cultures grown under low light and high light conditions. (A) Genes higher expressed in cultures grown under low light are depicted in dark grey while genes found to be higher expressed in cultures grown under high light conditions are depicted in grey. (B) ORFs identified to be unique to *Chl. phaeobacteroides* BS1 when compared to the other 11 green sulfur bacterial genomes are depicted in the same colours described above.

Genes up regulated under high light condition. From the 135 genes which are up regulated under high light conditions the most highly regulated are involved in phosphate uptake (Cphamn1_0512, Cphamn1_1229, Cphamn1_1230) or are hypothetical proteins. Among these up regulated genes 18 were found to be unique to BS1, of which 12 are hypothetical proteins with 5 (Cphamn1_0016, Cphamn1_0856, Cphamn1_0914, Cphamn1_0951, Cphamn1_2215) being even unique in the IMG database. The remaining 6 genes have unknown function (Cphamn1_2403), are involved in energy production and conversion like the arsenite oxidase

Results

(Cphamn1_2364 – small subunit, Cphamn1_2365 – large subunit), in cell wall/membrane/envelope biogenesis like the outer membrane efflux protein (Cphamn1_0863) and the efflux transporter (Cphamn1_0864) or in inorganic ion transport like the sodium/hydrogen exchanger (Cphamn1_1652).

Most of the here regulated genes with known function are involved in (i) inorganic ion transport like phosphate uptake (Cphamn1_1229 to Cphamn1_1237) and molybdenum uptake (Cphamn1_0451 to Cphamn1_0453), (ii) energy production and conversion like genes belonging to the nitrogenase coding *nif*-operon (Cphamn1_1748 to Cphamn1_1758) or (iii) coenzyme transport and metabolism like molybdenum cofactor biosynthesis (Cphamn1_2359, Cphamn1_2361, Cphamn1_2362 and Cphamn1_2366) and biotin biosynthesis (Cphamn1_2453 to Cphamn1_2459). In comparison to up regulated genes under low light conditions, more genes involved in inorganic ion transport and metabolism (18 genes vs. 2 genes), energy production and conversion (17 vs. 4) and coenzyme transport and metabolism (11 vs. 1) were highly transcribed under high light conditions. This is surely the case also because under this condition, large clusters of genes are being transcriptionally regulated, which obviously is not the case for the low light condition. Some of the ORFs identified by cDNA-SSH were again determined as up regulated under high light condition including a gene coding for a cytochrome c class I protein (Cphamn1_0009), an ammonium transporter (Cphamn1_1138) and the two hypothetical proteins (Cphamn1_1228 and Cphamn1_2363).

Genes up regulated under low light condition. A total number of 76 genes were found to be up regulated under low light conditions. Over one third (35.5%) of these genes code for hypothetical proteins (27 genes), with 19 of them being unique to BS1 and 6 (Cphamn1_0191, Cphamn1_0915, Cphamn1_1141, Cphamn1_1468, Cphamn1_1897 and Cphamn1_2005) also unique in the IMG database. From genes with known function the majority are involved in (i) replication, recombination and repair like endo- and excinucleases (Cphamn1_1984, Cphamn1_1412) or transposases (Cphamn1_0494, Cphamn1_1363, Cphamn1_1382, Cphamn1_2371, Cphamn1_2434) or (ii) translation and ribosomal structure like tRNAs (Cphamn1_R0001, Cphamn1_R0020, Cphamn1_R0021, Cphamn1_R0027, Cphamn1_R0033, Cphamn1_R0036) or ribosomal proteins (Cphamn1_0975, Cphamn1_1934). Also represented and of major interest are genes involved in (i) energy production and conversion like two

cytochromes (Cphamn1_2425, Cphamn1_2426) and a membrane bound proton translocating pyrophosphatase (Cphamn1_1101), (ii) posttranslational modification like heat shock proteins and chaperones (Cphamn1_0783, Cphamn1_1706, Cphamn1_1707) or a peroxiredoxin (Cphamn1_0848) and (iii) transcriptional regulation (Cphamn1_1095, Cphamn1_1366, Cphamn1_1637). In comparison to up regulated genes under high light conditions, more genes involved in replication, recombination and repair (9 genes vs. 2 genes) and translation and ribosomal structure (8 vs. 3) were highly transcribed under low light conditions. Interestingly 11 out of the 20 highest up regulated genes are unique for BS1 and 4 of them even unique in the IMG database. The occurrence of Cphamn1_2207 coding for a magnesium chelatase subunit H in the group of up regulated genes under low light conditions is contradictory to the cDNA-SSH results, but represents the gene with the lowest difference in expression in this group.

Only some genes are found to be closely located on the chromosome like two hypothetical proteins and a gene coding for a dinitrogenase iron-molybdenum cofactor biosynthesis protein of unknown function (Cphamn1_1075 to 1077) and also the two genes coding for a cytochrome B561 and a cytochrome c family protein (Cphamn1_2425, Cphamn1_2426). These two cytochromes, of which cytochrome B561 is closely related to phsC (thiosulfate reductase cytochrome b subunit) are always clustered in the genomes of 7 other *Chlorobi* (*Prosthecochloris aestuarii* DSM 271^T, *Chl. clathratiforme* DSM 5477^T, *Chl. luteolum* DSM 273^T, *Chl. phaeovibrioides* DSM 265, *Cba. parvum* NCIB 8327, *Chl. limicola* DSM 245^T and *Chl. phaeobacteroides* DSM 266^T) and several other bacterial strains belonging mainly to the group of sulfate reducers like the genera *Desulfovibrio* and *Desulfatibacillum*, or to phototrophic sulphur bacteria like *Allochromatium vinosum* DSM 180 and *Halorhodospira halophila* DSM 244. In *Chl. vibrioforme* and *Chl. luteolum* these genes are also clustered with a gene closely related to hppA membrane bound proton translocating pyrophosphatase (Cphamn1_1101) which is also upregulated under low light conditions in *Chl. phaeobacteroides* BS1. This inorganic pyrophosphatase is also present and not clustered with the two cytochromes in the other 5 *Chlorobi* and several other bacteria. The two other genes (phsA and B) present in the phs operon of *Salmonella typhimurium* are not present in either of the *Chlorobi* genomes.

Results

Genes highly transcribed under low light condition. When grown under low light condition, BS1 cultures still sustains a large amount of transcripts with the gene coding bacteriochlorophyll C binding protein (Cphamn1_2195) being the most transcribed (Suppl. Table 4). Among the 50 genes showing the highest transcript abundance there are genes involved in (i) chlorosome structure and photosynthesis like the chlorosome envelope protein (Cphamn1_0265), the photosystem P840 reaction center cytochrome c-551 (Cphamn1_0578) the bacteriochlorophyll *a* protein (Cphamn1_0841) and the bacteriochlorophyll *c* binding protein (Cphamn1_2195), or (ii) ribosomal structure (Cphamn1_2272, Cphamn1_2273, Cphamn1_2279, Cphamn1_2283, Cphamn1_R0006), or (iii) transcriptional regulation (Cphamn1_0720, Cphamn1_1366, Cphamn1_1367) and (iv) posttranslational modification (Cphamn1_0414, Cphamn1_0782, Cphamn1_2210). There are also 20 hypothetical proteins, 8 of them being unique to BS1 and two (Cphamn1_0719 and Cphamn1_0892) being unique in the IMG database. Only 5 genes of these 50 are significantly different transcribed, while two genes (Cphamn1_0841 and Cphamn1_R0006) were identified by cDNA-SSH but not by transcriptome sequencing.

Characterization of *Chlorobiaceae* from the chemocline of Lake Faro

The distribution of green sulfur bacteria found in the chemocline of Lake Faro was assessed through GSB specific 16S rRNA PCR amplification of DNA isolated from samples taken on several occasions in 2008 (Fig. 19 A). Several individual bands showing different melting types could be identified by DGGE. Four distinct bands were reamplified using the same GSB specific primers and sequenced. The sequence information of these short fragments revealed the presence of three different *Chlorobiaceae* species.

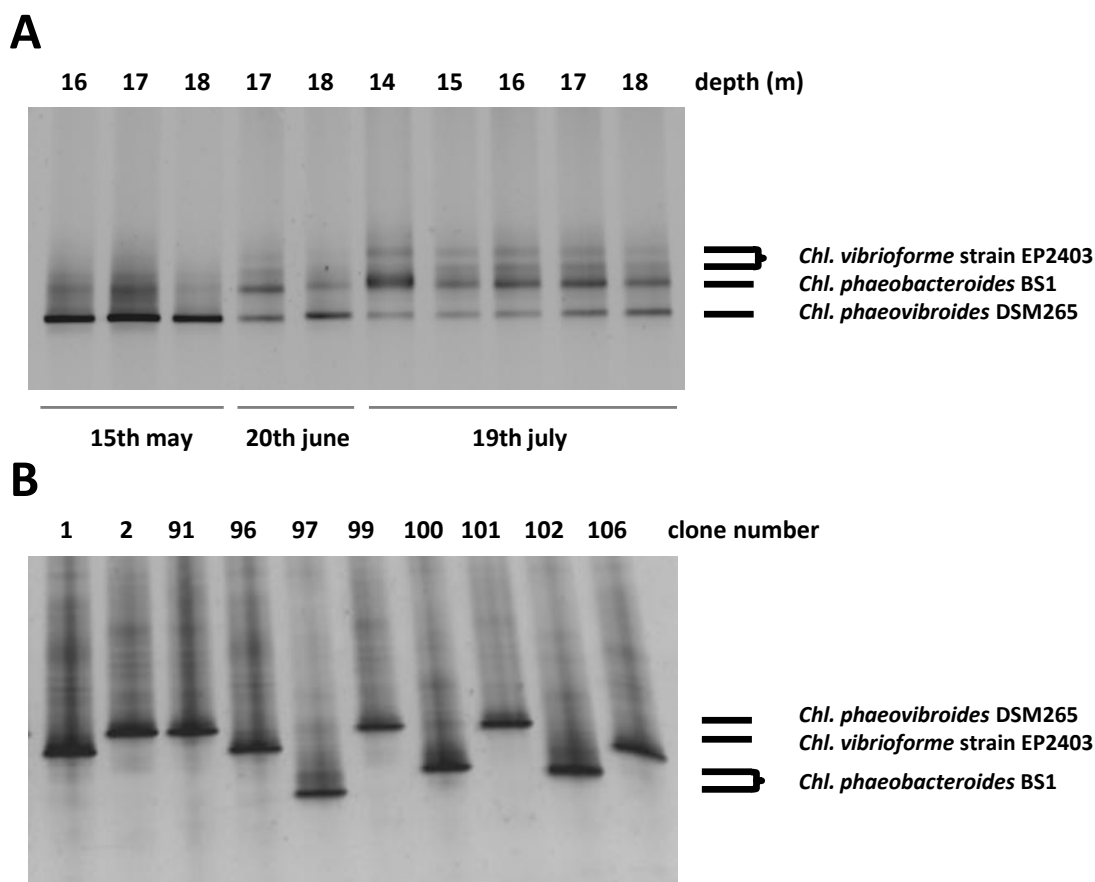


Fig.19. DGGE of 16S rRNA fragments amplified from: **A** environmental DNA with GSB specific primers (341f/GSB822r) and **B** cloned 16S and ITS fragments reamplified with universal primers (341f/907r). Sample depth and clone number are indicated on top of the respective image. Sampling dates are indicated at the bottom of the first image. Identity of individual bands was assessed through sequencing and are indicated on the right.

Results

The nucleotide sequence retrieved from the upper two bands was identical although showing slightly different melting type. Both 0.5 kb long fragments showed high similarity to *Chl. vibrioforme* (93% and 86% respectively) The more prominent middle band showed high similarity to *Chl. phaeobacteroides* BS1 (73%) while the lowermost band was identical to the sequence from *Chl. phaeovibroides* DSM 265. In the sample taken in May, *Chl. phaeovibroides* DSM 265 was the predominant green sulfur bacterium in the chemocline of Lake Faro. This distribution changes in the samples taken in June and July, where *Chl. phaeobacteroides* BS1 can also be detected with a strong presence in all investigated layers of the chemocline. The most striking changes can therefore be seen between samples taken at different times but not at different depths of the chemocline.

For more detailed information about the identity of the green sulfur bacteria present in the chemocline of Lake Faro, genomic fragments containing information of 16S rRNA gene and ITS were amplified and cloned. Screening of 106 individual clones led to the identification of 30 clones bearing sequence information related to green sulfur bacteria. DGGE analyses of these clones revealed 4 different melting types (Fig. 19B) which were identified through sequencing as *Chl. vibrioforme* EP2403 (eg. clone 1 and 96, Fig 19 B), *Chl. phaeovibroides* DSM 265 (eg. clone 2, 91, 99 and 101, Fig 19 B) and *Chl. phaeobacteroides* BS1 (eg. clone 97, 100 and 102, Fig 19B). All 6 clones containing sequence information most related to *Chl. phaeobacteroides* BS1 were sequenced showing 100% identity of 16S rRNA gene region. Only in the ITS region mutational changes were observed, with the occurrence of two distinct types. All clones showed three A↔G transitional mutations (Faro clone type 2, Fig. 20) and only one clone was bearing additional 2 A→G transitions (Faro clone type 1, Fig 20). In order to investigate how the two populations of *Chl. phaeobacteroides* BS1 present in the Black Sea and Lake Faro can be linked, fossil DNA retrieved from sediments of the Mediterranean Sea was also used as comparison (see next chapter).

Fig. 20 Nucleotide sequence from the genome of *Chl. phaeobacteroides* BS1 displaying the ITS region situated between 16S rRNA and 23S rRNA, which was amplified from DNA originating from the Faro chemocline and from fossil DNA fragments originating from Mediterranean Sea sediment samples (see next chapter). Transitional mutations are displayed shaded in black. Sequences of 16S rRNA (Cphamn_R0008), 23S rRNA (Cphamn_R0011), ileucine tRNA (Cphamn_R0009), and alanine tRNA (Cphamn_R0010) are underlined with names indicated above.

		<u>16S rRNA</u>				
BS1		<u>TGGATCACCT</u>	<u>CCTTTTAGTG</u>	<u>GAGATTGACT</u>	<u>GTCAGAAATG</u>	<u>GCAGGACAAG</u>
Faro clone type1		<u>TGGATCACCT</u>	<u>CCTTTTAGTG</u>	<u>GAGATTGACT</u>	<u>GTCAGAGATG</u>	<u>GCAGGACAAG</u>
Faro clone type2		<u>TGGATCACCT</u>	<u>CCTTTTAGTG</u>	<u>GAGATTGACT</u>	<u>GTCAGAAATG</u>	<u>GCAGGACAAG</u>
567-S5 clone1		<u>TGGATCACCT</u>	<u>CCTTTTAGTG</u>	<u>GAGATTGACT</u>	<u>GTCAGAAATG</u>	<u>GCAGGACAAG</u>
599-S1 clone5		<u>TGGATCACCT</u>	<u>CCTTTTAGTG</u>	<u>GAGATTGACT</u>	<u>GTCAGAAATG</u>	<u>GCAGGACAAG</u>
599-S1 clone6		<u>TGGATCACCT</u>	<u>CCTTTTAGTG</u>	<u>GAGATTGACT</u>	<u>GTCAGAAATG</u>	<u>GCAGGACAAG</u>
BS1		<u>CTCAAAGAGT</u>	<u>AATGGTCCGG</u>	<u>TTATCAGGCT</u>	<u>TTGGCGTTCA</u>	<u>TGATGCAACA</u>
Faro clone type1		<u>CTCAAAGAGT</u>	<u>AGTGATCCGG</u>	<u>TTATCAGGCT</u>	<u>TTGGCGTTCA</u>	<u>TGATGCAACA</u>
Faro clone type2		<u>CTCAAAGAGT</u>	<u>AGTGATCCGG</u>	<u>TTATCAGGCT</u>	<u>TTGGCGTTCA</u>	<u>TGATGCAACA</u>
567-S5 clone1		<u>CTCAAAGAGT</u>	<u>AATGGTCCGG</u>	<u>TTATCAGGCT</u>	<u>TTGGCGTTCA</u>	<u>TGATGCAACA</u>
599-S1 clone5		<u>CTCAAAGAGT</u>	<u>AATGGTCCGG</u>	<u>TTATCAGGCT</u>	<u>TTGGCGTTCA</u>	<u>TGATGCAACA</u>
599-S1 clone6		<u>CTCAAAGAGT</u>	<u>AATGGTCCGG</u>	<u>TTATCAGGCT</u>	<u>TTGGCGTTCA</u>	<u>TGATGCAACA</u>
BS1		<u>TTATTATTGC</u>	<u>TCACAAGGCG</u>	<u>ATAAGAAATT</u>	<u>TATTTGTGGA</u>	<u>AGTGGATTGG</u>
Faro clone type1		<u>TTATTATTGC</u>	<u>TCACAAGGCG</u>	<u>ATAAGAAATT</u>	<u>TATTTGTGGA</u>	<u>AGTGGATTGG</u>
Faro clone type2		<u>TTATTATTGC</u>	<u>TCACAAGGCG</u>	<u>ATAAGAAATT</u>	<u>TATTTGTGGA</u>	<u>AGTGGATTAG</u>
567-S5 clone1		<u>TTATTATTGC</u>	<u>TCACAAGGCG</u>	<u>ATAAGAAATT</u>	<u>TATTTGTGGA</u>	<u>AGTGGATTGG</u>
599-S1 clone5		<u>TTATTATTGC</u>	<u>TCACAAGGCG</u>	<u>ATAAGAAATT</u>	<u>TATTTGTGGA</u>	<u>AGTGGATTGG</u>
599-S1 clone6		<u>TTATTATTGC</u>	<u>TCACAAGGCG</u>	<u>ATAAGAAATT</u>	<u>TATTTGTGGA</u>	<u>AGTGGATTGG</u>
		<u>tRNA-Ile -></u>				
BS1		<u>GAAACCCTGA</u>	<u>TTCGCTGGCC</u>	<u>CTGCTCGAAC</u>	<u>CGGGCCTGTA</u>	<u>GCTCAGTTGG</u>
Faro clone type1		<u>GAAACCCTGA</u>	<u>TTCGCTGGCC</u>	<u>CTGCTCGAAC</u>	<u>CGGGCCTGTA</u>	<u>GCTCAGTTGG</u>
Faro clone type2		<u>GAAACCCTGA</u>	<u>TTCGCTGGCC</u>	<u>CTGCTCGAAC</u>	<u>CGGGCCTGTA</u>	<u>GCTCAGTTGG</u>
567-S5 clone1		<u>A</u> <u>GAAACCCTGA</u>	<u>TTCGCTGGCC</u>	<u>CTGCTCGAAC</u>	<u>CGGGCCTGTA</u>	<u>GCTCAGTTGG</u>
599-S1 clone5		<u>GAAACCCTGA</u>	<u>TTCGCTGGCC</u>	<u>CTGCTCGAAC</u>	<u>CGGGCCTGTA</u>	<u>GCTCAGTTGG</u>
599-S1 clone6		<u>GAAACCCTGA</u>	<u>TTCGCTGGCC</u>	<u>CTGCTCGAAC</u>	<u>CGGGCCTGTA</u>	<u>GCTCAGTTGG</u>
BS1		<u>TTAGAGCGCA</u>	<u>CGCCTGATAA</u>	<u>GCGTGAGGTC</u>	<u>AGTGGTTCAA</u>	<u>CTCCACTCAG</u>
Faro clone type1		<u>TTAGAGCGCA</u>	<u>CGCCTGATAA</u>	<u>GCGTGAGGTC</u>	<u>AGTGGTTCAA</u>	<u>CTCCACTCAG</u>
Faro clone type2		<u>TTAGAGCGCA</u>	<u>CGCCTGATAA</u>	<u>GCGTGAGGTC</u>	<u>AGTGGTTCAA</u>	<u>CTCCACTCAG</u>
567-S5 clone1		<u>T</u> <u>C</u> <u>A</u> <u>G</u> <u>A</u> <u>G</u> <u>A</u> <u>G</u> <u>C</u> <u>G</u> <u>C</u> <u>A</u>	<u>CGCCTGATAA</u>	<u>GCGTGAGGTC</u>	<u>AGTGGTTCAA</u>	<u>CTCCACTCAG</u>
599-S1 clone5		<u>TTAG</u> <u>C</u> <u>G</u> <u>C</u> <u>G</u> <u>C</u> <u>A</u>	<u>CGCCTGATAA</u>	<u>GCGTGAGGTC</u>	<u>AGTGGTTCAA</u>	<u>CTCCACTCAG</u>
599-S1 clone6		<u>TTAGAGCGCA</u>	<u>CGCCTGATAA</u>	<u>GCGTGAGGTC</u>	<u>AGTGGTTCAA</u>	<u>CTCCACTCAG</u>
		<u>tRNA-Ala -></u>				
BS1		<u>GCCCACTAAC</u>	<u>AGTTAAAGGC</u>	<u>GCGTAAGAGG</u>	<u>CTGAATTGTT</u>	<u>ATTGGGGCTT</u>
Faro clone type1		<u>GCCCACTAAC</u>	<u>AGTTAAAGGC</u>	<u>GCGTAAGAGG</u>	<u>CTGAATTGTT</u>	<u>ATTGGGGCTT</u>
Faro clone type2		<u>GCCCACTAAC</u>	<u>AGTTAAAGGC</u>	<u>GCGTAAGAGG</u>	<u>CTGAATTGTT</u>	<u>ATTGGGGCTT</u>
567-S5 clone1		<u>GCCCACTAAC</u>	<u>AGTTAAAGGC</u>	<u>GCGTAAGAGG</u>	<u>CTGAATTGTT</u>	<u>ATTGGGGCTT</u>
599-S1 clone5		<u>GCCCACTAAC</u>	<u>AGTTAAAGGC</u>	<u>GCGTAAGAGG</u>	<u>CTGAATTGTT</u>	<u>ATTGGGGCTT</u>
599-S1 clone6		<u>GCCCACTAAC</u>	<u>AGTTAAAGGC</u>	<u>GCGTAAGAGG</u>	<u>CTGAATTGTT</u>	<u>ATTGGGGCCT</u>

Results

Fig. 20 continued

BS1	<u>TAGCTCAGTT</u>	<u>GGTAGAGCGC</u>	<u>CTGCTTTGCA</u>	<u>AGCAGGAGGT</u>	<u>CAACGGTTCG</u>
Faro clone type1	<u>TAGCTCAGTT</u>	<u>GGTAGAGCGC</u>	<u>CTGCTTTGCA</u>	<u>AGCAGGAGGT</u>	<u>CAACGGTTCG</u>
Faro clone type2	<u>TAGCTCAGTT</u>	<u>GGTAGAGCGC</u>	<u>CTGCTTTGCA</u>	<u>AGCAGGAGGT</u>	<u>CAACGGTTCG</u>
567-S5 clone1	<u>TAGCTCAGTT</u>	<u>GGTAGAGCGC</u>	<u>CTGCTTTGCA</u>	<u>AGCAGGAGGT</u>	<u>CAACGGTTCG</u>
599-S1 clone5	<u>TAGCTCAGTT</u>	<u>GGTAGAGCGC</u>	<u>CTGCTTTGCA</u>	<u>AGCAGGAGGT</u>	<u>CAACGGTTCG</u>
599-S1 clone6	<u>TAGCTCAGTT</u>	<u>GGTAGAGCGC</u>	<u>CTGCTTTGCA</u>	<u>AGCAGGAGGT</u>	<u>CAACGGTTCG</u>
BS1	<u>ACCCCGTTAA</u>	<u>GCTCCACACA</u>	<u>CGAAAATAGA</u>	<u>CGTGTAAGCA</u>	<u>CTGAAAGGTG</u>
Faro clone type1	<u>ACCCCGTTAA</u>	<u>GCTCCACACA</u>	<u>CGAAAATAGA</u>	<u>CGTGTAAGCA</u>	<u>CTGAAAGGTG</u>
Faro clone type2	<u>ACCCCGTTAA</u>	<u>GCTCCACACA</u>	<u>CGAAAATAGA</u>	<u>CGTGTAAGCA</u>	<u>CTGAAAGGTG</u>
567-S5 clone1	<u>ACCCCGTTAA</u>	<u>GCTCCACACA</u>	<u>CGAAAATAGA</u>	<u>CGTGTAAGCA</u>	<u>CTGAAAGGTG</u>
599-S1 clone5	<u>ACCCCGTTAA</u>	<u>GCTCCACACA</u>	<u>CGAAAATAGA</u>	<u>CGTGTAAGCA</u>	<u>CTGAAAGGTG</u>
599-S1 clone6	<u>ACCCCGTTAA</u>	<u>GCTCCACACA</u>	<u>CGAAAATAGA</u>	<u>CGTGTAAGCA</u>	<u>CTGAAAGGTG</u>
BS1	<u>CATGTTATTT</u>	<u>GACATAGCTG</u>	<u>GTAAGAATGA</u>	<u>AATGCAAAAAG</u>	<u>CATTTAACGG</u>
Faro clone type1	<u>CATGTTATTT</u>	<u>GACATAGCTG</u>	<u>GTAAGAATGA</u>	<u>AATGCAAAAAG</u>	<u>CATTTAACGG</u>
Faro clone type2	<u>CATGTTATTT</u>	<u>GACATAGCTG</u>	<u>GTAAGAATGA</u>	<u>AATGCAAAAAG</u>	<u>CATTTAACGG</u>
567-S5 clone1	<u>CATGTTATTT</u>	<u>GACATAGCTG</u>	<u>GTAAGAATGA</u>	<u>AATGCAAAAAG</u>	<u>CATTTAACGG</u>
599-S1 clone5	<u>CATGTTATTT</u>	<u>GACATAGCTG</u>	<u>GTAAGAATGA</u>	<u>AATGCAAAAAG</u>	<u>CATTTAACGG</u>
599-S1 clone6	<u>CATGTTATTT</u>	<u>GACATAGCTG</u>	<u>GTAAGAATGA</u>	<u>AATGCAAAAAG</u>	<u>CATTTAACGG</u>
BS1	<u>AAAAGTTCTT</u>	<u>AGTGAACATA</u>	<u>TAAACTTTCC</u>	<u>TGTTGATGTG</u>	<u>AGTGATACTC</u>
Faro clone type1	<u>AAAAGTTCTT</u>	<u>AGTGAACATA</u>	<u>TAAACTTTCC</u>	<u>TGTTGATGTG</u>	<u>AGTGATACTC</u>
Faro clone type2	<u>AAAAGTTCTT</u>	<u>AGTGAACATA</u>	<u>TAAACTTTCC</u>	<u>TGTTGATGTG</u>	<u>AGTGATACTC</u>
567-S5 clone1	<u>AAAAGTTCTT</u>	<u>AGTGAACATA</u>	<u>TAAACTTTCC</u>	<u>TGTTGATGTG</u>	<u>AGTGATACTC</u>
599-S1 clone5	<u>AAAAGTTCTT</u>	<u>AGTGAACATA</u>	<u>TAAACTTTCC</u>	<u>TGTTGATGTG</u>	<u>AGTGATACTC</u>
599-S1 clone6	<u>AAAAGTTCTT</u>	<u>AGTGAACATA</u>	<u>TAAACTTTCC</u>	<u>TGTTGATGTG</u>	<u>AGTGATACTC</u>
23S rRNA ->					
BS1	<u>ATCAATAATA</u>	<u>GGTTTTTTGG</u>	<u>TTAAGTTACT</u>	<u>AAGGGCGTAC</u>	
Faro clone type1	<u>ATCAATAATA</u>	<u>GGTTTTTTGG</u>	<u>TTAAGTTACT</u>	<u>AAGGGCGTAC</u>	
Faro clone type2	<u>ATCAATAATA</u>	<u>GGTTTTTTGG</u>	<u>TTAAGTTACT</u>	<u>AAGGGCGTAC</u>	
567-S5 clone1	<u>ATCAATAATA</u>	<u>GGTTTTTTGG</u>	<u>TTAAGTTACT</u>	<u>AAGGGCGTAC</u>	
599-S1 clone5	<u>ATCAATAATA</u>	<u>GGTTTTTTGG</u>	<u>TTAAGTTACT</u>	<u>AAGGGCGTAC</u>	
599-S1 clone6	<u>ATCAATAATA</u>	<u>GGTTTTTTGG</u>	<u>TTAAGTTACT</u>	<u>AAGGGCGTAC</u>	

Distribution of molecular markers in sediments

The concentration of the carotenoid isorenieratene was measured in sediment samples from different locations in the Black Sea and Mediterranean Sea (Fig. 21, Table 4). Samples from the Eastern Mediterranean Sea were taken from the sediment surface layer (Z0) or the corresponding sapropel layers (S1, S4 and S5) from sediment cores from various locations mainly in the Aegean Sea. These sapropel layers were previously described and represent layers of sediment which was deposited under anoxic conditions 8,000 (S1), 124,000 (S4) and 176,000 (S5) years ago (Emeis K.-C. et al., 2000).

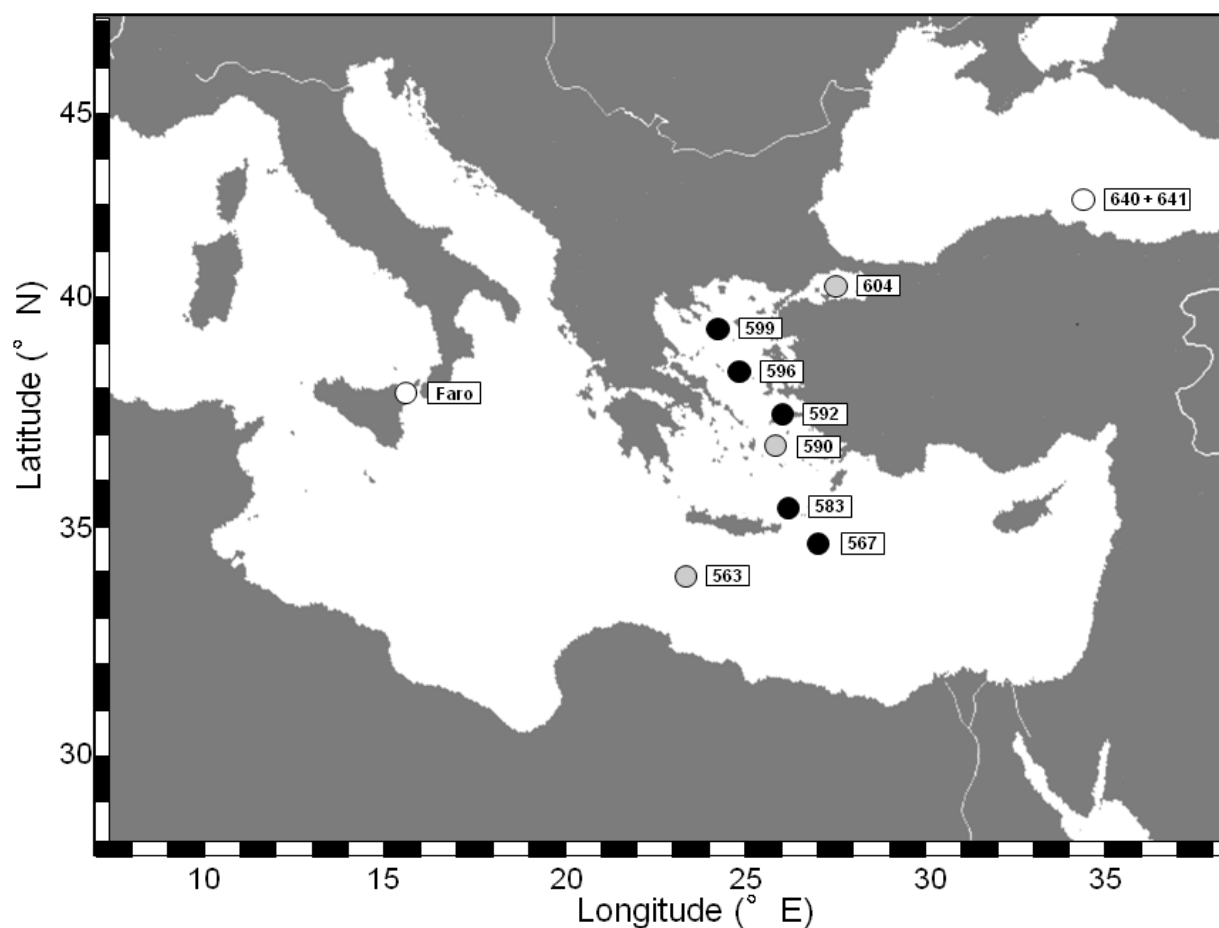


Fig. 21 Geographic map of the eastern Mediterranean basin and the Black Sea. Locations where sediment samples contained isorenieratene and BS1 fossil DNA are depicted with black circles; locations where sediment samples contained only isorenieratene are depicted with grey circles; current locations where *Chl. phaeobacteroides* BS1 was identified in the chemocline are depicted with white circles.

Sample Name	Station	Position	Water depth m	Sapropel name	Multicorer	Gravity corer (cm below top)	Isorenieratene		DNA	
							Average ng (g sediment) ⁻¹	SIdev ng (g sediment) ⁻¹	BS1DNA %	totalDNA ng (g sediment) ⁻¹
Mediterranean Sea										
563-S1	563	33°43.07'N 23°29.97'E	1878	S1	21-24		343.21	320.58	n.d.	
567-Z0	567	34°48.83'N 27°16.97'E	2154	Z0		0-4	21.03	17.70	n.d.	
567-S1				S1		14-24	74.00	10.77	1.82E-04	32.55
567-S4				S4		318-324	180.96	174.17	6.70E-05	39.65
567-S5				S5		404-409	n.a.		1.02E-04	10.80
583-S1	583	35°42.60'N 26°31.49'E	1230	S1		41-58	116.20	7.90	4.96E-05	33.70
590-Z0	590	37°16.46'N 26°11.52'E	581	Z0	0-4		22.88		n.d.	
592-S1	592	37°47.64'N 26°15.85'E	1148	S1		215-230	94.78	1.60	3.04E-05	7.80
596-S1	596	38°57.22'N 24°45.16'E	881	S1		150-160	230.88	144.76	4.64E-04	4.00
599-S1	599	39°45.34'N 24°5.59'E	1359	S1		117-127	63.70	37.36	3.53E-04	15.60
604-Z0	604	40°50.36'N 27°47.28'E	570	Z0	0-4		20.43		n.d.	
604-S1				S1		94-102	302.19	212.79	n.d.	
Black Sea										
641.22-1	641.22	42°13.55'N 36°29.59'E	848		Fluff		767.52		4.34E-02	25714.28
641.22-2					3.5		2164.18	1269.46	4.88E-03	11927.56
641.22-3					6.5		405.54	51.51	3.69E-03	10554.11
641.22-4					19-20		105.90	59.47	n.d.	
641.22-5					43-44		208.59	45.90	n.d.	
640.22-6	640.22	42°13.545'N 36°29.597'E	844			57.5	404.14	313.26	n.d.	
640.22-7						77.5	163.18	44.56	n.d.	
640.22-8						83.5	205.35	155.45	n.d.	
640.22-9						125.5	10.32	13.12	n.d.	
640.22-10c						834-837.5	743.84	143.20	n.d.	

Table 4. (depicted on previous page) Amounts of isorenieratene and DNA concentrations measured in different sediment samples originating from multiple sampling sites in the Black and the Mediterranean Sea.

Samples from the Black Sea originate from two sediment cores taken with a multicorer and a gravity corer from the same location. In all investigated samples isorenieratene was detected (Suppl. Table 5). The distribution of isorenieratene isolated from the sample station 641.22 in the Black Sea shows high amounts of this carotenoid in the recent sediment (Fig. 22). With increasing depth isorenieratene amounts decrease displaying a small peak increase around the depth of 60 cm. In a sample taken at 837 cm depth under sediment surface, where the EEM Sapropel is situated (equivalent to sapropel S5 described above), high amounts of isorenieratene could also be detected. In the other samples from the Mediterranean Sea isorenieratene was always present, with higher concentrations in the sapropel layers. In samples taken from the surface of the sediment isorenieratene could also be identified, and although in low amounts, but not less than 20 ng per g sediment.

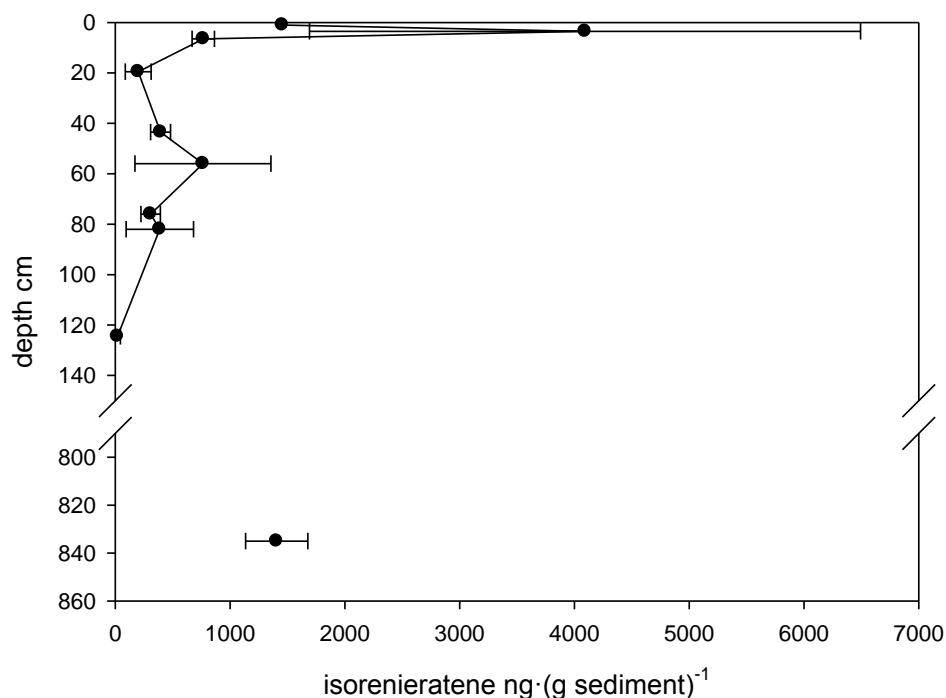


Fig.22. Distribution of isorenieratene in samples taken at different depths of a sediment core at station 641.22 in the Black Sea (Fig. 21, Table 4)

Results

For some samples DNA extracts were also investigated for the occurrence of sequences of *Chl. phaeobacteroides* BS1 and of other species. Using highly specific primers sequences originating from the BS1-genome could be amplified using qPCR. The measured values were first calculated as percentage of DNA amplified with universal primers and corresponding to total extracted DNA also as amount per g sediment. Specific DNA originating from BS1 genome could be detected in the upper segments of the Black Sea sample and in the deep samples from the Mediterranean Sea (Table 4). No BS1 sequences could be amplified from samples originating from recent samples from the Mediterranean Sea. Although higher amounts of both BS1 DNA and isorenieratene were measured in the Black Sea samples, no correlation could be detected between the corresponding values from investigated samples (Fig. 23).

Sequences amplified from the sediments of the Mediterranean Sea samples are covering a region of 386 bp located in the ITS sequence of BS1. Three different sequence types could be identified which harbor changes in the amplified sequence (Fig. 20). Two types contain one single transitional mutation, $A \rightarrow G$ (599-S1 clone 5) and $T \rightarrow C$ (599-S1 clone 6) both found in sequences from sample 599-S1. Another sequence amplified from sample 567-S5 displays two transitional mutations ($G \rightarrow A$ and $T \rightarrow C$). All identified mutations are distributed on different locations on the ITS sequence of *Chl. phaeobacteroides* BS1. These transitions differ in location also when compared to sequences of BS1 retrieved from the chemocline of Lake Faro described in the preceding chapter.

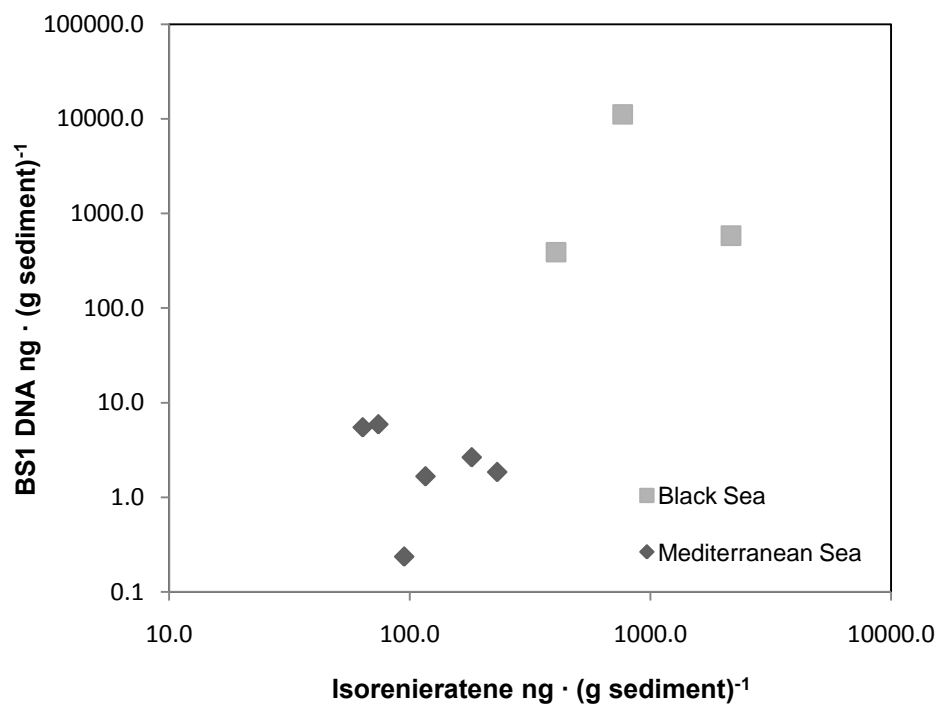


Fig.23. Measured amounts of isorenieratene plotted against corresponding measured amounts of *Chl. phaeobacteroides* BS1 genomic DNA. Samples originating from the Black Sea are depicted as light grey squares and samples originating from the Mediterranean Sea are depicted as grey diamonds. Values are plotted in logarithmic scale.

Distribution of *Chlorobiaceae* in the chemocline of Lake Sakinaw

The distribution of the pigment BChl *e* in samples originating from the chemocline of Lake Sakinaw was investigated (Fig. 24A). Samples taken in May 2008 show a slightly different distribution when compared to samples taken in 2009 (experiments with samples from 2009 were performed by Anne Köhler). The range of Bchl *e* distribution is located deeper with very low amounts above 35m and a peak around 37-38 m. The samples originating from July 2009 display elevated amounts of measured BChl *e* above 34m and peak amounts around 35-36m. In contrast to 2008 less amounts of BChl *e* were detected below 37m. Additionally, light intensity measurements were performed in May 2008 reaching to the depth of 38m below surface (Fig.25). Only minute amounts of light are reaching the chemocline with $0.05 \mu\text{mol quanta m}^{-2} \text{s}^{-1}$ measured at 34 m. At the depth where the BChl *e* peak was detected, the intensity drops to $0.029 \mu\text{mol quanta m}^{-2} \text{s}^{-1}$ at 36 m, while $0.0002 \mu\text{mol quanta m}^{-2} \text{s}^{-1}$ were measured at the depth of 38 m where the BChl *e* concentration reaches its maximum.

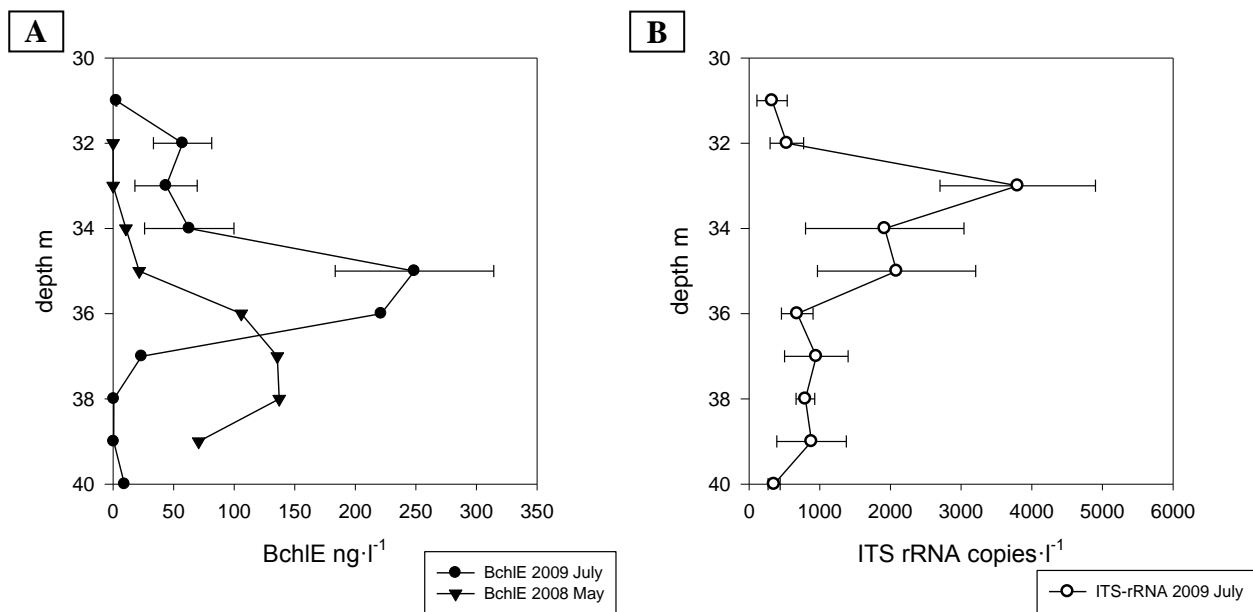


Fig 24. The distribution of BChl *e* measured through HPLC (A) and ITS rRNA from the predominant GSB assessed through RT-qPCR (B) originating from the chemocline of Lake Sakinaw

The activity of the predominant BChl *e* containing green sulfur bacterium found in the chemocline of Lake Sakinaw was assessed through RT-qPCR for samples taken in July 2009 (Fig. 24B). In agreement with the inferred pattern of pigment distribution specific ITS transcripts were detected in all investigated samples. Peak amounts correlating with high activity can be observed at the depth of 33 m with decreasing activity at 34-35m. Regions above 32 m and below 36 m show very low activity patterns. Although BChl *e* concentrations at 33 m are much lower than at deeper depths cells thriving at these depths are more active due to the higher light intensity. These activity patterns show clear correlation with light intensity which drops dramatically when reaching pigment rich layers in the chemocline as shown in measurements from 2008.

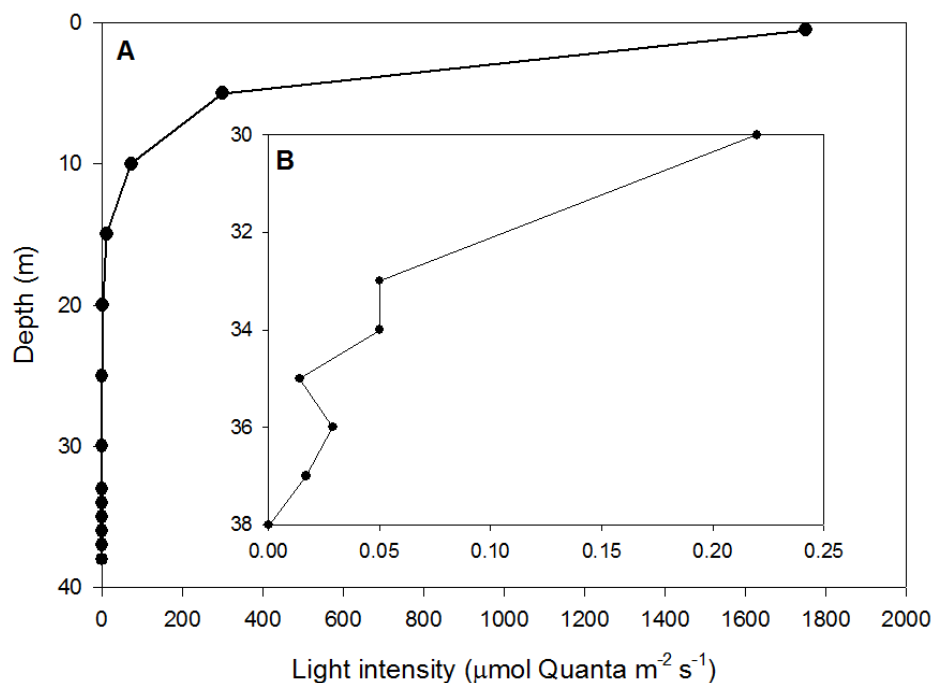


Fig 25. Depth profile of the light intensity distribution measured in the Lake Sakinaw during the sampling session in May 2008 (A). Expand view of light intensities measured below 30 m is shown inserted (B). (E. Gies and T. Beatty, unpublished data)

DISCUSSION

Adaptation of *Chromatiaceae* toward absorption of specific wavelengths of light

Structure of the *puf* operons in strain 970 and *Trv. winogradskyi*

All *puf* operons sequenced in this study follow the arrangement *pufBALMC* common to other purple sulfur bacteria (Tuschak et al., 2005). Like other *Gammaproteobacteria* from the family *Chromatiaceae* such as *Allochromatium vinosum* and *Lamprocystis purpurea* (Tuschak et al., 2005; Yutin and Béjà, 2005), strain 970 has multiple copies of *pufBA*. Instead of the three copies found in these other species, only two copies are present in strain 970, however, and the occurrence of an ORF downstream of *pufA*₂ that is not related to the genes typical for the *puf* operon renders a presence of a third copy of LHC genes unlikely. Accordingly, the *puf* operon structure detected in strain 970 represents a novel type among the anoxygenic phototrophic proteobacteria. In addition, the two *pufA* copies are also unusually long with *pufA*₂ spanning over 261 nt. Because the sequenced part of the *puf* operons of *Trv. winogradskyi* did not extend beyond *pufC*, it remains unclear whether additional *pufBA* copies are present in these two strains. Since a partial sequence of *bchZ* was detected upstream of *pufBA* in both *Trv. winogradskyi* strains, the *puf* genes are likely to be part of a photosynthesis gene cluster as in other purple bacteria (Beja et al., 2002). In contrast no sequence of *bchZ* was detected upstream of *pufBA* in strain 970. No other known bacterial sequence shows such an unusual arrangement of the *puf* operon. In *Citromicrobium bathyomarinum* strain JL354 a second incomplete photosynthetic operon consisting only of *pufLMC* and *pufCBA* genes could be identified by whole-genome sequencing (Jiao et al., 2010). The sequence similarity between the two *pufLM* genes in the same genome is less than 70%. Since no second *pufLM* sequence could be detected in strain 970 it remains unclear how the photosynthesis gene cluster is organized in this bacterium. The investigated sequence resembles a complete *puf* operon and transcriptional analysis with specific primers clearly shows transcriptional activity in photosynthetic active cultures of strain 970.

Transcriptional regulation of the *puf* operon in strain 970

Besides light intensity and oxygen concentrations that affect the transcription of *puf* genes via several repressors and transactivators (Bauer and Bird 1996; Gregor and Klug 1999), the expression of *puf* genes is also regulated via the stability of their mRNA transcripts. With regard to the latter, differential degradation rates of the polycistronic mRNA are caused by intercistronic secondary structures of the transcripts (Rauhut and Klug 1999). In the present study, intercistronic hairpin loop structures were found between *pufA* and *pufL* in all the investigated *puf* operons. Similar structures were previously shown to exert stabilizing effects on the short *pufBA* mRNA segment by protecting it against 3' to 5' exonucleases (Klug et al., 1987; Chen et al., 1988). A significantly longer half life of the *pufB₁A₁* transcript compared to that of the *pufLM* mRNA was previously also determined in strains of *Rhodobacter capsulatus* (Klug et al., 1987; Klug, 1993), where transcripts of *pufB₁A₁* and *pufLM* display half lives of 33 min and 8 min, respectively, which are in the same range as the values determined for strain 970. It is concluded, that the increased stability of the *pufBA* mRNA segment causes a predominance of *pufB₁A₁* transcripts over the *pufLM* mRNA in strain 970. Furthermore, the ratio of the two transcripts doubled under light-limiting conditions. Therefore our results indicate that transcriptional regulation of *puf* genes in strain 970 follows the patterns known for other phototrophic proteobacteria.

So far, the reason for the low abundance of *pufB₂A₂* transcripts remain elusive. No putative sites of transcriptional terminators could be found between the *pufC* and *pufB₂* intercistronic region and only a strong secondary structure downstream of *pufA₂* that is followed by several uracil residues displays features of a described transcriptional terminator for the *puf* operon of *Rhodospirillum rubrum* (Bélangier and Gingras, 1988). This suggests that the additional copies of *pufBA* genes are within the co-transcribed *puf* operon and possibly also the presence of additional destabilizing, yet unrecognized, RNA structures upstream or within the *pufB₂A₂* transcripts. In this context it is noteworthy that the nucleotide sequence of *pufA₂* but not *pufA₁* was found to harbor two consensus sequences that were earlier suggested as recognition sites for *Escherichia coli* RNase E (GAUUU) Fig. 8, (Ehretsmann et al., 1992).

Significance of amino-acid substitutions in the LHC1 polypeptides

The α and β polypeptides of LHC1 encompass a single transmembrane α helical segment with a conserved histidine that ligates the Mg atom of the BChl macrocycle (Zuber and Brunisholz, 1991). Mutational exchange of this residue results in either the complete loss or severely limited expression of LHC1 (Bylina et al., 1988; Olsen et al., 1994, 1997; Davis et al., 1997). Additional interactions between the polypeptide and BChl include hydrogen bonding between the BChl C3¹ acetyl group and α Trp⁺¹¹ or β Trp⁺⁹ (Olsen et al., 1994; Sturgis et al., 1997).

The sequence analysis of the LHC1 polypeptides of strain 970 revealed a conspicuous difference to most or all other known sequence types. The change in polarity of the N- and C-terminal domains framing the membrane spanning α -helices of both LHC1 polypeptides is unlikely to impact the absorption pattern as similar changes are also found in sequences from *Trv. winogradskyi*, *Cfl. aurantiacus* and *Lpc. purpurea*. Furthermore, the C-terminal region of the LHC1 α polypeptide of other phototrophic proteobacteria was shown to be post-translationally processed (Bérard et al., 1986; Wiessner et al., 1990; Nagashima et al., 1994). Therefore differences in the primary structure of this region, which could occur due to the unusual length of LHC1 α polypeptides from strain 970 and a possible interference with the spatial arrangement of the light harvesting complex, may not affect the absorption properties of the resulting complex.

In contrast, the deletion of an amino acid between α His⁰ and α Trp⁺¹¹ is found in only four other species, one of them being *Tch. tepidum* that also exhibits a red shifted Q_y absorption maximum at 915 nm (Madigan, 2003). The formation of a Ca²⁺ binding site in this region of the polypeptide is thought to be responsible for the absorption shift in this bacterium (Kimura et al., 2008). Although *pufA*₁ and *pufA*₂ of strain 970 display this deletion as well, the Q_y red shift cannot be attributed solely to this region, because the same sequence pattern was also determined for the two *Trv. winogradskyi* strains that do not exhibit a red-shifted Q_y absorption. However, sequence analysis of the LHC1 polypeptides from strain 970 identified additional candidate amino acids that may cause the highly specific and extreme red shift of the Q_y band in this bacterium. One striking difference is the α His⁺¹¹ that follows α Trp⁺¹⁰. This substitution combined with the deletion between α His⁰ and α Trp⁺¹¹ directly affects the interaction with the BChl C3¹ acetyl group. Based on our modeling of the strain 970 α -polypeptide an interaction

between αHis^{+11} and BChla is likely. Previous studies showed that the substitution of αTrp^{+11} with a histidine residue in *Rbc. sphaeroides* leads to a slight red shift in the Q_y absorption maximum (Sturgis et al., 1997). We therefore propose that the combination of the replacement and the deletion of one amino acid leads to considerable conformational changes in the LHC1 structure of strain 970 causing the change in the Q_y absorption.

Conspicuously no similarities could be found in the sequence comparison with LHC1 polypeptides isolated previously from *Roseospirillum (Rss.) parvum*, another purple sulfur bacterium displaying a red shifted Q_y absorption maximum at 909 nm (Tuschak et al., 2004). The α -polypeptide from *Rss. parvum* harbors differences at the residues αCys^{+3} , αGly^{+5} and αHis^{+6} found in close proximity to the conserved histidine residue (αHis^0). Additionally, the β -polypeptide shows a unique residue βCys^{-4} and another change at the position βPhe^{+9} . Comparative 3D-models indicate that αCys^{+3} , βCys^{-4} and βPhe^{+9} are in close proximity to the BChla molecule. This comparison shows that effects on the Q_y absorption can result from different positions in the polypeptide sequence.

A sequence position that is exclusively shared between strain 970 and *Tch. tepidum* ATCC43061^T is the residue βTrp^{-8} , which was previously suggested to interact with BChla (Ma et al., 2009). Indeed, our 3-D modeling of the β -polypeptide of strain 970 suggests that the replacement of βPhe^{-8} by βTrp^{-8} results in hydrogen bonding to the acetyl carbonyl of BChla. In combination, the changes involving the residues βTrp^{-8} and αHis^{+11} together with the deletion of one amino acid may explain the red-shift of Q_y in *Tch. tepidum* ATCC43061^T and strain 970 compared to other bacteria including the two strains of *Trv. winogradskyi* and also *Rss. parvum*.

Phylogeny of the unusual LHC1 in strain 970

The phylogenetic analyses indicate a monophyletic origin of the LHC1 polypeptides of strain 970, *Trv. winogradskyi* strains 06511 and DSM6702^T, and *Tch. tepidum* ATCC43061^T. Based on the phylogenetic branching pattern, amino acid substitutions leading to red-shifted Q_y absorption patterns could have accumulated gradually and started with a sequence similar to that found in *Trv. winogradskyi* strains that display common spectral properties. All substitutions present in the LHC1 sequence from *Tch. tepidum* ATCC43061^T could also be found in strain 970. Additional substitutions found solely in strain 970 could then have accumulated and caused the extreme red shift of the Q_y absorption toward 963 nm. In contrast to the *pufBA* phylogeny, our analysis of 16S rRNA gene sequences as well as of *pufLM* sequences clearly indicated a more distant phylogenetic relationship between *Tch. tepidum* ATCC43061^T, and the closely related strain 970 and *Trv. winogradskyi* strains. This might even reflect the different habitat of the moderate thermophile *Tch. tepidum*. Horizontal gene transfer has previously been taken in consideration to explain inconsistencies between phylogenies of *puf* and 16S rRNA gene sequences (Nagashima et al., 1997). Due to the small sizes of the antenna polypeptides, however, such sequence differences might also reflect mere statistical fluctuations (Nagashima et al., 1996). Although *Rss. parvum* displays similar red-shifted Q_y absorption to *Tch. tepidum*, its distant phylogenetic relationship revealed in both analyses emphasizes the parallel evolution of patterns involved in the light harvesting properties of purple sulfur bacteria. Comparative genomics of the *Tch. tepidum* ATCC43061^T, strain 970 and *Trv. winogradskyi* 06511 and DSM6702^T potentially will provide a deeper insight into the origin of the extreme red-shifted light-harvesting complexes of strain 970.

The isolation of new types of anoxygenic phototrophs (such as *Rss. parvum*; Glaeser and Overmann 1999) expressing light-harvesting complexes with absorption maxima above 900 nm suggests that a selection of red-shifted light harvesting complexes has occurred in littoral sediments. This can be attributed to the discontinuous water coverage of these sandy sediments, which in contrast to pelagic habitats leads to an higher amount of far-red and near-infrared light reaching the sediment. Therefore, additional efforts were made to identify new strains exerting red-shifted absorption patterns. The search for new *pufLM* sequences in the diverse habitats of Little Sippewissett Saltmarsh did not yield novel close relatives of strain 970. Most retrieved

sequences (i.e. 8 clone types) clustered with *Roseobacter* species and one clone type with *Congergibacter litoralis* DSM 17192. These proteobacteria are aerobic anoxygenic phototrophs and usually exist in marine habitats, especially in nearshore waters. Another clone type showed close relationship to *Thiorhodococcus mannitoliphagus* ATCC BAA-1228, a *Gammaproteobacterium* initially isolated from an microbial mats located in an estuary on the White Sea coast (Rabold et al., 2006), a similar habitat like the Sippewissett Saltmarsh. The last retrieved sequence is closely related to bacteria belonging to the genus *Halochromatium*, which resembles the halophilic species of the family *Chromatiaceae*. All these isolated sequences represent species with no specific adaptation towards near infrared light absorption, indicating that the adaptation to the 900-1000 nm wavelength region, be it by lateral gene transfer or independent evolution of one lineage, may have occurred only rarely during the evolution of benthic *Chromatiaceae*.

The adaptation of *Chlorobiaceae* to growth at low light conditions

The detection of extreme low light intensities at depths where the green sulfur bacterium *Chl. phaeobacteroides* BS1 was shown to grow with only light as energy source, has led to questions about the molecular properties enabling this adaptation. Previous studies described physiological features like the increased BChl *e* content and the presence of geranyl homologs of BChl *e* (Manske et al., 2005), the extreme low light saturated growth rate (Overmann et al., 1992a) or the low maintenance requirements (Marschall et al., 2010). The fact that cells cultivated at low light intensities resemble increased adaptational features when compared to cells cultivated at high light intensities enables most of these experimental approaches. In order to identify the genetic determinants of this preadaptation, the transcriptomes of cultures grown under these two different light intensities were compared in the present study. Additionally whole genome comparison with the other currently available GSB genomes was used to identify unique features of the BS1 genome.

While the chemocline of the Black Sea represents a unique marine habitat, in some lacustrine environments chemoclines with low light conditions are also present. The identification of another *Chlorobi* strain adapted to low light intensities in the chemocline of Lake Sakinaw herefore opened new perspectives in investigating this trait. First measurements assessed the BChl *e* content, distribution and activity pattern of this newly described bacterium in order to compare the growth conditions in this lake to those of the Black Sea chemocline. Although the chemocline of Lake Faro is not located at great depths, the presence of the same geranyl homologs of BChl *e* as in BS1 was intriguing. The precise description of the green sulfur bacterial community was therefore needed to reveal the possible link to the BS1 strain and also a possible low light adaptation.

The Black Sea, as a well described model for past anoxic environments, enables also the use of BS1 as a precise indicator in the investigation of sediments. The occurrence of the carotenoid isorenieratene, commonly used as molecular marker for anoxic environments, was therefore compared against the occurrence of fossil DNA of BS1 in sediments from the Black Sea and the Mediterranean Sea. For this purpose, sediments which were previously described to have been deposited under anoxic conditions and present sediments were investigated.

Genes up-regulated under high light condition

The imposed light intensity of $3 \mu\text{mol quanta}\cdot\text{m}^{-2}\cdot\text{s}^{-1}$ represents the condition where the culture is light saturated but shows no light inhibition (Manske et al., 2005). This condition was chosen for comparison to low light intensities which resemble the *in-situ* situation in the chemocline. Transcripts highly regulated under this high light intensity reveal which genes are becoming unessential in conditions of low light availability and hereby lead to a more detailed description of the low light adaptation of *Chl. phaeobacteroides* BS1. Many of the high regulated 135 genes are part of major metabolic pathways or are part of an operon and will be discussed as distinctive groups.

Nitrogen fixation. Like many other bacteria BS1 is able to fix nitrogen as a source for biosynthetic needs. Genes involved in the nitrogen fixation are clustered in the *nif*-operon, which is found to be down regulated under low light conditions. The positive transcriptional regulator *nifA* (Cphamn1_1748) together with other 8 genes (Cphamn1_1751-58) of this operon are highly transcribed only under high light availability. Because nitrogen fixation is an high energy demanding process, exact control of its function and expression under limiting energy conditions is mandatory for free living autotrophic bacteria. In most bacteria the presence of oxygen is the major negative regulator for nitrogenase transcription and activity (Schmitz et al., 2002). But a close linkage between nitrogenase regulation and ammonium availability and light intensity could also be detected in the phototrophic purple bacterium *Rhodobacter capsulatus* (Masepohl et al., 2002). Another two nitrogen regulatory proteins P-II (Cphamn1_0108, Cphamn1_1137) are also similarly regulated and interestingly both are co-localized with two genes coding for an ammonium transporter (Cphamn1_0107, Cphamn1_1138). Ammonium is then used in the amidation with glutamate to form glutamine, reaction which is part of the metabolism of nitrogen and is being catalyzed by the enzyme glutamine synthetase (Eisenberg et al., 1987). The genes coding for this enzyme are also found to be up regulated in high light (Cphamn1_0953) together with an transcriptional regulator from the AsnC family, which is an important regulatory system of the amino acid metabolism and related processes (Kumarevel et al., 2008). While hydrogen is produced along with ammonia as a product of nitrogen fixation, hydrogen utilization is typically mediated by uptake hydrogenases that catalyze the oxidation of hydrogen (Rey et al., 2006). The hydrogenase transfers electrons to ferredoxins and cytochromes, thus contributing to the

Discussion

recycling of electrons to nitrogenase (Willison et al., 1983). Therefore the up-regulation of 4 genes coding for the nickel-dependent hydrogenase (Cphamn1_1590-93) can directly be linked to the up regulation of nitrogenase activity. The high number of regulated genes coding for many proteins involved in nitrogen fixation is one of the facts which make this process energy demanding. But more important is the fact that this process also needs reduced ferredoxins, which are more scarcely produced under low light conditions and is first of all needed for the reductive citric acid pathway. A negative control of this energy consuming processes is therefore one of the features *Chl. phaeobacteroides* BS1 is regulating in order to adapt to low light availability.

Molybdenum transport and Mo cofactor biosynthesis. Many enzymes like nitrogenase, sulphite oxidase and arsenite oxidase require cofactors which have incorporated molybdenum in their structure (Schwarz and Mendel, 2006). It is therefore not surprising that together with the regulation of nitrogenase, a simultaneous regulation of its cofactor synthesis and therefore molybdenum transport occurs. Genes responsible for the molybdenum transport are coding for molybdenum and molybdate ABC transporter (Cphamn1_0451, 0453 respectively) and in between these two a gene (Cphamn1_0452) coding for a TOBE domain-containing protein responsible for the recognition of small ligands such as molybdenum were found to be upregulated at high light. Molybdenum cofactor synthesis genes (Cphamn1_2359, 2361, 2362 and 2366) are clustered together with other up regulated genes. Two genes coding for hypothetical proteins are found in close vicinity (Cphamn1_2358 and 2363) with the latter being unique to BS1. In between cofactor synthesis genes there are also two genes coding for the arsenite oxidase small and large subunit (Cphamn1_2364 and 2365), another enzyme requiring molybdate cofactors as mentioned above. These data show clearly that all these genes showing correlations in this metabolic pathway are also correlated in their regulation when being down regulated at light conditions where the energy yield is low.

Phosphate transport. A big cluster of genes (Cphamn1_1225-1237) resembling an operon coding for genes involved in phosphate uptake was found to be similarly regulated. The main genes coding for an ABC type phosphate transporter are present twice in this operon. Two copies of ATP-binding protein PstB (Cphamn1_1231, 1236) are flanking a tandem of inner membrane subunit proteins PstC (Cphamn1_1232, 1234) and PstA (Cphamn1_1233, 1235). Additionally there are two phosphate binding proteins (Cphamn1_1229, 1230) two phosphate uptake

regulators PhoU (Cphamn1_1237, 1238). This genetic assembly can also be found in other bacteria belonging to the *Chlorobi* phylum. Usually these transporters are multicomponent systems typically composed of a periplasmic substrate-binding protein, one or two reciprocally homologous integral inner-membrane proteins and one or two peripheral membrane ATP-binding proteins that couple energy to the active transport system (Ames, 1986). The role of the three 5' flanking hypothetical proteins (Cphamn1_1226, Cphamn1_1227 and Cphamn1_1228) which seem to be co-regulated is unknown and the latter gene was also detected as up-regulated by cDNA-SSH. Homologs of these genes could be identified in three other *Chlorobi* (*Chl. limicola* DSM 245^T, *Chl. phaeobacteroides* DSM 266^T, and *Prosthecochloris aestuarii* DSM 271^T). The last gene found to be cotranscribed with this cluster is coding for a glycotransferase (Cphamn1_1225) which is involved in cell wall biogenesis, but the link to the genes involved in phosphate transport is unknown and could represent just a coincidence. Other up regulated genes that can be linked to phosphate uptake are Cphamn1_1536 coding for a phytase and Cphamn1_0512 coding for a alkaline phosphatase. The phytase is a secreted enzyme which hydrolyses phytate to release inorganic phosphate, while the latter represents a means for the bacteria to generate free phosphate groups for uptake and use, which is supported by the fact that alkaline phosphatase is usually produced by the bacteria only during phosphate starvation (Horiuchi et al., 1959). As seen for the molybdenum transport, BS1 regulates some energy demanding transport systems probably in order to save energy for more important metabolic pathways.

Biotin synthesis. Another example of a highly regulated secondary metabolism pathway is the biotin synthesis pathway. Like in 9 other *Chlorobi* genomes, genes coding for proteins involved in biotin biosynthesis (Cphamn_2453-2459) are clustered in an operon which in our experiments was shown to be co-regulated. Five of these genes (Cphamn1_2453, 2454, 2457, 2458 and 2459) code for enzymes involved in the second stage of biotin synthesis from primelate (Lin and Cronan, 2011) while biosynthesis protein BioC (Cphamn1_2455) is involved in the synthesis of primelate. The gene coding for a hypothetical protein has unknown functions and has homologs also present in all nine *Chlorobi* genomes mentioned before. Biotin is an enzyme cofactor indispensable for CO₂ fixation and the down-regulation of the genes involved of its metabolic pathway are congruent with the lower photosynthetic activity expected at these low

Discussion

light intensities. However, a second copy of biotin synthase BioB (Cphamn1_0208) was not down-regulated, but the impact of this regulatory feature on biotin synthesis is still unclear.

Other up-regulated genes under high light conditions. Most of these regulated genes not organized in bigger clusters or operons are involved in energy production or conversion pathways. Two genes coding for subunits of the succinate dehydrogenase (Cecchini et al., 2002) were found to be up-regulated, (i) succinate dehydrogenase and fumarate reductase iron-sulfur protein (Cphamn1_0285) and (ii) a putative succinate dehydrogenase subunit C (Cphamn1_0286). But other copies of genes involved in the assembly of the succinate dehydrogenase enzyme (Cphamn1_0284, 1699, 2514, 2515 and 2516) show no transcriptional regulation leading to the conclusion that only some additional copies are being regulated. Another gene is coding for NADH dehydrogenase I subunit D (Cphamn1_1604), being the only gene in the NADH dehydrogenase operon showing significant but low regulation. The plastoquinol-plastocyanin reductase (Cphamn1_1987) is part of the cytochrome b6f complex and involved in photosynthesis, but like above it represents only one significant but low regulated subunit of a larger complex. A gene coding for a cytochrome *c* class I protein (Cphamn1_0009) was also found to be down-regulated through both used methods, Illumina sequencing and cDNA SSH. It presumably codes for the sulfite dehydrogenase cytochrome subunit, being then also involved in the photosynthesis pathway by providing the electron donors for the reductive CO₂ cycle (inorganic reduced sulfur compounds) through sulfide oxidation. Another protein which could be associated to these regulated genes is the cytochrome *c* assembly protein (Cphamn1_2044), which is involved in the assembly of periplasmic c-type cytochromes.

Some of the up-regulated genes are involved in amino acid transport and metabolism like a aminoacyl-histidine dipeptidase (Cphamn1_1387), a pyruvate carboxyltransferase (Cphamn1_1747), and a gene (Cphamn1_1650) coding for a Na⁺/proline symporter. Others, like the two copies of cobyrinic acid ac-diamide synthase (Cphamn1_0038 and 0681), are involved in the biosynthesis of cobalamine (vitamin B₁₂) which is a cofactor of enzymes including isomerases, methyltransferases and dehalogenases. Genes involved in transport are the inorganic ion transport Fe²⁺ transport system protein A (Cphamn1_0621) or the tripartite ATP-independent periplasmic transporter with unknown function (Cphamn1_0426).

Genes detected only by cDNA-SSH. Out of 9 protein coding ORF found to be differentially expressed by cDNA-SSH 4 were also detected via transcriptome sequencing. Interestingly the two genes coding for hypothetical proteins were detected also by transcriptome sequencing, and one of them (Cphamn1_2363) being also unique to BS1 when compared to other *Chlorobi*. The other five genes are also involved in major metabolic pathways, two proteins being involved in the reductive citric acid cycle. The oxoglutarate ferredoxin oxidoreductase (Cphamn1_0326) resembles the beta subunit of the enzyme catalyzing the carboxylation of succinyl-CoA to 2-oxoglutarate. But because other three genes involved in this carboxylation step (Cphamn1_0327, Cphamn1_1033 and Cphamn1_1034) showed no detectable change in their transcription, the meaning of this positive hit remains inconclusive. The gene coding for ferredoxin (Cphamn1_1091) was also found to be up-regulated, being the direct electron donor for CO₂ fixation reactions in the reductive citric acid cycle. Another two genes are coding proteins which are involved in the photosynthetic complex. While FMO-protein (Cphamn1_0841) is part of this complex, resembling the base plate connecting the chlorosomes to the reaction center, the second gene codes for the magnesium chelatase subunit H (Cphamn1_2207), a protein involved in the bacteriochlorophyll biosynthesis. Again this gene coding for a enzyme subunit is only one of several genes (Cphamn1_2205, Cphamn1_1048, Cphamn1_1047, and Cphamn1_1046) which were not further detected as differentially transcribed. The last gene detected only by cDNA-SSH dapD (Cphamn1_0020) is coding the 2,3,4,5-tetrahydropyridine-2-carboxylate N-succinyltransferase involved in the lysine biosynthesis. In general, ORFs detected to be up regulated at high light intensities by cDNA-SSH, are involved with pathways which are directly coupled with the turnover of the increased energy available at high light intensities.

Genes up-regulated under low light condition

Under low light condition ($0.15 \mu\text{mol quanta}\cdot\text{m}^{-2}\cdot\text{s}^{-1}$) the transcriptome of *Chl. phaeobacteroides* BS1 still contains transcripts of a majority of the identified 2524 ORFs in the genome. In comparison to cultures grown under higher light intensities ($3 \mu\text{mol quanta}\cdot\text{m}^{-2}\cdot\text{s}^{-1}$), 76 genes are being up-regulated indicating potential relevance for the specific adaptation to low light intensities.

General stress proteins. A group of 13 different up-regulated genes can be associated with stress response. Proteins like the heat shock protein Hsp20 (Cphamn1_1706), chaperonine GroEL (Cphamn1_0783) and molecular chaperone DnaK (Cphamn1_1707) have major impact on refolding mature proteins unfolded by stress. These three genes do not show a very large increase of transcripts with DnaK being 3.04-fold, Hsp20 2.63-fold and GroEL 1.72-fold up-regulated. GroEL was shown to be slightly up regulated in cultures of *Prochlorococcus marinus* MED4 cultivated at high light intensities (Pandhal et al., 2007). However the levels of these transcripts remained high even after prolonged exposure to high light suggesting an importance for cellular function maintenance and not only for stress response. The molecular chaperone DnaK (Hsp70) requires ATP for refolding proteins (Glover and Lindquist, 1998) and Hsp20 a small heat shock protein acts ATP-independent (Jakob and Buchner, 1994). Due to the genomic neighborhood these two genes could be co-transcribed. Although their transcription is not highly elevated, the accumulation of chaperones is of crucial importance for cellular function maintenance. During low protein turnover misfolded proteins and modifications of proteins such as carbonylation and illegitimate disulfite bond formation tend to accumulate (Nyström, 2004). The availability of stress proteins which are refolding damaged proteins or initiate the proteolysis are therefore of increased need. Other stress related genes are involved in DNA repair mechanisms like the DNA mismatch endonuclease Vsr (Cphamn1_1412), which recognizes a TG mismatched base pair, generated after spontaneous deamination of methylated cytosines, and cleaves the phosphate backbone on the 5' side of the thymine (Tsutakawa et al., 1999). Also the excinuclease ABC C subunit domain-containing protein (Cphamn1_1984) and two uncharacterized CRISPR-associated proteins (Cphamn1_2160, Cphamn1_2334) are predicted to be involved in DNA repair. The gene coding for purine nucleoside phosphorylase (Cphamn1_1782) is also being up-regulated, which helps in the need for recovery of bases and

nucleosides from degraded RNA and DNA. All these proteins with their ability to prolong protein functionality or protect against damages are therefore directly involved in the conservation of maintenance energy.

Transcriptional regulators. These proteins play a major role in modulating gene expression and thus reacting to environmental changes. For the tradeoff between proliferation and maintenance the sigma factor σ^S is thought to be the main regulator (Nystrom, 2003). A gene coding for this regulator could not be found in the genomic sequence of *Chl. phaeobacteroides* BS1. Nevertheless 4 different transcriptional regulators are found to be up-regulated under low light condition. Two genes coding for sigma-24 regulators (Cphamn1_1095, Cphamn1_1366) are believed to belong to the ECF subfamily involved in the response to extracytoplasmatic stimuli. These alternative sigma factors were found to be transcribed constitutively in *E. coli* during active growth and during starvation or the stationary phase (Sharma and Chatterji, 2010). Even if not belonging to the essential housekeeping sigma factors in *E. coli*, the inactivation of the σ^{24} resulted in loss of viability (De Las Peñas et al., 1997). The up-regulation of σ^{24} in *E. coli* coincided with the entry into stationary phase pinpointing the important role this sigma factor plays during this phase (Costanzo and Ades, 2006). The transcription of σ^{24} is regulated by the protein DskA and the small molecule (p)ppGpp, which represents the general signal for starvation stress. In the BS1 transcriptome no up-regulation of the transcriptional regulator TraR/DskA family (Cphman1_1886) could be detected under low light intensities. Another regulator found to be up-regulated belongs to the MarR family (Cphamn1_1673) which are often involved in the development of antibiotic resistance and oxidative stress agents (Alekhshun and Levy, 1999). The fourth gene codes for a putative anti-sigma regulatory factor, serine-protein kinase (Cphamn1_1139) which in *Bacillus subtilis* controls the general stress regulon and is activated by cell stresses such as stationary phase and heat shock (Voelker et al., 1996). The most up-regulated factor in *E. coli* during starvation was σ^{38} which like σ^S is absent in the genomic sequence of *Chl. phaeobacteroides* BS1. Future experiments with cultures of BS1 grown at lower light intensities could bring more insight on transcriptional regulation under adverse conditions.

Energy production. A group of genes involved in energy production and conversion were found to be up-regulated under low light condition. The cytochrome B561 coding gene (Cphamn1_2425) is closely related to the *phsC* thiosulfate reductase cytochrome b subunit. In

Discussion

Salmonella typhimurium thiosulfate reductase is involved in the production of hydrogen sulfate from thiosulfate and is encoded by the *phs*-operon (Heinzinger et al., 1995). In seven other genomes from bacteria belonging to the *Chlorobi* group and also various other sulfate-reducing and some iron-oxidizing bacteria, a *phsC* homologous cytochrome B561 is present but two other genes *phsA* and *phsB* of the *phs*-operon are missing or have not been identified based on sequence comparisons. Instead all these bacteria have an uncharacterized cytochrome c family protein coding gene clustering with the putative cytochrome B561 coding gene. This new genetic environment therefore leads to the assumption of a different function as predicted for this cytochrome B561. Cytochrome *c* from BS1 (Cphamn1_2426) has eight heme binding CxxCH groups like the hydroxylamine oxidoreductase of *Nitrosomonas europaea* (Bertini et al., 2006) or an octa-heme cytochrome *c*₃ believed to be involved in thiosulfate reduction in *Desulfovibrio gigas* (Sieker et al., 1986). Interestingly in both *Chl. vibrioforme* and *Pelodictyon luteolum* the two up-regulated cytochrome genes group with a gene coding for a *hppA* membrane bound proton translocating pyrophosphatase. This gene (Cphamn1_1101) was also found to be also upregulated under low light conditions in *Chl. phaeobacteroides* BS1 thus raising the question of a probable transcriptional co-regulation and the functional relation of these three genes. Membrane bound proton-translocating pyrophosphatases (H⁺-PPase) couple inorganic phosphate PPi energy with an electrochemical proton gradient across biological membranes (Serrano et al., 2007). In *Rhodospirillum rubrum* H⁺-PPase appears to be transcriptionally induced in response to a variety of conditions that constrain cell bioenergetics (López-Marqués et al., 2004). The characterization of a *Rhodospirillum rubrum* H⁺-PPase mutant strain revealed the importance of its presence under low light conditions (García-Contreras et al., 2004). It has been shown that this enzyme is essential for the up-keep of an H⁺ gradient at conditions where the photosynthetic electron transport chain is not sufficient. It has been further hypothesized that under low energy conditions PP_i-dependent H⁺ gradient produced by H⁺-PPase might become the main energy source (Nyrén and Strid, 1991). Further experiments using BS1 cultures could therefore lead to more insights in a possible implication of these interesting genes in the energetic production and conversion system of this green sulfur bacterium.

Other up-regulated genes. Despite the up-regulation of nitrogenase related genes only in high light, a gene coding for the dinitrogenase iron-molybdenum cofactor biosynthesis protein (Cphamn1_1076) is being up-regulated under low light conditions. Enzymes requiring an iron-

molybdenum cofactor can also be found in the sulfur metabolism, opening the possibility that this detected gene is also involved in other pathways than nitrogen fixation. Another isolated hit was a gene coding for the polysulphide reductase *NrfD* (Cphamn1_1865), but as the other 6 genes of the previously described *nrf* operon (Hussain et al., 1994) are missing, the function of this isolated gene remains inconclusive. Other genes code for enzymes like the phosphoserine phosphatase *SerB* (Cphamn1_0341) involved in the biosynthesis of serine from carbohydrates, or the phosphoenolpyruvate-protein phosphotransferase (Cphamn1_0363) which is involved in carbohydrate transport. Nonetheless for most of the up-regulated genes no functional description could be found because of the classification as coding for hypothetical proteins. Through this experiment many of the genes belonging to this category could for the first time be linked to a physiological condition. More than 70% (19 out of 27) genes were found to be unique to the genome of *Chl. phaeobacteroides* BS1 when compared to the genomes of other bacteria belonging to the *Chlorobi* phylum. When compared to all sequenced genomes available at the IMG database 6 of these genes were found to be unique, altogether revealing possible new genes involved in this unequaled low light adaptation.

But not only differentially transcribed genes could open a new perspective to this physiological feature. Also constitutively expressed genes with high abundance in low light conditions harbor interesting features. Besides genes involved in chlorosomes structure, photosynthesis, ribosomal structure, transcriptional regulation and posttranslational modifications, genes coding for hypothetical proteins represent with 20 out of the 50 most transcribed genes a high percentage of these constitutively expressed genes. These hypothetical proteins therefore need to be of major importance during cell development not only under low light conditions. The usage of *Chl. phaeobacteroides* BS1 as a model organism has the potential of unraveling some of these poorly described features of bacterial genomes.

Distribution of *Chlorobiaceae* in different chemoclines and their molecular markers in marine sediments

The Black Sea represents a unique marine habitat and its deep situated chemocline resembles an extreme low light habitat where *Chl. phaeobacteroides* BS1 is the only photosynthetic bacterium. Although they are not situated as deep, in some lacustrine environments chemoclines with low light conditions are also present due to higher absorption in the photic zone above it. While brown coloured, BChl *e* containing *Chlorobiaceae* are more adapted to low light, the occurrence of such bacterial strains in habitats similar to the Black Sea was therefore investigated.

***Chlorobiaceae* in Sakinaw Lake.** In the chemocline of the meromictic fresh water fjord Lake Sakinaw, BChl *e* was detected previously (T. Beatty, unpublished data) and light intensity measurements indicated that low light conditions prevailed at these depths. Isolated 16S rRNA nucleotide sequences indicate that the bacterium thriving at these depths is most related to *Chl. clathratiforme* BU-1 (A Köhler, unpublished data). Since the concentration of photosynthetic pigments found in green sulfur bacteria is maintained constant and at a maximum during light limited growth (Montesinos et al., 1983), BChl *e* can serve as an indicator of green sulfur bacterial biomass. The patterns of BChl *e* measured on two consecutive years indicate the prevalence of a stable GSB population in the chemocline. The pigment distributions are relatively similar although the highest amount measured in 2009 was 2m above the corresponding depth in 2008. This difference of the peak amounts of BChl *e* may also reflect different positions of the chemocline or different underwater light penetration occurring at the time of sampling.

While the determination of biomass distribution clearly identifies the depth where this bacterium mostly occurs in the chemocline, no conclusions can be made upon the activity pattern. The concentration of the internal transcribed spacer (ITS)-RNA has previously been shown to reflect the activity of bacterial cells (Schmid et al., 2001). The occurrence of active GSB in depths above 33 m is limited by higher O₂ levels in the layers above the chemocline. During sampling in May 2008 measured O₂ concentrations dropped from 2 ml l⁻¹ at 32 m to 0.1 ml l⁻¹ at 33 m (Beatty T. and Gies E., personal communication). The activity patterns measured for the 2009 samples correlate with light intensities showing high activity in regions

with the highest light intensity reaching the chemocline. Although BChl *e* concentrations at 33 m are much lower than at depths below, cells thriving at this level are more active due to increased amount of available energy. Below this active layer light limitation occurs which is reflected in the light intensity measurements performed in 2008, where light intensity dropped dramatically from 0.029 $\mu\text{mol quanta m}^{-2} \text{s}^{-1}$ at 36 m to 0.0002 $\mu\text{mol quanta m}^{-2} \text{s}^{-1}$ at 38 m. This correlates with peak BChl *e* amounts detected around 37 m, and also shows how cells thriving at these depth try to adapt to the low light through accumulation of additional pigments. Nevertheless this increased light limitation leads to a dramatically decreased activity below 36 m depth despite of this high accumulation of photosynthetic pigments. The detection of low amounts of ITS transcripts in depths where almost no pigments were detectable could be due to the different sensitivity of the used methods.

Therefore, this *Chlorobium* strain represents another low light adapted bacterium thriving in the chemocline of Lake Sakinaw. The light intensities reaching the active layer of this bacterium were 0.05 $\mu\text{mol quanta m}^{-2} \text{s}^{-1}$, which is similar to light intensities in the Black Sea chemocline.

***Chlorobiaceae* in Faro Lake.** In contrast to the chemoclines of Lake Sakinaw and the Black Sea, Lake Faro harbours a chemocline at the lesser depth around 15m. Pigment measurements indicated the presence of BChl *e* containing geranyl ester homologs (A Sacca, unpublished data) which were identified also in the GSB strain *Chl. phaeobacteroides* BS1 present in the Black Sea (Manske et al., 2005). GSB specific 16S rRNA PCR amplification and DGGE revealed the presence of three distinct *Chlorobi* strains in the chemocline of Lake Faro. One of them was identified as *Chl. phaeobacteroides* BS1, showing 100% identity in the 16S rRNA gene region. These strains were shown to persist over a longer period of time with slight shifts of distribution during the sampling period. While *Chl. phaeovibroides* DSM 265 dominates in samples taken in May, *Chl. phaeobacteroides* BS1 is more abundant in samples taken July. Although the strain *Chl. phaeobacteroides* BS1 was shown to be perfectly adapted to low light conditions in the Black Sea, no correlation of its abundance with increasing depth in the chemocline of Lake Faro can be observed. Eventual light intensity measurements, and an isolate of the observed strain could give more insight on the distribution pattern observed. The availability of a second habitat where this bacterial strain is present opens also the possibility to observe its adaptational versatility and also the impact of competition from other *Chlorobi* strains.

Distribution of GSB molecular markers in sediments. The pigment isorenieratene and its degradation products have previously been used as an indicator of past water column anoxia (Passier et al., 1999; Menzel et al., 2002). This correlation has been made on the assumption that isorenieratene is a molecular marker for green sulfur bacteria, which thrive in an anoxic photic environment. But carotenoids show a limited diversity which cannot provide a differentiation between GSB representants displaying contrasting physiology and ecology. Previous investigations have shed some doubts on this assumption, showing that isorenieratene could also have originated from allochthonous sources (Coolen and Overmann, 2007). Using fossil DNA as molecular marker, a higher diversity of GSB sequences present in the sapropel layers has been identified, including mostly typical freshwater or brackish water species. Additionally, traces of isorenieratene were identified in intermediate layers and in samples from the sediment surface, but amounts were too low to enable firm interpretation.

In order to reconfirm these findings, several samples from the Mediterranean Sea were investigated for their isorenieratene content. For this task a more sensitive method was chosen, using mass spectrometry with a narrow mass range of 528.0-532.0 followed by two events of collision induced dissociation, in order to exclusively identify isorenieratene amounts. Sediment samples from the sapropel S1 (8.000 years old) and one sample from sapropel S4 (124.000 years old) originate from stations spread around the Aegean Sea, East Mediterranean Basin and the Marmara Sea. All these old samples show amounts of isorenieratene ranging from 343.2-63.7 ng per g sediment. Lower but still relevant amounts of isorenieratene were identified samples from the top layers (Z0) of sediments. These represent recently deposited sediments and the presence of an extended water anoxia reaching to the photic zone can definitely be excluded in this case. This finding reconfirms the assumption that deposited isorenieratene can originate from allochthonous sources and shows the importance of the usage of fossil DNA markers when this option is available.

The fossil DNA isolated from these samples was also investigated for the content of BS1 sequences. Sequences identical to BS1 sequences were detected in the upper sediment layers of the Black Sea. But in the Black Sea samples, where it can certainly be assumed that BS1 is the only green sulfur bacterium present in the chemocline (Manske et al., 2005), no correlation between isorenieratene and DNA amounts can be observed. Samples from the Mediterranean Sea S1 sapropel, which was deposited at approximatively at the same time when the inflow of

Mediterranean water via the Bosphorus has started to happen (Degens and Ross, 1972), also bear sequences identical to BS1 genomic ITS sequence. It can be therefore be assumed that the green sulfur bacteria present now in the chemocline of the Black Sea represent direct descendants of the Mediterranean BS1 population. The fact that BS1 could also be detected in the S5 sapropel, which is 172,000 years old, shows the persistency of this green sulfur bacterium in the Mediterranean Basin.

The ITS sequences similar to BS1 retrieved from sapropel layers below the Mediterranean Sea show minimal divergence by bearing only 1 altered base (two clones from station 599-S1) or 2 altered bases in the older sapropel S5 (567-S5). The investigation of the chemocline of Lake Faro situated on Sicily near the Strait of Messina revealed the presence of 3 distinct *Chlorobi* strains. One of these strains was identified as bearing identical 16S rDNA sequence as *Chl. phaeobacteroides* BS1, with differences only in the ITS region. Five investigated clones were bearing 3 transitional mutations with one clone with additional 2 transitional changes in the ITS region, which were all different from the changes occurring in the fossil sequences from the Mediterranean sapropels. This imposes that the BS1 strain present in Mediterranean Sea at the deposition time of these sapropels shows closer relationship to present BS1 cultures from the Black Sea. Therefore the BS1 strain found in Lake Faro represents a lineage which was geographically isolated much earlier from the Black Sea lineage, as the time of the sapropel deposition 172.000 years ago.

Nonetheless, the question arises how this strictly anaerobic photosynthetic bacterium can survive and overcome periods during which no anoxic water body reaches the photic zone, case which can be assumed for periods between sapropel deposition. The identification of *Chl. phaeobacteroides* BS1 strain in the chemocline of Lake Faro, Sicily offers a simple and interesting theory. This lake, which is located near and connected to the Strait of Messina represents a niche where anaerobic bacteria thrive when conditions do not allow survival in the open sea water body. From such niches recolonization easily can occur when conditions with extended water body anoxia reaching the photic zone are reestablished. Considering the long lasting occurrence and distribution of *Chl. phaeobacteroides* BS1 throughout various investigated regions, predisposes this bacterium and its fossil DNA markers as suitable aid for the reconstruction of the paleoceanography in the Mediterranean Sea Basin.

Conclusions

Different aspects of adaptation towards the availability and quality of light were successfully revealed during the course of this study. These two aspects were assessed through the analysis of newly isolated bacterial strains, which showed physiological adaptation towards long wavelengths of light and low light intensities. In order to gain additional information from possible similar adaptations of other bacterial strains, natural samples originating from different suitable locations were also successfully investigated.

The unusual absorption patterns found in several *Gammaproteobacteria* containing BChl *a* was examined through sequencing of *pufBA* genes coding for the light harvesting antenna proteins. This comparison of *pufBA* sequences revealed a monophyletic origin of the LHC1 polypeptides present in the bacterial species strain 970, *Thr. winogradskyi* and *Tch. tepidum*. For the first time it could be shown, how a gradual accumulation of amino acid substitutions is leading to an increasing red-shifted Q_y absorption. The availability of such newly isolated strains enables a more profound investigation of previously described features which were believed to be responsible for its altered absorption spectrum. Nevertheless site directed mutagenesis remains a powerful method for testing these substitutions and will certainly help understand how these single features contribute to the changes in the absorption properties. Although 3D modeling is very helpful for the visualization of pigment protein interaction, the lack of crystal structures of LH1 polypeptides originating from *Gammaproteobacteria* hampers a precise comparison. The assembled sequences revealed also that strain 970 harbors a new *puf* operon architecture but transcriptional analysis showed that the second copy of *pufBA* has no further implications on the absorption pattern. Additionally, the search for new *pufLM* sequences in the diverse habitats of Little Sippewissett Saltmarsh did not yield novel close relatives of strain 970, indicating that the adaptation to the 900-1000 nm wavelength region, be it by lateral gene transfer or independent evolution of one lineage, may have occurred only rarely during the evolution of benthic *Chromatiaceae*.

The more complex physiological aspects of adaptation towards low light availability were assessed using three habitats where such conditions were identified. Available enrichment cultures and complete genetic information from the extremely low light adapted bacterium *Chl.*

phaeobacteroides BS1 facilitated whole transcriptome sequencing. The comparison of transcripts present at two different light conditions revealed multiple genes with possible implications in the low light adaptation. Furthermore the organization of multiple genes in operons and other co-regulated genes which are regulated by photosynthetic activity represents another novel information which could be retrieved from such data. The regulation of high energy demanding metabolic pathways and of multiple gene copies enables an insight in the management of transcripts in order to lower the maintenance energy. Although the implication of some poorly characterized genes remains unclear some up-regulated genes reveal interesting findings. The identification of genes with implication in the upkeep of an H⁺ gradient at conditions where the photosynthetic electron transport chain is not sufficient together offer interesting candidates for future investigations. Also the regulation of several stress proteins, which are crucial for prolonged protein functionality under conditions of low protein turnover represent potential candidates with implications in the poorly understood stress regulon during conditions of energy conservation. Together with *in silico* subtractive hybridization, transcriptome analysis led to the identification of multiple hypothetical proteins with possible implications for the adaptation towards low light conditions. These uncharacterized proteins showed high abundance of transcripts under both investigated conditions emphasizing their constitutive expression. In general, the transcriptome retrieved from low light grown cultures, which resembles the *in situ* conditions in the Black Sea chemocline, still contains transcripts of a majority of the predicted 2524 ORFs. Nonetheless, among most actively regulated transcripts many are coding for hypothetical proteins, some of them even being unique to the genome of *Chl. phaeobacteroides* BS1. This study therefore identified several interesting targets for future investigations of such poorly described genomic regions.

The investigation of green sulfur bacterial strains in the chemoclines from Lake Sakinaw and Faro revealed the versatility of adaptation in this group. Part of this versatility is based on the advantage that chlorosomes can accumulate pigments without a higher demand for proteins, which allow these bacteria to thrive at such low light intensities. The identification of a strain closely related to *Chl. clathratiforme* BU-1 also shows that adaptation to very low light intensities is not restricted only to *Chl. phaeobacteroides* BS1. Nonetheless, this bacterium represents the best described low adapted strain so far, and the comparison with this newly identified strain with similar adaptations but different location will help elucidate how *Chlorobi*

Discussion

strains can thrive under such conditions. In contrast to the chemoclines in the Black Sea and Lake Sakinaw where only one photosynthetic species is present, three species belonging to the GSB were found to coexist in Lake Faro. The identified close relationship between the two strains of BS1 present in these two locations where different conditions prevail opens new opportunities for the investigation of this unmatched adaptation to low light intensities. Additionally, the distribution of molecular markers found in sediments from the Eastern Mediterranean Sea and the Black Sea demonstrate the persistency of *Chl. phaeobacteroides* BS1 in this region. The usage of DNA as a molecular marker was shown to have clear advantages over pigment analysis because of its higher diversity. Phylogenetic analysis of retrieved fossil DNA enabled firm interpretation of the relationship and the distribution of the green sulfur bacteria in past anoxic water environments. The great potential in the usage of *Chl. phaeobacteroides* BS1 as model organism has therefore again been demonstrated, and future studies including the newly described habitats can elucidate even more molecular determinants of the adaptation of anoxygenic phototrophic bacteria to different light conditions.

APPENDIX

App. Table 1. 331 unique ORFs of the green sulfur bacterium *Chl. phaeobacteroides* BS1 genome identified by *in silico* subtractive hybridization based on BLASTP alignments against 11 other GSB genomes. ORFs which were found to be differentially regulated are marked in bold type.

Locus Tag	ORF Name	Length	Unique in IMG
Cphamn1_0016	hypothetical protein	46aa	Yes
Cphamn1_0025	hypothetical protein	43aa	No
Cphamn1_0027	aminotransferase class V	455aa	No
Cphamn1_0034	hypothetical protein	66aa	No
Cphamn1_0036	hypothetical protein	45aa	Yes
Cphamn1_0044	hypothetical protein	101aa	Yes
Cphamn1_0045	hypothetical protein	87aa	No
Cphamn1_0046	CHAP domain containing protein	332aa	No
Cphamn1_0047	hypothetical protein	154aa	No
Cphamn1_0048	hypothetical protein	34aa	Yes
Cphamn1_0051	hypothetical protein	80aa	Yes
Cphamn1_0054	hypothetical protein	173aa	No
Cphamn1_0060	amidohydrolase	440aa	No
Cphamn1_0061	hypothetical protein	35aa	Yes
Cphamn1_0062	hypothetical protein	104aa	No
Cphamn1_0082	hypothetical protein	84aa	Yes
Cphamn1_0083	protein of unknown function nitrogen fixation	73aa	No
Cphamn1_0092	hypothetical protein	60aa	No
Cphamn1_0116	-	117aa	No
Cphamn1_0120	hypothetical protein	191aa	No
Cphamn1_0139	hypothetical protein	340aa	No
Cphamn1_0145	hypothetical protein	206aa	No
Cphamn1_0151	hypothetical protein	99aa	No
Cphamn1_0166	hypothetical protein	81aa	No
Cphamn1_0186	hypothetical protein	253aa	No
Cphamn1_0187	hypothetical protein	198aa	No
Cphamn1_0190	transcriptional regulator, XRE family	69aa	No
Cphamn1_0191	hypothetical protein	207aa	Yes
Cphamn1_0209	hypothetical protein	40aa	Yes
Cphamn1_0210	hypothetical protein	267aa	No
Cphamn1_0212	hypothetical protein	229aa	No
Cphamn1_0213	hypothetical protein	177aa	No
Cphamn1_0214	hypothetical protein	284aa	No
Cphamn1_0215	putative excisionase	98aa	No
Cphamn1_0217	phage/plasmid primase, P4 family	486aa	No
Cphamn1_0219	hypothetical protein	61aa	Yes

Appendix

Locus Tag	ORF Name	Length	Unique in IMG
Cphamn1_0220	phage terminase, small subunit, P27 family	166aa	No
Cphamn1_0221	hypothetical protein	34aa	Yes
Cphamn1_0223	hypothetical protein	61aa	No
Cphamn1_0227	hypothetical protein	154aa	No
Cphamn1_0231	hypothetical protein	67aa	No
Cphamn1_0232	PilT protein domain protein	135aa	No
Cphamn1_0234	hypothetical protein	113aa	No
Cphamn1_0235	hypothetical protein	50aa	Yes
Cphamn1_0243	hypothetical protein	62aa	No
Cphamn1_0244	DNA polymerase beta domain protein region	131aa	No
Cphamn1_0245	protein of unknown function DUF86	141aa	No
Cphamn1_0335	hypothetical protein	591aa	No
Cphamn1_0336	Piwi domain protein	474aa	No
Cphamn1_0370	lipopolysaccharide biosynthesis protein	334aa	No
Cphamn1_0374	hypothetical protein	209aa	No
Cphamn1_0375	glycosyl transferase group 1	383aa	No
Cphamn1_0376	hypothetical protein	119aa	No
Cphamn1_0379	hypothetical protein	179aa	No
Cphamn1_0382	hypothetical protein	459aa	No
Cphamn1_0385	NAD-dependent epimerase/dehydratase	677aa	No
Cphamn1_0394	hypothetical protein	49aa	No
Cphamn1_0399	hypothetical protein	70aa	No
Cphamn1_0425	hypothetical protein	83aa	Yes
Cphamn1_0450	hypothetical protein	39aa	Yes
Cphamn1_0468	hypothetical protein	75aa	Yes
Cphamn1_0471	NADH dehydrogenase subunit E (EC 1.6.5.3) (IMGterm)	195aa	No
Cphamn1_0482	hypothetical protein	87aa	No
Cphamn1_0483	-	112aa	No
Cphamn1_0486	hypothetical protein	50aa	Yes
Cphamn1_0491	hypothetical protein	40aa	Yes
Cphamn1_0494	transposase, IS5 family, putative	498aa	No
Cphamn1_0522	hypothetical protein	74aa	Yes
Cphamn1_0526	hypothetical protein	261aa	No
Cphamn1_0555	protein of unknown function DUF81	408aa	No
Cphamn1_0556	conserved hypothetical cytosolic protein	88aa	No
Cphamn1_0557	transcriptional regulator, XRE family	89aa	No
Cphamn1_0561	hypothetical protein	44aa	No
Cphamn1_0563	hypothetical protein	230aa	No
Cphamn1_0564	hypothetical protein	58aa	No
Cphamn1_0575	hypothetical protein	52aa	Yes
Cphamn1_0613	Protein of unknown function DUF1810	168aa	No

Locus Tag	ORF Name	Length	Unique in IMG
Cphamn1_0632	hypothetical protein	30aa	Yes
Cphamn1_0639	hypothetical protein	66aa	No
Cphamn1_0643	thiamine biosynthesis protein ThiS	73aa	No
Cphamn1_0646	Mov34/MPN/PAD-1 family protein	146aa	No
Cphamn1_0648	SirA family protein	82aa	No
Cphamn1_0650	hypothetical protein	201aa	No
Cphamn1_0654	hypothetical protein	86aa	No
Cphamn1_0655	TonB-dependent receptor	768aa	No
Cphamn1_0664	transposase, IS5 family, putative	498aa	No
Cphamn1_0678	hypothetical protein	84aa	No
Cphamn1_0689	hypothetical protein	250aa	No
Cphamn1_0690	hypothetical protein	263aa	No
Cphamn1_0691	mobilizable transposon, xis protein	115aa	No
Cphamn1_0693	hypothetical protein	71aa	No
Cphamn1_0694	Serine/threonine protein phosphatase-like protein	247aa	No
Cphamn1_0695	hypothetical protein	225aa	No
Cphamn1_0696	CheD	327aa	No
Cphamn1_0697	amino acid/amide ABC transporter membrane protein 1, HAAT family (TC 3.A.1.4.-) (IMGterm)	297aa	No
Cphamn1_0703	hypothetical protein	151aa	No
Cphamn1_0707	type III restriction protein res subunit	1099aa	No
Cphamn1_0711	hypothetical protein	36aa	Yes
Cphamn1_0719	hypothetical protein	42aa	Yes
Cphamn1_0722	transposase, IS5 family, putative	498aa	No
Cphamn1_0730	Isoprenylcysteine carboxyl methyltransferase	236aa	No
Cphamn1_0731	hypothetical protein	93aa	No
Cphamn1_0740	hypothetical protein	60aa	No
Cphamn1_0749	type III restriction protein res subunit	992aa	No
Cphamn1_0751	N-6 DNA methylase	686aa	No
Cphamn1_0754	hypothetical protein	447aa	No
Cphamn1_0757	hypothetical protein	208aa	No
Cphamn1_0760	putative anti-sigma regulatory factor, serine/threonine protein kinase	490aa	No
Cphamn1_0761	hypothetical protein	211aa	No
Cphamn1_0801	hypothetical protein	278aa	Yes
Cphamn1_0802	hypothetical protein	591aa	No
Cphamn1_0803	hypothetical protein	680aa	No
Cphamn1_0804	hypothetical protein	274aa	No
Cphamn1_0822	type III restriction-modification system restriction subunit	52aa	No
Cphamn1_0824	sulfotransferase	326aa	No
Cphamn1_0827	hypothetical protein	49aa	Yes
Cphamn1_0836	hypothetical protein	59aa	Yes

Appendix

Locus Tag	ORF Name	Length	Unique in IMG
Cphamn1_0856	hypothetical protein	50aa	Yes
Cphamn1_0862	hypothetical protein	68aa	Yes
Cphamn1_0863	outer membrane efflux protein	443aa	No
Cphamn1_0864	efflux transporter, RND family, MFP subunit	345aa	No
Cphamn1_0866	hypothetical protein	82aa	No
Cphamn1_0867	hypothetical protein	187aa	No
Cphamn1_0872	protein of unknown function DUF86	114aa	No
Cphamn1_0875	hypothetical protein	159aa	No
Cphamn1_0881	hypothetical protein	233aa	No
Cphamn1_0882	hypothetical protein	450aa	No
Cphamn1_0891	transcriptional regulator, AbrB family	96aa	No
Cphamn1_0892	hypothetical protein	64aa	Yes
Cphamn1_0893	Radical SAM domain protein	681aa	No
Cphamn1_0901	hypothetical protein	48aa	Yes
Cphamn1_0913	hypothetical protein	33aa	Yes
Cphamn1_0914	hypothetical protein	42aa	Yes
Cphamn1_0915	hypothetical protein	51aa	Yes
Cphamn1_0928	hypothetical protein	63aa	No
Cphamn1_0931	hypothetical protein	65aa	No
Cphamn1_0946	hypothetical protein	37aa	No
Cphamn1_0950	hypothetical protein	66aa	No
Cphamn1_0951	hypothetical protein	52aa	Yes
Cphamn1_0954	hypothetical protein	82aa	Yes
Cphamn1_0979	hypothetical protein	87aa	No
Cphamn1_1022	Methyltransferase type 11	273aa	No
Cphamn1_1032	hypothetical protein	45aa	No
Cphamn1_1036	hypothetical protein	156aa	No
Cphamn1_1056	hypothetical protein	46aa	Yes
Cphamn1_1073	hypothetical protein	40aa	Yes
Cphamn1_1075	hypothetical protein	82aa	No
Cphamn1_1083	protein of unknown function DUF86	83aa	No
Cphamn1_1100	hypothetical protein	169aa	Yes
Cphamn1_1129	hypothetical protein	56aa	No
Cphamn1_1141	hypothetical protein	65aa	Yes
Cphamn1_1142	hypothetical protein	70aa	No
Cphamn1_1143	hypothetical protein	77aa	No
Cphamn1_1147	hypothetical protein	212aa	No
Cphamn1_1150	protein of unknown function DUF262	687aa	No
Cphamn1_1151	hypothetical protein	743aa	No
Cphamn1_1155	hypothetical protein	31aa	No
Cphamn1_1158	HNH endonuclease	360aa	No

Locus Tag	ORF Name	Length	Unique in IMG
Cphamn1_1160	putative addiction module antidote protein, CopG/Arc/MetJ family	83aa	No
Cphamn1_1161	plasmid stabilization system	104aa	No
Cphamn1_1182	putative glycosyltransferase	281aa	No
Cphamn1_1209	hypothetical protein	37aa	Yes
Cphamn1_1210	hypothetical protein	72aa	No
Cphamn1_1220	hypothetical protein	64aa	Yes
Cphamn1_1245	hypothetical protein	109aa	Yes
Cphamn1_1248	hypothetical protein	59aa	No
Cphamn1_1250	CRISPR-associated protein, Csm1 family (IMGterm)	850aa	No
Cphamn1_1253	CRISPR-associated protein, Csm2 family (IMGterm)	141aa	No
Cphamn1_1255	CRISPR-associated protein, Csm4 family (IMGterm)	338aa	No
Cphamn1_1256	CRISPR-associated protein, Csm5 family (IMGterm)	380aa	No
Cphamn1_1264	hypothetical protein	34aa	No
Cphamn1_1284	hypothetical protein	32aa	Yes
Cphamn1_1297	-	496aa	No
Cphamn1_1298	hypothetical protein	44aa	No
Cphamn1_1308	Rhodanese domain protein	430aa	No
Cphamn1_1309	methyltransferase	334aa	No
Cphamn1_1310	Nitrilase/cyanide hydratase and apolipoprotein N-acyltransferase	311aa	No
Cphamn1_1312	hypothetical protein	116aa	No
Cphamn1_1319	hypothetical protein	66aa	Yes
Cphamn1_1328	hypothetical protein	486aa	No
Cphamn1_1329	hypothetical protein	355aa	No
Cphamn1_1330	hypothetical protein	497aa	No
Cphamn1_1362	hypothetical protein	79aa	No
Cphamn1_1365	hypothetical protein	47aa	Yes
Cphamn1_1375	hypothetical protein	65aa	No
Cphamn1_1382	transposase, IS5 family, putative	498aa	No
Cphamn1_1383	hypothetical protein	76aa	No
Cphamn1_1384	Radical SAM domain protein	330aa	No
Cphamn1_1385	Radical SAM domain protein	417aa	No
Cphamn1_1397	hypothetical protein	339aa	No
Cphamn1_1401	PilT protein domain protein	126aa	No
Cphamn1_1403	hypothetical protein	210aa	No
Cphamn1_1409	hypothetical protein	285aa	No
Cphamn1_1410	Flavodoxin-like protein	175aa	No
Cphamn1_1413	DNA-cytosine methyltransferase	420aa	No
Cphamn1_1414	hypothetical protein	635aa	No
Cphamn1_1416	NERD domain protein	578aa	No
Cphamn1_1417	hypothetical protein	540aa	Yes

Appendix

Locus Tag	ORF Name	Length	Unique in IMG
Cphamn1_1418	hypothetical protein	322aa	No
Cphamn1_1424	hypothetical protein	192aa	Yes
Cphamn1_1431	-	62aa	No
Cphamn1_1432	transposase, IS5 family, putative	498aa	No
Cphamn1_1449	hypothetical protein	70aa	No
Cphamn1_1455	-	430aa	No
Cphamn1_1468	hypothetical protein	49aa	Yes
Cphamn1_1500	hypothetical protein	99aa	No
Cphamn1_1501	alpha/beta hydrolase fold	340aa	No
Cphamn1_1537	hypothetical protein	34aa	Yes
Cphamn1_1539	hypothetical protein	235aa	No
Cphamn1_1540	hypothetical protein	454aa	No
Cphamn1_1541	hypothetical protein	104aa	No
Cphamn1_1543	hypothetical protein	124aa	No
Cphamn1_1546	hypothetical protein	142aa	No
Cphamn1_1548	hypothetical protein	239aa	No
Cphamn1_1549	hypothetical protein	196aa	No
Cphamn1_1565	hypothetical protein	97aa	No
Cphamn1_1566	Methyltransferase type 11	199aa	No
Cphamn1_1568	phosphoserine aminotransferase apoenzyme (EC 2.6.1.52) (IMGterm)	360aa	No
Cphamn1_1570	HAD-superfamily hydrolase, subfamily IA, variant 3	223aa	No
Cphamn1_1573	-	165aa	No
Cphamn1_1581	hypothetical protein	70aa	No
Cphamn1_1594	hypothetical protein	478aa	No
Cphamn1_1595	protein of unknown function DUF21	347aa	No
Cphamn1_1596	hypothetical protein	59aa	Yes
Cphamn1_1622	Outer membrane protein (porin)-like protein	333aa	No
Cphamn1_1652	transporter, CPA2 family (2.A.37) (IMGterm)	392aa	No
Cphamn1_1656	hypothetical protein	77aa	No
Cphamn1_1667	hypothetical protein	61aa	Yes
Cphamn1_1671	helicase domain protein	1066aa	No
Cphamn1_1672	hypothetical protein	604aa	No
Cphamn1_1673	hypothetical protein	409aa	No
Cphamn1_1676	PglZ domain protein	832aa	No
Cphamn1_1677	hypothetical protein	1171aa	No
Cphamn1_1678	hypothetical protein	174aa	No
Cphamn1_1680	hypothetical protein	1203aa	No
Cphamn1_1681	Domain of unknown function DUF1788	196aa	No
Cphamn1_1682	Protein of unknown function DUF1819 putative inner membrane	204aa	No
Cphamn1_1684	AIG2 family protein	185aa	No

Locus Tag	ORF Name	Length	Unique in IMG
Cphamn1_1686	hypothetical protein	53aa	No
Cphamn1_1687	hypothetical protein	30aa	No
Cphamn1_1705	hypothetical protein	85aa	No
Cphamn1_1725	proteinase inhibitor I4 serpin	431aa	No
Cphamn1_1743	hypothetical protein	54aa	No
Cphamn1_1744	hypothetical protein	156aa	No
Cphamn1_1780	hypothetical protein	34aa	Yes
Cphamn1_1784	hypothetical protein	39aa	Yes
Cphamn1_1785	Hpt protein	139aa	No
Cphamn1_1833	hypothetical protein	43aa	No
Cphamn1_1881	hypothetical protein	143aa	No
Cphamn1_1890	hypothetical protein	45aa	No
Cphamn1_1897	hypothetical protein	57aa	Yes
Cphamn1_1903	hypothetical protein	56aa	Yes
Cphamn1_1905	hypothetical protein	75aa	No
Cphamn1_1912	hypothetical protein	45aa	Yes
Cphamn1_1921	transposase, IS4 family (IMGterm)	498aa	No
Cphamn1_1927	cobalamin B12-binding domain protein	288aa	No
Cphamn1_1928	O-antigen polymerase	415aa	No
Cphamn1_1935	-	63aa	No
Cphamn1_1936	YcfA family protein	74aa	No
Cphamn1_1937	hypothetical protein	74aa	No
Cphamn1_1942	hypothetical protein	72aa	No
Cphamn1_1944	Excinuclease ABC C subunit domain protein	84aa	No
Cphamn1_1947	protein of unknown function DUF86	111aa	No
Cphamn1_1951	YcfA family protein	74aa	No
Cphamn1_1952	hypothetical protein	74aa	No
Cphamn1_1956	hypothetical protein	72aa	No
Cphamn1_1958	protein of unknown function DUF86	111aa	No
Cphamn1_1961	PilT protein domain protein	131aa	No
Cphamn1_1962	hypothetical protein	88aa	No
Cphamn1_1966	hypothetical protein	51aa	No
Cphamn1_1979	hypothetical protein	53aa	Yes
Cphamn1_1980	hypothetical protein	67aa	No
Cphamn1_1981	alpha-2-HS-glycoprotein	111aa	No
Cphamn1_1983	hypothetical protein	89aa	No
Cphamn1_1985	hypothetical protein	81aa	No
Cphamn1_2005	hypothetical protein	61aa	Yes
Cphamn1_2021	hypothetical protein	84aa	No
Cphamn1_2057	hypothetical protein	62aa	Yes
Cphamn1_2094	hypothetical protein	58aa	Yes
Cphamn1_2114	hypothetical protein	51aa	Yes

Appendix

Locus Tag	ORF Name	Length	Unique in IMG
Cphamn1_2120	hypothetical protein	42aa	No
Cphamn1_2128	hypothetical protein	77aa	No
Cphamn1_2143	hypothetical protein	177aa	No
Cphamn1_2147	hypothetical protein	296aa	No
Cphamn1_2169	hypothetical protein	98aa	No
Cphamn1_2179	hypothetical protein	57aa	Yes
Cphamn1_2197	hypothetical protein	41aa	Yes
Cphamn1_2206	hypothetical protein	102aa	No
Cphamn1_2215	hypothetical protein	85aa	Yes
Cphamn1_2219	hypothetical protein	55aa	No
Cphamn1_2221	prevent-host-death family protein	77aa	No
Cphamn1_2229	hypothetical protein	150aa	No
Cphamn1_2250	TfoX domain protein	90aa	No
Cphamn1_2255	hypothetical protein	31aa	No
Cphamn1_2265	hypothetical protein	43aa	Yes
Cphamn1_2317	hypothetical protein	31aa	No
Cphamn1_2323	hypothetical protein	219aa	No
Cphamn1_2337	hypothetical protein	183aa	No
Cphamn1_2338	hypothetical protein	76aa	Yes
Cphamn1_2354	Bile acid:sodium symporter	300aa	No
Cphamn1_2355	hypothetical protein	68aa	Yes
Cphamn1_2363	hypothetical protein	422aa	No
Cphamn1_2364	arsenite oxidase, small subunit	165aa	No
Cphamn1_2365	arsenite oxidase, large subunit	853aa	No
Cphamn1_2393	hypothetical protein	143aa	No
Cphamn1_2396	hypothetical protein	203aa	No
Cphamn1_2397	hypothetical protein	66aa	No
Cphamn1_2398	hypothetical protein	85aa	No
Cphamn1_2399	putative acetyltransferase	66aa	No
Cphamn1_2400	hypothetical protein	54aa	No
Cphamn1_2402	Methyltransferase type 11	159aa	No
Cphamn1_2403	Cupin 2 conserved barrel domain protein	115aa	No
Cphamn1_2404	hypothetical protein	90aa	No
Cphamn1_2410	hypothetical protein	97aa	No
Cphamn1_2411	hypothetical protein	174aa	No
Cphamn1_2412	hypothetical protein	121aa	No
Cphamn1_2423	hypothetical protein	39aa	No
Cphamn1_2427	hypothetical protein	47aa	No
Cphamn1_2434	transposase, IS4 family (IMGterm)	498aa	No
Cphamn1_2451	hypothetical protein	59aa	No
Cphamn1_2469	hypothetical protein	157aa	No
Cphamn1_2470	hypothetical protein	133aa	No

Locus Tag	ORF Name	Length	Unique in IMG
Cphamn1_2480	hypothetical protein	61aa	Yes
Cphamn1_2483	hypothetical protein	41aa	Yes
Cphamn1_2494	hypothetical protein	136aa	No
Cphamn1_2507	hypothetical protein	49aa	No
Cphamn1_2540	GTP-binding signal recognition particle SRP54, G-domain	137aa	No
Cphamn1_2551	hypothetical protein	133aa	No
Cphamn1_2552	hypothetical protein	196aa	No
Cphamn1_2553	hypothetical protein	77aa	Yes
Cphamn1_2554	hypothetical protein	616aa	No

Appendix

App. Table 2. Protein coding genes of *Chl. phaeobacteroides* BS1 that display significant differential expression between low and high light conditions. ORFs which were found to be unique to *Chl. phaeobacteroides* BS1 are marked in bold type and ORFs which were found to be differentially regulated through cDNA SSH are marked in italics. (CPB: counts per base meaning log base2 transformed mean expression per base of each gene; QN: normalized quantile)

ORF name	CPB high light	CPB low light	QN high light	QN low light	Δ low:high light	unique in IMG
Up regulated genes under high light condition						
<i>Cphamn1_0009 - cytochrome c class I</i>	36.55	12.44	5.27	3.58	-1.70	
Cphamn1_0016 - hypothetical protein	4.28	1.31	2.09	0.48	-1.61	Yes
Cphamn1_0025 - hypothetical protein	0.81	0.00	-0.44	-10.00	-9.56	
Cphamn1_0038 - Cobyrinic acid ac-diamide synthase	40.09	16.34	5.40	3.96	-1.44	
Cphamn1_0039 - hypothetical protein	6.31	0.97	2.70	0.09	-2.61	
Cphamn1_0107 - ammonium transporter	46.09	1.19	5.60	0.36	-5.24	
Cphamn1_0108 - nitrogen regulatory protein P-II	19.30	1.72	4.36	0.86	-3.50	
Cphamn1_0129 - PHP domain-containing protein	4.52	0.15	2.16	-2.52	-4.68	
Cphamn1_0135 - IstB domain-containing protein ATP-binding protein	0.11	0.00	-3.59	-10.00	-6.41	
Cphamn1_0137 - hypothetical protein	14.00	4.25	3.87	2.10	-1.77	
Cphamn1_0216 - hypothetical protein	0.80	0.03	-0.46	-4.26	-3.81	
Cphamn1_0257 - hypothetical protein	2.50	0.41	1.28	-1.08	-2.36	
Cphamn1_0285 - succinate dehydrogenase and fumarate reductase iron-sulfur protein	33.23	13.07	5.14	3.67	-1.47	
Cphamn1_0286 - CoB--CoM heterodisulfide reductase	36.67	15.48	5.28	3.89	-1.39	
Cphamn1_0423 - FolC bifunctional protein	5.38	1.95	2.43	1.01	-1.41	
Cphamn1_0426 - Tripartite ATP-independent periplasmic transporter DctQ component	1.45	0.21	0.45	-2.05	-2.49	
Cphamn1_0451 - molybdenum ABC transporter, periplasmic molybdate-binding protein	27.83	8.53	4.90	3.04	-1.86	
Cphamn1_0452 - TOBE domain-containing protein	15.89	5.95	4.06	2.56	-1.50	
Cphamn1_0453 - molybdate ABC transporter, inner membrane subunit	11.23	3.52	3.54	1.86	-1.69	
Cphamn1_0488 - phosphatidate cytidyltransferase	36.27	9.48	5.27	3.20	-2.07	
Cphamn1_0511 - hypothetical protein	46.72	1.45	5.64	0.61	-5.04	
Cphamn1_0512 - Alkaline phosphatase	50.19	0.20	5.75	-2.17	-7.92	
Cphamn1_0513 - YibE/F family protein	6.48	0.87	2.75	-0.07	-2.81	
Cphamn1_0571 - transcriptional regulator, XRE family	81.73	36.71	6.45	5.10	-1.35	
Cphamn1_0573 - putative transcriptional regulator	37.09	15.64	5.30	3.90	-1.40	
Cphamn1_0600 - rnhA ribonuclease H	2.48	0.32	1.26	-1.42	-2.68	
Cphamn1_0620 - hypothetical protein	21.31	8.37	4.50	3.01	-1.49	
Cphamn1_0621 - FeoA family protein	37.08	15.86	5.30	3.93	-1.37	
Cphamn1_0665 - hypothetical protein	2.75	0.63	1.42	-0.51	-1.93	
Cphamn1_0668 - CMP/dCMP deaminase zinc-binding	7.73	1.52	3.00	0.68	-2.32	
Cphamn1_0681 - Cobyrinic acid ac-diamide synthase	180.81	69.62	7.59	6.01	-1.58	
Cphamn1_0683 - hypothetical protein	113.61	40.27	6.94	5.24	-1.70	
Cphamn1_0685 - hypothetical protein	83.21	37.28	6.48	5.12	-1.36	

ORF name	CPB high light	CPB low light	QN high light	QN low light	Δ low:high light	unique in IMG
Cphamn1_0856 - hypothetical protein	1.09	0.10	-0.01	-3.04	-3.02	Yes
Cphamn1_0863 - outer membrane efflux protein	8.21	0.14	3.08	-2.66	-5.74	
Cphamn1_0864 - efflux transporter, RND family, MFP subunit	27.97	0.91	4.91	0.01	-4.90	
Cphamn1_0865 - heavy metal efflux pump, CzCA family	2.61	0.44	1.34	-0.98	-2.32	
Cphamn1_0888 - hypothetical protein	84.64	39.06	6.52	5.20	-1.32	
Cphamn1_0889 - transcriptional regulator, XRE family	111.50	42.66	6.92	5.33	-1.59	
Cphamn1_0914 - hypothetical protein	2.20	0.02	1.11	-4.80	-5.91	Yes
Cphamn1_0951 - hypothetical protein	1.69	0.27	0.69	-1.73	-2.42	Yes
Cphamn1_0952 - transcriptional regulator, AsnC family	107.11	14.48	6.84	3.80	-3.04	
Cphamn1_0953 - glutamine synthetase catalytic region	169.78	21.80	7.49	4.36	-3.12	
Cphamn1_1136 - hypothetical protein	82.28	8.89	6.46	3.11	-3.35	
Cphamn1_1137 - nitrogen regulatory protein P-II	1169.64	83.62	10.29	6.28	-4.01	
<i>Cphamn1_1138 - ammonium transporter</i>	298.49	4.92	8.31	2.31	-5.99	
Cphamn1_1166 - UspA domain-containing protein	5.56	1.92	2.47	1.00	-1.47	
Cphamn1_1212 - hypothetical protein	27.89	2.31	4.91	1.26	-3.65	
Cphamn1_1213 - tRNA guanosine-2'-O-methyltransferase	26.14	4.00	4.81	2.02	-2.79	
Cphamn1_1225 - phospholipid/glycerol acyltransferase	18.77	1.18	4.32	0.34	-3.98	
Cphamn1_1226 - hypothetical protein	373.83	0.76	8.61	-0.26	-8.88	
Cphamn1_1227 - hypothetical protein	84.47	0.67	6.50	-0.44	-6.94	
<i>Cphamn1_1228 - hypothetical protein</i>	83.39	0.69	6.48	-0.41	-6.89	
Cphamn1_1229 - phosphate binding protein	266.32	1.56	8.13	0.72	-7.41	
Cphamn1_1230 - ABC-type phosphate transport system periplasmic component-like protein	264.84	2.60	8.11	1.42	-6.69	
Cphamn1_1231 - phosphate ABC transporter, ATPase subunit	46.35	1.16	5.61	0.32	-5.29	
Cphamn1_1232 - phosphate ABC transporter, inner membrane subunit PstC	4.31	0.32	2.10	-1.39	-3.48	
Cphamn1_1233 - phosphate ABC transporter, inner membrane subunit PstA	6.13	0.39	2.65	-1.18	-3.82	
Cphamn1_1234 - phosphate ABC transporter, inner membrane subunit PstC	6.06	1.00	2.62	0.13	-2.49	
Cphamn1_1235 - phosphate ABC transporter, inner membrane subunit PstA	13.66	2.95	3.83	1.60	-2.23	
Cphamn1_1237 - phosphate uptake regulator, PhoU	25.78	10.97	4.79	3.40	-1.39	
Cphamn1_1271 - hypothetical protein	186.74	11.90	7.67	3.51	-4.15	
Cphamn1_1312 - hypothetical protein	3.68	1.02	1.84	0.15	-1.68	
Cphamn1_1387 - aminoacyl-histidine dipeptidase	4.26	0.74	2.08	-0.32	-2.40	
Cphamn1_1389 - hypothetical protein	29.05	8.26	4.97	2.99	-1.98	
Cphamn1_1390 - hypothetical protein	273.61	74.68	8.17	6.12	-2.05	
Cphamn1_1391 - transcriptional regulator, ArsR family	323.63	95.84	8.44	6.48	-1.96	
Cphamn1_1475 - hypothetical protein	61.50	3.27	6.03	1.75	-4.29	
Cphamn1_1534 - Inorganic pyrophosphatase	10.33	1.18	3.42	0.35	-3.07	
Cphamn1_1535 - TonB-dependent receptor	22.32	0.27	4.57	-1.67	-6.24	
Cphamn1_1536 - phytase	22.92	10.10	4.62	3.28	-1.33	
Cphamn1_1543 - hypothetical protein	4.99	0.75	2.31	-0.29	-2.60	

Appendix

ORF name	CPB high light	CPB low light	QN high light	QN low light	Δ low:high light	unique in IMG
Cphamn1_1554 - FAD-dependent pyridine nucleotide-disulphide oxidoreductase	332.23	5.79	8.48	2.53	-5.96	
Cphamn1_1562 - hypothetical protein	25.49	9.51	4.78	3.20	-1.58	
Cphamn1_1590 - hydrogenase maturation protease	7.99	0.35	3.05	-1.29	-4.33	
Cphamn1_1591 - Ni/Fe-hydrogenase, b-type cytochrome subunit	19.86	0.31	4.41	-1.44	-5.85	
Cphamn1_1592 - nickel-dependent hydrogenase large subunit	80.62	0.97	6.41	0.09	-6.32	
Cphamn1_1593 - hydrogenase (NiFe) small subunit HydA	25.37	0.37	4.77	-1.22	-6.00	
Cphamn1_1604 - NADH dehydrogenase (quinone)	26.97	11.58	4.86	3.48	-1.38	
Cphamn1_1644 - protein tyrosine phosphatase	83.03	4.84	6.47	2.28	-4.19	
Cphamn1_1650 - SSS sodium solute transporter superfamily	1.34	0.20	0.32	-2.09	-2.41	
Cphamn1_1652 - sodium/hydrogen exchanger	57.68	2.42	5.95	1.32	-4.63	
Cphamn1_1653 - hypothetical protein	165.23	6.80	7.45	2.72	-4.73	
Cphamn1_1694 - two component transcriptional regulator, winged helix family	31.52	13.08	5.07	3.67	-1.41	
Cphamn1_1705 - hypothetical protein	10.49	2.38	3.45	1.29	-2.16	
Cphamn1_1747 - pyruvate carboxyltransferase	29.47	0.32	4.99	-1.41	-6.40	
Cphamn1_1748 - transcriptional regulator, NifA, Fis Family	8.10	0.17	3.06	-2.38	-5.44	
Cphamn1_1751 - nifH nitrogenase reductase	689.84	52.39	9.41	5.62	-3.79	
Cphamn1_1752 - nitrogen regulatory protein P-II	366.90	18.75	8.59	4.14	-4.44	
Cphamn1_1753 - nitrogen regulatory protein P-II	1642.56	65.95	10.89	5.94	-4.95	
Cphamn1_1754 - nitrogenase molybdenum-iron protein alpha chain	38.97	1.33	5.34	0.50	-4.85	
Cphamn1_1755 - nitrogenase molybdenum-iron protein beta chain	19.51	0.64	4.38	-0.49	-4.86	
Cphamn1_1756 - nitrogenase MoFe cofactor biosynthesis protein NifE	27.28	0.74	4.87	-0.31	-5.19	
Cphamn1_1757 - Nitrogenase	13.94	0.76	3.86	-0.27	-4.13	
Cphamn1_1758 - nitrogenase cofactor biosynthesis protein NifB	18.41	0.58	4.29	-0.61	-4.91	
Cphamn1_1809 - pyruvoyl-dependent arginine decarboxylase	26.01	9.71	4.80	3.23	-1.57	
Cphamn1_1831 - hypothetical protein	21.50	8.29	4.51	3.00	-1.51	
Cphamn1_1950 - hypothetical protein	0.11	0.00	-3.71	-10.00	-6.29	
Cphamn1_1985 - hypothetical protein	0.12	0.00	-3.48	-10.00	-6.52	
Cphamn1_1987 - Plastoquinol--plastocyanin reductase	22.11	9.83	4.56	3.24	-1.31	
Cphamn1_2002 - GTP-dependent nucleic acid-binding protein EngD	1.97	0.20	0.93	-2.15	-3.08	
Cphamn1_2044 - cytochrome c assembly protein	22.74	10.05	4.61	3.28	-1.33	
Cphamn1_2129 - hydrogenase/sulfur reductase, beta subunit	20.72	8.52	4.46	3.04	-1.42	
Cphamn1_2142 - hypothetical protein	0.06	0.00	-6.14	-10.00	-3.86	
Cphamn1_2214 - hypothetical protein	6.61	2.12	2.79	1.12	-1.67	
Cphamn1_2215 - hypothetical protein	5.61	0.93	2.49	0.05	-2.44	Yes
Cphamn1_2216 - Class I peptide chain release factor	3.40	0.78	1.72	-0.22	-1.94	
Cphamn1_2229 - hypothetical protein	23.37	9.80	4.64	3.24	-1.40	
Cphamn1_2309 - obgE GTPase ObgE	47.18	19.10	5.65	4.17	-1.48	
Cphamn1_2320 - hypothetical protein	12.24	5.03	3.66	2.35	-1.31	
Cphamn1_2328 - hypothetical protein	0.49	0.00	-1.24	-10.00	-8.76	
Cphamn1_2332 - outer membrane protein-like protein	0.13	0.00	-3.34	-10.00	-6.66	

ORF name	CPB high light	CPB low light	QN high light	QN low light	Δ low:high light	unique in IMG
Cphamn1_2358 - hypothetical protein	9.87	4.03	3.35	2.03	-1.32	
Cphamn1_2359 - molybdopterin biosynthesis MoaE protein	20.05	5.69	4.42	2.51	-1.92	
Cphamn1_2361 - molybdenum cofactor synthesis domain-containing protein	4.04	1.10	1.98	0.26	-1.72	
Cphamn1_2362 - moaC bifunctional molybdenum cofactor biosynthesis protein MoaC/MogA	19.26	3.07	4.35	1.65	-2.70	
Cphamn1_2363 - hypothetical protein	627.53	88.22	9.32	6.38	-2.94	
Cphamn1_2364 - arsenite oxidase, small subunit	137.34	3.65	7.22	1.91	-5.32	
Cphamn1_2365 - arsenite oxidase, large subunit	84.56	3.51	6.51	1.85	-4.65	
Cphamn1_2366 - molybdenum cofactor biosynthesis protein A	23.34	5.76	4.64	2.52	-2.12	
Cphamn1_2372 - hypothetical protein	0.52	0.00	-1.14	-10.00	-8.86	
Cphamn1_2394 - cytoplasmic alpha-amylase	51.11	20.28	5.78	4.25	-1.53	
Cphamn1_2403 - Cupin 2 conserved barrel domain-containing protein	7.89	2.08	3.03	1.09	-1.94	
Cphamn1_2453 - adenosylmethionine-8-amino-7-oxononanoate amino-transferase	1.23	0.19	0.17	-2.22	-2.40	
Cphamn1_2454 - dethiobiotin synthase	4.63	0.56	2.20	-0.67	-2.87	
Cphamn1_2455 - biotin biosynthesis protein BioC	3.65	0.74	1.82	-0.31	-2.13	
Cphamn1_2456 - hypothetical protein	2.98	0.43	1.53	-1.03	-2.57	
Cphamn1_2457 - 8-amino-7-oxononanoate synthase	7.62	1.31	2.98	0.48	-2.50	
Cphamn1_2458 - Biotin synthase	2.84	0.33	1.46	-1.37	-2.83	
Cphamn1_2459 - biotin/acetyl-CoA-carboxylase ligase	4.66	0.21	2.21	-2.02	-4.23	
Cphamn1_R0023 - Val tRNA	0.26	0.00	-2.12	-10.00	-7.88	
Cphamn1_R0031 - Ser tRNA	0.11	0.00	-3.63	-10.00	-6.37	
Cphamn1_R0043 - Pro tRNA	0.11	0.00	-3.76	-10.00	-6.24	
Cphamn1_R0051 - Phe tRNA	4.37	0.77	2.11	-0.24	-2.36	
Cphamn1_R0055 - ffs	0.30	0.00	-1.92	-10.00	-8.08	
Up-regulated genes under low light condition						
Cphamn1_0188 - N-6 DNA methylase	0.00	0.01	-10.00	-5.65	4.35	
Cphamn1_0191 - hypothetical protein	0.02	0.07	-7.79	-3.48	4.31	Yes
Cphamn1_0200 - camphor resistance protein CrcB	3.50	9.43	1.77	3.19	1.42	
Cphamn1_0242 - esterase/lipase, putative	1.43	4.43	0.43	2.16	1.74	
Cphamn1_0328 - hypothetical protein	20.93	63.13	4.48	5.88	1.40	
Cphamn1_0341 - phosphoserine phosphatase SerB	5.08	13.05	2.33	3.67	1.33	
Cphamn1_0363 - phosphoenolpyruvate-protein phosphotransferase	6.05	8.49	2.62	3.93	1.31	
Cphamn1_0494 - transposase, IS5 family, putative	0.00	0.00	-9.77	-5.90	3.88	
Cphamn1_0507 - permease	0.09	1.36	-4.26	0.52	4.79	
Cphamn1_0508 - redox-active disulfide protein 2	1.25	6.83	0.21	2.73	2.52	
Cphamn1_0783 - groEL chaperonin GroEL	15.30	56.82	4.00	5.72	1.72	
Cphamn1_0848 - alkyl hydroperoxide reductase/ Thiol specific antioxidant / Mal allergen	43.07	170.47	5.49	7.27	1.78	
Cphamn1_0915 - hypothetical protein	1.52	8.21	0.52	2.98	2.47	Yes

Appendix

ORF name	CPB high light	CPB low light	QN high light	QN low light	Δ low:high light	unique in IMG
Cpham1_0975 - rpmG 50S ribosomal protein L33	20.81	78.96	4.47	6.21	1.74	
Cpham1_1075 - hypothetical protein	0.17	0.85	-2.85	-0.09	2.76	
Cpham1_1076 - Dinitrogenase iron-molybdenum cofactor biosynthesis protein	11.84	75.64	3.61	6.15	2.54	
Cpham1_1077 - hypothetical protein	6.07	19.43	2.63	4.19	1.57	
Cpham1_1083 - hypothetical protein	0.17	0.80	-2.90	-0.18	2.73	
Cpham1_1095 - sigma-24 (FecI-like)	3.64	11.45	1.82	3.46	1.65	
Cpham1_1101 - hppA membrane-bound proton-translocating pyrophosphatase	5.96	17.51	2.60	4.06	1.47	
Cpham1_1139 - putative anti-sigma regulatory factor, serine/threonine protein kinase	49.76	174.14	5.74	7.33	1.59	
Cpham1_1141 - hypothetical protein	0.27	2.16	-2.07	1.14	3.21	Yes
Cpham1_1142 - hypothetical protein	0.36	1.69	-1.68	0.84	2.52	
Cpham1_1149 - type III restriction protein res subunit	2.97	8.72	1.53	3.08	1.55	
Cpham1_1150 - hypothetical protein	2.97	10.98	1.53	3.41	1.88	
Cpham1_1248 - hypothetical protein	4.28	12.41	2.09	3.57	1.48	
Cpham1_1264 - hypothetical protein	99.56	296.31	6.75	8.14	1.39	
Cpham1_1331 - hypothetical protein	50.98	154.87	5.77	7.13	1.36	
Cpham1_1363 - Integrase catalytic region	0.05	0.03	-7.23	-4.37	2.87	
Cpham1_1366 - RNA polymerase, sigma-24 subunit, ECF subfamily	436.25	1841.74	8.83	10.63	1.79	
Cpham1_1371 - hypothetical protein	1.59	4.79	0.59	2.27	1.68	
Cpham1_1375 - hypothetical protein	24.46	201.23	4.71	7.57	2.86	
Cpham1_1382 - transposase, IS5 family, putative	0.00	0.00	-10.00	-6.14	3.86	
Cpham1_1403 - hypothetical protein	240.38	695.99	8.01	9.57	1.56	
Cpham1_1412 - DNA mismatch endonuclease Vsr	3.77	12.63	1.88	3.61	1.73	
Cpham1_1468 - hypothetical protein	0.00	0.78	-10.00	-0.22	9.78	Yes
Cpham1_1508 - Glyoxalase/bleomycin resistance protein/dioxygenase	4.91	14.46	2.28	3.80	1.51	
Cpham1_1637 - transcriptional regulator, MarR family	4.64	14.91	2.20	3.84	1.64	
Cpham1_1706 - heat shock protein Hsp20	19.78	144.44	4.40	7.04	2.63	
Cpham1_1707 - dnaK molecular chaperone DnaK	10.17	92.62	3.40	6.44	3.04	
Cpham1_1782 - purine nucleoside phosphorylase	13.83	40.62	3.85	5.25	1.40	
Cpham1_1816 - Ag473	98.13	307.86	6.72	8.20	1.48	
Cpham1_1817 - bifunctional aconitate hydratase 2/2-methylisocitrate dehydratase	5.01	21.29	2.32	4.32	2.01	
Cpham1_1833 - hypothetical protein	0.00	0.32	-10.00	-1.40	8.60	
Cpham1_1865 - Polysulphide reductase NrfD	1.13	3.20	0.03	1.71	1.68	
Cpham1_1881 - hypothetical protein	18.72	58.71	4.32	5.77	1.45	

ORF name	CPB high light	CPB low light	QN high light	QN low light	Δ low:high light	unique in IMG
Cphamn1_1897 - hypothetical protein	0.34	3.82	-1.74	1.97	3.71	Yes
Cphamn1_1913 - dTDP-4-dehydrorhamnose 3,5-epimerase	5.68	15.85	2.51	3.93	1.42	
Cphamn1_1925 - glycosyl transferase family 2	28.92	91.34	4.96	6.42	1.47	
Cphamn1_1926 - hypothetical protein	0.00	0.03	-10.00	-4.29	5.71	
Cphamn1_1934 - S23 ribosomal protein	1.28	3.58	0.24	1.88	1.64	
Cphamn1_1951 - YcfA family protein	0.00	1.50	-10.00	0.65	10.65	
Cphamn1_1961 - PilT protein domain-containing protein	10.78	26.45	3.49	5.35	1.87	
Cphamn1_1980 - hypothetical protein	0.00	0.41	-10.00	-1.06	8.94	
Cphamn1_1984 - Excinuclease ABC C subunit domain-containing protein	4.57	20.25	2.17	4.25	2.08	
Cphamn1_2005 - hypothetical protein	1.59	4.24	0.59	2.09	1.50	Yes
Cphamn1_2116 - YbaK/prolyl-tRNA synthetase associated region	44.90	166.78	5.56	7.25	1.69	
Cphamn1_2120 - hypothetical protein	0.33	2.62	-1.82	1.43	3.25	
Cphamn1_2141 - hypothetical protein	1.58	9.19	0.59	3.16	2.57	
Cphamn1_2160 - CRISPR-associated protein, Cse2 family	0.49	2.02	-1.22	1.06	2.29	
Cphamn1_2204 - TonB-dependent receptor	69.89	335.52	6.22	8.31	2.08	
<i>Cphamn1_2207 - magnesium chelatase subunit H</i>	8.17	21.74	3.07	4.36	1.28	
Cphamn1_2334 - CRISPR-associated protein Cas2	1.93	5.36	0.88	2.43	1.55	
Cphamn1_2371 - transposase IS4 family protein	0.03	0.05	-7.48	-3.76	3.72	
Cphamn1_2423 - hypothetical protein	0.00	0.39	-10.00	-1.14	8.86	
Cphamn1_2424 - hypothetical protein	0.61	7.95	-0.92	2.94	3.86	
Cphamn1_2425 - cytochrome B561	1.42	17.40	0.41	4.05	3.64	
Cphamn1_2426 - cytochrome c family protein	1.83	13.04	0.79	3.66	2.87	
Cphamn1_2434 - transposase, IS5 family, putative	0.00	0.01	-10.00	-4.92	5.08	
Cphamn1_2491 - hypothetical protein	11.23	60.10	3.54	5.81	2.27	
Cphamn1_R0001 - Thr tRNA	0.00	1.68	-10.00	0.82	10.82	
Cphamn1_R0020 - Leu tRNA	0.00	0.03	-10.00	-4.16	5.84	
Cphamn1_R0021 - Lys tRNA	0.51	3.47	-1.18	1.84	3.01	
Cphamn1_R0027 - Leu tRNA	4.19	11.24	2.05	3.44	1.39	
Cphamn1_R0033 - Met tRNA	3.57	17.08	1.80	4.02	2.23	
Cphamn1_R0036 - Cys tRNA	0.63	2.71	-0.90	1.48	2.38	

Appendix

App. Table 3. Protein coding genes of *Chl. phaeobacteroides* BS1 with the 50 highest transcript numbers registrated under low light conditions. ORFs which were found to be unique to *Chl. phaeobacteroides* BS1 are marked in bold type and ORFs which were found to be differentially regulated through cDNA SSH are marked in italics. (CPB: counts per base, meaning log base2 transformed mean expression per base of each gene; QN: normalized quantile)

ORF name	CPB high light	CPB low light	QN high light	QN low light	Δ low:high light	unique in IMG
Cphamn1_2195 - bacteriochlorophyll C binding protein	7577.27	14788.59	13.37	13.37	0.00	
Cphamn1_1392 - RNP-1 like RNA-binding protein	2502.30	6195.52	11.47	12.04	0.57	
Cphamn1_1042 - hypothetical protein	1355.07	3206.79	10.63	11.47	0.84	
Cphamn1_0433 - hypothetical protein	1613.09	2281.80	10.86	10.96	0.11	
<i>Cphamn1_R0045 - -</i>	2864.37	2195.98	12.04	10.89	-1.15	
Cphamn1_0689 - hypothetical protein	1394.05	1878.57	10.66	10.66	0.00	
<i>Cphamn1_1366 - RNA polymerase, sigma-24 subunit, ECF subfamily</i>	436.25	1841.74	8.83	10.63	1.79	
Cphamn1_2210 - heat shock protein Hsp20	1062.80	1820.52	10.14	10.60	0.47	
Cphamn1_2272 - rpsM 30S ribosomal protein S13	1327.94	1428.53	10.43	10.43	0.00	
Cphamn1_1710 - peptidoglycan-associated lipoprotein	825.08	1367.24	9.57	10.33	0.76	
Cphamn1_1769 - hypothetical protein	502.35	1189.79	9.01	10.14	1.13	
Cphamn1_1838 - adenylylsulfate reductase, beta subunit	892.93	1030.09	9.70	9.93	0.23	
Cphamn1_0720 - transcriptional regulator, CopG family	928.75	775.34	9.93	9.70	-0.23	
<i>Cphamn1_1403 - hypothetical protein</i>	240.38	695.99	8.01	9.57	1.56	
Cphamn1_0254 - hypothetical protein	718.13	682.94	9.45	9.53	0.08	
Cphamn1_1368 - hypothetical protein	314.06	680.22	8.35	9.45	1.09	
Cphamn1_1265 - hypothetical protein	256.95	651.86	8.09	9.32	1.23	
Cphamn1_2273 - rpmJ 50S ribosomal protein L36	387.16	531.09	8.69	9.06	0.37	
Cphamn1_0823 - hypothetical protein	279.36	477.97	8.19	8.84	0.66	
Cphamn1_R0006 - 23S ribosomal RNA	371.22	475.71	8.60	8.83	0.24	
<i>Cphamn1_0841 - bacteriochlorophyll A protein</i>	221.23	473.95	7.89	8.79	0.90	
Cphamn1_0721 - addiction module toxin, ReE/StbE family	699.59	467.10	9.42	8.77	-0.65	
Cphamn1_0892 - hypothetical protein	231.33	433.24	7.96	8.68	0.72	Yes
Cphamn1_2279 - rpsE 30S ribosomal protein S5	286.34	406.75	8.23	8.60	0.37	
Cphamn1_0163 - single-strand binding protein	346.29	402.62	8.54	8.59	0.04	
Cphamn1_0306 - 4Fe-4S ferredoxin iron-sulfur binding domain-containing protein	211.76	402.49	7.82	8.54	0.72	
Cphamn1_2173 - hypothetical protein	281.17	385.64	8.20	8.48	0.28	
Cphamn1_0234 - hypothetical protein	269.56	373.52	8.14	8.44	0.30	
Cphamn1_0106 - RNP-1 like RNA-binding protein	145.41	345.16	7.30	8.38	1.08	
Cphamn1_0126 - zinc finger CDGSH-type domain-containing protein	408.90	340.51	8.77	8.35	-0.42	
<i>Cphamn1_2204 - TonB-dependent receptor</i>	69.89	335.52	6.22	8.31	2.08	

Appendix

ORF name	CPB high light	CPB low light	QN high light	QN low light	Δ low:high light	unique in IMG
Cphamn1_0124 - iojap-like protein	295.70	332.27	8.29	8.29	0.00	
Cphamn1_1010 - phosphoribosylformylglycinamide synthase, purS	537.06	320.41	9.06	8.27	-0.80	
Cphamn1_1243 - hypothetical protein	120.88	315.87	7.05	8.23	1.18	
Cphamn1_0265 - chlorosome envelope protein B	397.16	308.03	8.71	8.20	-0.51	
<i>Cphamn1_1816 - Ag473</i>	98.13	307.86	6.72	8.20	1.48	
Cphamn1_2538 - hypothetical protein	149.66	303.96	7.33	8.19	0.85	
Cphamn1_1850 - hypothetical protein	187.82	302.70	7.67	8.17	0.49	
Cphamn1_0690 - hypothetical protein	499.20	297.02	8.99	8.15	-0.84	
<i>Cphamn1_1264 - hypothetical protein</i>	99.56	296.31	6.75	8.14	1.39	
Cphamn1_0719 - hypothetical protein	227.85	291.48	7.94	8.12	0.18	Yes
Cphamn1_0179 - acpP acyl carrier protein	441.21	287.34	8.84	8.09	-0.76	
Cphamn1_0693 - hypothetical protein	178.78	277.16	7.57	8.04	0.47	
Cphamn1_0414 - outer membrane chaperone Skp (OmpH)	130.79	276.01	7.17	8.01	0.84	
Cphamn1_2283 - rpsN 30S ribosomal protein S14	238.79	271.32	7.99	7.97	-0.02	
Cphamn1_0578 - photosystem P840 reaction center cytochrome c-551	120.22	264.03	7.04	7.94	0.89	
Cphamn1_1367 - putative transmembrane anti-sigma factor	141.52	254.13	7.28	7.89	0.61	
Cphamn1_0782 - groES co-chaperonin GroES	93.68	252.61	6.65	7.88	1.23	
Cphamn1_0691 - mobilizable transposon, xis protein	114.41	250.51	6.96	7.87	0.91	
Cphamn1_1071 - hypothetical protein	218.28	245.44	7.87	7.85	-0.02	

REFERENCES

- Airs, R.L., Atkinson, J.E., and Keely, B.J. (2001). Development and application of a high resolution liquid chromatographic method for the analysis of complex pigment distributions. *J Chromat* 917, 167–177.
- Alekshun, M.N., and Levy, S.B. (1999). The mar regulon: multiple resistance to antibiotics and other toxic chemicals. *Trends in Microbiology* 7, 410–413.
- Altschul, S.F., Madden, T.L., Schäffer, A.A., Zhang, J., Zhang, Z., Miller, W., and Lipman, D.J. (1997). Gapped BLAST and PSI-BLAST: a new generation of protein database search programs. *Nucleic Acids Res* 25, 3389–3402.
- Ames, G.F.L. (1986). Bacterial Periplasmic Transport Systems: Structure, Mechanism, and Evolution. *Annu. Rev. Biochem.* 55, 397–425.
- Anbar, A.D., and Knoll, A.H. (2002). Proterozoic Ocean Chemistry and Evolution: A Bioinorganic Bridge? *Science* 297, 1137–1142.
- Arnold, K., Bordoli, L., Kopp, J., and Schwede, T. (2006). The SWISS-MODEL workspace: a web-based environment for protein structure homology modelling. *Bioinformatics* 22, 195–201.
- Balch, W.E., Fox, G.E., Magrum, L.J., Woese, C.R., and Wolfe, R.S. (1979). Methanogens: reevaluation of a unique biological group. *Microbiol Rev* 43, 260–296.
- Beja, O., Suzuki, M.T., Heidelberg, J.F., Nelson, W.C., Preston, C.M., Hamada, T., Eisen, J.A., Fraser, C.M., and DeLong, E.F. (2002). Unsuspected diversity among marine aerobic anoxygenic phototrophs. *Nature* 415, 630–633.
- Bélangier, G., and Gingras, G. (1988). Structure and expression of the *puf* operon messenger RNA in *Rhodospirillum rubrum*. *J. Biol. Chem* 263, 7639–7645.
- Benson, D.A., Karsch-Mizrachi, I., Lipman, D.J., Ostell, J., and Wheeler, D.L. (2008). GenBank. *Nucleic Acids Res* 36, D25–D30.
- Bérard, J., Bélangier, G., Corriveau, P., and Gingras, G. (1986). Molecular cloning and sequence of the B880 holochrome gene from *Rhodospirillum rubrum*. *J. Biol. Chem* 261, 82–87.
- Berman, H.M., Westbrook, J., Feng, Z., Gilliland, G., Bhat, T.N., Weissig, H., Shindyalov, I.N., and Bourne, P.E. (2000). The Protein Data Bank. *Nucleic Acids Res* 28, 235–242.
- Bertini, I., Cavallaro, G., and Rosato, A. (2006). Cytochrome c: Occurrence and Functions. *Chemical Reviews* 106, 90–115.

References

- Blankenship, R., and Matsuura, K. (2003). Antenna Complexes from Green photosynthetic Bacteria. In *Light-harvesting antennas in photosynthesis*, B.R. Green, and W.W. Parson, eds. (Springer), pp. 195–211.
- Borrego, C.M., Arellano, J.B., Abella, C.A., Gillbro, T., and Garcia-Gil, J. (1999). The molar extinction coefficient of bacteriochlorophyll e and the pigment stoichiometry in *Chlorobium phaeobacteroides*. *Photosynthesis Research* 60, 257–264.
- Brune, D.C. (1989). Sulfur oxidation by phototrophic bacteria. *Biochim. Biophys. Acta* 975, 189–221.
- Bullard, J.H., Purdom, E., Hansen, K.D., and Dudoit, S. (2010). Evaluation of statistical methods for normalization and differential expression in mRNA-Seq experiments. *BMC Bioinformatics* 11, 94.
- Bullough, P.A., Qian, P., and Hunter, C.N. (2008). Reaction Center-Light-Harvesting Core Complexes of Purple Bacteria. In *The Purple Phototrophic Bacteria*, (Springer Netherlands), pp. 155–179.
- Bylina, E.J., Robles, S.J., and Youvan, D.C. (1988). Directed mutations affecting the putative bacteriochlorophyll-binding sites in the light-harvesting I antenna of *Rhodobacter capsulatus*. *Isr. J. Chem.* 28, 73–78.
- Campbell, E.A., Korzheva, N., Mustaev, A., Murakami, K., Nair, S., Goldfarb, A., and Darst, S.A. (2001). Structural Mechanism for Rifampicin Inhibition of Bacterial RNA Polymerase. *Cell* 104, 901–912.
- Cecchini, G., Schröder, I., Gunsalus, R.P., and Maklashina, E. (2002). Succinate dehydrogenase and fumarate reductase from *Escherichia coli*. *Biochimica et Biophysica Acta (BBA) - Bioenergetics* 1553, 140–157.
- Chen, C.-Y.A., Beatty, J.T., Cohen, S.N., and Belasco, J.G. (1988). An intercistronic stem-loop structure functions as an mRNA decay terminator necessary but insufficient for puf mRNA stability. *Cell* 52, 609–619.
- Chew, A.G.M., Frigaard, N.-U., and Bryant, D.A. (2007). Bacteriochlorophyllide c C-82 and C-121 Methyltransferases Are Essential for Adaptation to Low Light in *Chlorobaculum tepidum*. *J Bacteriol.* 189, 6176–6184.
- Chomczynski, P., and Sacchi, N. (1987). Single-step method of RNA isolation by acid guanidinium thiocyanate-phenol-chloroform extraction. *Anal. Biochem* 162, 156–159.
- Cogdell, R.J., Howard, T.D., Isaacs, N.W., McLuskey, K., and Gardiner, A.T. (2002). Structural factors which control the position of the Qy absorption band of bacteriochlorophyll a in purple bacterial antenna complexes. *PhotosyRes* 74, 135–141.
- Cogdell, R.J., Isaacs, N.W., Howard, T.D., McLuskey, K., Fraser, N.J., and Prince, S.M. (1999). How photosynthetic bacteria harvest solar energy. *J. Bacteriol* 181, 3869–3879.

- Conroy, M.J., Westerhuis, W.H., Parkes-Loach, P.S., Loach, P.A., Hunter, C.N., and Williamson, M.P. (2000). The solution structure of *Rhodobacter sphaeroides* LH1[beta] reveals two helical domains separated by a more flexible region: structural consequences for the LH1 complex. *J Mol Biol* 298, 83–94.
- Coolen, M.J.L., and Overmann, J. (2000). Functional Exoenzymes as Indicators of Metabolically Active Bacteria in 124,000-Year-Old Sapropel Layers of the Eastern Mediterranean Sea. *Appl Environ Microbiol* 66, 2589–2598.
- Coolen, M.J.L., and Overmann, J. (2007). 217 000-year-old DNA sequences of green sulfur bacteria in Mediterranean sapropels and their implications for the reconstruction of the paleoenvironment. *Environ Microbiol* 9, 238–249.
- Costanzo, A., and Ades, S.E. (2006). Growth phase-dependent regulation of the extracytoplasmic stress factor, sigmaE, by guanosine 3',5'-bispyrophosphate (ppGpp). *J. Bacteriol.* 188, 4627–4634.
- Davis, C.M., Bustamante, P.L., Todd, J.B., Parkes-Loach, P.S., McGlynn, P., Olsen, J.D., McMaster, L., Hunter, C.N., and Loach, P.A. (1997). Evaluation of Structure–Function Relationships in the Core Light-Harvesting Complex of Photosynthetic Bacteria by Reconstitution with Mutant Polypeptides. *Biochemistry* 36, 3671–3679.
- Degens, E.T., and Ross, D.A. (1972). Chronology of the Black Sea over the last 25,000 years. *Chemical Geology* 10, 1–16.
- Dietrich, G., Kalle, K., Krauss, W., and Siedler, G. (1975). *Allgemeine Meereskunde* (Berlin, Stuttgart: Gebrüder Bornträger).
- Eccles, J., and Honig, B. (1983). Charged amino acids as spectroscopic determinants for chlorophyll in vivo. *Proc. Natl. Acad. Sci. U.S.A* 80, 4959–4962.
- Ehretsmann, C.P., Carpousis, A.J., and Krisch, H.M. (1992). Specificity of *Escherichia coli* endoribonuclease RNase E: in vivo and in vitro analysis of mutants in a bacteriophage T4 mRNA processing site. *Genes & Development* 6, 149–159.
- Eisenberg, D., Almassy, R.J., Janson, C.A., Chapman, M.S., Suh, S.W., Cascio, D., and Smith, W.W. (1987). Some evolutionary relationships of the primary biological catalysts glutamine synthetase and RuBisCO. *Cold Spring Harb Symp Quant Biol* 52, 483–490.
- Eisen, J.A., Nelson, K.E., Paulsen, I.T., Heidelberg, J.F., Wu, M., Dodson, R.J., Deboy, R., Gwinn, M.L., Nelson, W.C., Haft, D.H., et al. (2002). The complete genome sequence of *Chlorobium tepidum* TLS, a photosynthetic, anaerobic, green-sulfur bacterium. *Proc. Natl. Acad. Sci. U.S.A* 99, 9509–9514.
- Emeis K.-C., Sakamoto T., Wehausen R., and Brumsack H.-J. (2000). The sapropel record of the eastern Mediterranean Sea - results of Ocean Drilling Program Leg 160. *Palaeogeography, Palaeoclimatology, Palaeoecology* 158, 371–395.

References

- Frigaard, N.-U. (1997). Light-harvesting structures in green sulfur bacteria. Odense University.
- Frigaard, N.-U., Chew, A.G.M., Li, H., Maresca, J.A., and Bryant, D.A. (2003). *Chlorobium tepidum*: insights into the structure, physiology, and metabolism of a green sulfur bacterium derived from the complete genome sequence. *Photosyn. Res* 78, 93–117.
- Ganapathy, S., Oostergetel, G.T., Wawrzyniak, P.K., Reus, M., Gomez Maqueo Chew, A., Buda, F., Boekema, E.J., Bryant, D.A., Holzwarth, A.R., and de Groot, H.J.M. (2009). Alternating syn-anti bacteriochlorophylls form concentric helical nanotubes in chlorosomes. *Proc. Natl. Acad. Sci. U.S.A.* 106, 8525–8530.
- García-Contreras, R., Celis, H., and Romero, I. (2004). Importance of *Rhodospirillum rubrum* H⁺-Pyrophosphatase under Low-Energy Conditions. *Journal of Bacteriology* 186, 6651–6655.
- Garcia, D., Parot, P., Verméglio, A., and Madigan, M.T. (1986). The light-harvesting complexes of a thermophilic purple sulfur photosynthetic bacterium *Chromatium tepidum*. *Biochimica et Biophysica Acta (BBA) - Bioenergetics* 850, 390–395.
- Garcia-Pichel, F. (1999). Cyanobacteria. In *Encyclopedia of Microbiology*, J. Lederberg, ed. (San Diego: Academic Press)
- Gates, D.M. (1965). *Energy exchange in the biosphere* (New York: Harper & Row).
- Van Gemerden, H., and Mas, J. (1995). Ecology of phototrophic sulfur bacteria. In *Anoxygenic photosynthetic bacteria.*, R. Blankenship, M.T. Madigan, and C.E. Bauer, eds. (Dordrecht, The Netherlands: Kluwer Academic Publishers), pp. 49–85.
- Glaeser, J., and Overmann, J. (1999). Selective enrichment and characterization of *Roseospirillum parvum*, gen. nov. and sp. nov., a new purple nonsulfur bacterium with unusual light absorption properties. *Arch Microbiol* 171, 405–416.
- Glaeser, J., Bañeras, L., Rütters, H., and Overmann, J. (2002). Novel bacteriochlorophyll e structures and species-specific variability of pigment composition in green sulfur bacteria. *Arch Microbiol* 177, 475–485.
- Glover, J.R., and Lindquist, S. (1998). Hsp104, Hsp70, and Hsp40: a novel chaperone system that rescues previously aggregated proteins. *Cell* 94, 73–82.
- Gottschalk, G. (1986). *Bacterial metabolism* (Springer New York).
- Gudowska-Nowak, E., Newton, M.D., and Fajer, J. (1990). Conformational and environmental effects on bacteriochlorophyll optical spectra: correlations of calculated spectra with structural results. *The Journal of Physical Chemistry* 94, 5795–5801.
- Guex, N., and Peitsch, M.C. (1997). SWISS-MODEL and the Swiss-PdbViewer: an environment for comparative protein modeling. *Electrophoresis* 18, 2714–2723.

- Heinzinger, N.K., Fujimoto, S.Y., Clark, M.A., Moreno, M.S., and Barrett, E.L. (1995). Sequence analysis of the *phs* operon in *Salmonella typhimurium* and the contribution of thiosulfate reduction to anaerobic energy metabolism. *J Bacteriol* *177*, 2813–2820.
- Horiuchi, T., HORIUCHI, S., and MIZUNO, D. (1959). A Possible Negative Feedback Phenomenon controlling Formation of Alkaline Phosphomonoesterase in *Escherichia coli*. *Nature* *183*, 1529–1530.
- Hussain, H., Grove, J., Griffiths, L., Busby, S., and Cole, J. (1994). A seven-gene operon essential for formate-dependent nitrite reduction to ammonia by enteric bacteria. *Mol. Microbiol.* *12*, 153–163.
- Jakob, U., and Buchner, J. (1994). Assisting spontaneity: the role of Hsp90 and small Hsps as molecular chaperones. *Trends in Biochemical Sciences* *19*, 205–211.
- Jensen, M.A., Webster, J.A., and Straus, N. (1993). Rapid identification of bacteria on the basis of polymerase chain reaction-amplified ribosomal DNA spacer polymorphisms. *Appl. Environ. Microbiol.* *59*, 945–952.
- Jiao, N., Zhang, R., and Zheng, Q. (2010). Coexistence of Two Different Photosynthetic Operons in *Citromicrobium bathyomarinum* JL354 As Revealed by Whole-Genome Sequencing. *Journal of Bacteriology* *192*, 1169–1170.
- Karrasch, S., Bullough, P.A., and Ghosh, R. (1995). The 8.5 Å projection map of the light-harvesting complex I from *Rhodospirillum rubrum* reveals a ring composed of 16 subunits. *EMBO J* *14*, 631–638.
- Kimura, Y., Hirano, Y., Yu, L., Suzuki, H., Kobayashi, M., and Wang, Z. (2008). Calcium ions are involved in the unusual red shift of the light-harvesting 1 Q(y) transition of the core complex in thermophilic purple sulfur bacterium *Thermochromatium tepidum*. *JBiolChem* *283*, 13867–13873.
- Kirk, J.T.O. (1983). *Light and Photosynthesis in Aquatic Ecosystems* (Cambridge: Cambridge University Press).
- Klug, G. (1993). The role of mRNA degradation in the regulated expression of bacterial photosynthesis genes. *Mol. Microbiol* *9*, 1–7.
- Klug, G., Adams, C.W., Belasco, J., Doerge, B., and Cohen, S.N. (1987). Biological consequences of segmental alterations in mRNA stability: effects of deletion of the intergenic hairpin loop region of the *Rhodobacter capsulatus* *puf* operon. *EMBO J* *6*, 3515–3520.
- Koepke, J., Hu, X., Muenke, C., Schulten, K., and Michel, H. (1996). The crystal structure of the light-harvesting complex II (B800-850) from *Rhodospirillum rubrum*. *Structure* *4*, 581–597.

References

- Kumarevel, T., Nakano, N., Ponnuraj, K., Gopinath, S.C.B., Sakamoto, K., Shinkai, A., Kumar, P.K.R., and Yokoyama, S. (2008). Crystal structure of glutamine receptor protein from *Sulfolobus tokodaii* strain 7 in complex with its effector l-glutamine: implications of effector binding in molecular association and DNA binding. *Nucleic Acids Research* 36, 4808–4820.
- Lane, D.J. (1991). 16S/23S rRNA sequencing. In *Nucleic Acid Techniques in Bacterial Systematics*, E. Stackebrandt, and M. Goodfellow, eds. (Chichester UK: John Wiley & Sons), pp. 115–175.
- Larkin, M.A., Blackshields, G., Brown, N.P., Chenna, R., McGettigan, P.A., McWilliam, H., Valentin, F., Wallace, I.M., Wilm, A., Lopez, R., et al. (2007). Clustal W and Clustal X version 2.0. *Bioinformatics* 23, 2947–2948.
- De Las Peñas, A., Connolly, L., and Gross, C.A. (1997). SigmaE is an essential sigma factor in *Escherichia coli*. *J. Bacteriol.* 179, 6862–6864.
- Lin, S., and Cronan, J.E. (2011). Closing in on complete pathways of biotin biosynthesis. *Mol Biosyst.*
- De Long, S.K., Kinney, K.A., and Kirisits, M.J. (2008). Prokaryotic Suppression Subtractive Hybridization PCR cDNA Subtraction, a Targeted Method To Identify Differentially Expressed Genes. *Appl. Environ. Microbiol.* 74, 225–232.
- López-Marqués, R.L., Pérez-Castiñeira, J.R., Losada, M., and Serrano, A. (2004). Differential Regulation of Soluble and Membrane-Bound Inorganic Pyrophosphatases in the Photosynthetic Bacterium *Rhodospirillum rubrum* Provides Insights into Pyrophosphate-Based Stress Bioenergetics. *J Bacteriol* 186, 5418–5426.
- Ludwig, W., Strunk, O., Westram, R., Richter, L., Meier, H., Yadhukumar, Buchner, A., Lai, T., Steppi, S., Jobb, G., et al. (2004). ARB: a software environment for sequence data. *Nucleic Acids Research* 32, 1363–1371.
- Madigan, M.T. (1984). A Novel Photosynthetic Purple Bacterium Isolated from a Yellowstone Hot Spring. *Science* 225, 313–315.
- Madigan, M.T. (2003). Anoxygenic phototrophic bacteria from extreme environments. *Photosyn. Res* 76, 157–171.
- Ma, F., Kimura, Y., Yu, L., Wang, P., Ai, X., Wang, Z., and Zhang, J. (2009). Specific Ca²⁺-binding motif in the LH1 complex from photosynthetic bacterium *Thermochromatium tepidum* as revealed by optical spectroscopy and structural modeling. *FEBS Journal* 276, 1739–1749.
- Manske, A.K., Glaeser, J., Kuypers, M.M.M., and Overmann, J. (2005). Physiology and Phylogeny of Green Sulfur Bacteria Forming a Monospecific Phototrophic Assemblage at a Depth of 100 Meters in the Black Sea. *Appl Environ Microbiol* 71, 8049–8060.

- Manske, A.K., Henssge, U., Glaeser, J., and Overmann, J. (2008). Subfossil 16S rRNA Gene Sequences of Green Sulfur Bacteria in the Black Sea and Their Implications for Past Photic Zone Anoxia. *Appl. Environ. Microbiol.* *74*, 624–632.
- Maresca, J.A., Gomez Maqueo Chew, A., Ponsatí, M.R., Frigaard, N.-U., Ormerod, J.G., and Bryant, D.A. (2004). The bchU gene of *Chlorobium tepidum* encodes the c-20 methyltransferase in bacteriochlorophyll c biosynthesis. *J. Bacteriol* *186*, 2558–2566.
- Marschall, E., Jogler, M., Hessge, U., and Overmann, J. (2010). Large-scale distribution and activity patterns of an extremely low-light-adapted population of green sulfur bacteria in the Black Sea. *Environ. Microbiol* *12*, 1348–1362.
- Masepohl, B., Drepper, T., Paschen, A., Gross, S., Pawlowski, A., Raabe, K., Riedel, K.-U., and Klipp, W. (2002). Regulation of nitrogen fixation in the phototrophic purple bacterium *Rhodobacter capsulatus*. *J. Mol. Microbiol. Biotechnol* *4*, 243–248.
- McLuskey, K., Prince, S.M., Cogdell, R.J., and Isaacs, N.W. (2001). The Crystallographic Structure of the B800-820 LH3 Light-Harvesting Complex from the Purple Bacteria *Rhodospseudomonas acidophila* Strain 7050. *Biochemistry* *40*, 8783–8789.
- Menzel, D., Hopmans, E.C., van Bergen, P.F., de Leeuw, J.W., and Sinninghe Damsté, J.S. (2002). Development of photic zone euxinia in the eastern Mediterranean Basin during deposition of Pliocene sapropels. *Marine Geology* *189*, 215–226.
- Montesinos, E., Guerrero, R., Abella, C., and Esteve, I. (1983). Ecology and Physiology of the Competition for Light Between *Chlorobium limicola* and *Chlorobium phaeobacteroides* in Natural Habitats. *Appl. Environ. Microbiol.* *46*, 1007–1016.
- Murray, J.W., Jannasch, H.W., Honjo, S., Anderson, R.F., Reeburgh, W.S., Top, Z., Friederich, G.E., Codispoti, L.A., and Izdar, E. (1989). Unexpected changes in the oxic/anoxic interface in the Black Sea. *Nature* *338*, 411–413.
- Muyzer, G., and Smalla, K. (1998). Application of denaturing gradient gel electrophoresis (DGGE) and temperature gradient gel electrophoresis (TGGE) in microbial ecology. *Antonie Van Leeuwenhoek* *73*, 127–141.
- Muyzer, G., Hottenträger, S., Teske, A., and Waver, C. (1995). Denaturing gradient gel electrophoresis of PCR-amplified 16S rDNA - a new molecular approach to analyse the genetic diversity of mixed microbial communities. In *Molecular microbial ecology manual*, A.D.L. Akkermans, J.D. Van Elsas, and F.J. De Bruijn, eds. (Dordrecht, The Netherlands: Kluwer), pp. 3.4.4.1–3.4.4.22.
- Nagashima, K.V., Hiraishi, A., Shimada, K., and Matsuura, K. (1997). Horizontal transfer of genes coding for the photosynthetic reaction centers of purple bacteria. *J. Mol. Evol* *45*, 131–136.

References

- Nagashima, K.V., Matsuura, K., Ohyama, S., and Shimada, K. (1994). Primary structure and transcription of genes encoding B870 and photosynthetic reaction center apoproteins from *Rubrivivax gelatinosus*. *J. Biol. Chem* 269, 2477–2484.
- Nagashima, K.V.P., Matsuura, K., and Shimada, K. (1996). The nucleotide sequence of the puf operon from the purple photosynthetic bacterium, *Rhodospirillum rubrum*: Comparative analyses of light-harvesting proteins and the cytochrome subunits associated with the reaction centers. *Photosynthesis Research* 50, 61–70.
- Nyrén, P., and Strid, Å. (1991). Hypothesis: the physiological role of the membrane-bound proton-translocating pyrophosphatase in some phototrophic bacteria. *FEMS Microbiology Letters* 77, 265–270.
- Nystrom, T. (2003). Conditional senescence in bacteria: death of the immortals. *Mol Microbiol* 48, 17–23.
- Nyström, T. (2004). Stationary-phase physiology. *Annual Review of Microbiology* 58, 161–181.
- Ochman, H., Ayala, F.J., and Hartl, D.L. (1993). Use of polymerase chain reaction to amplify segments outside boundaries of known sequences. *Meth. Enzymol* 218, 309–321.
- Olsen, J.D., Sockalingum, G.D., Robert, B., and Hunter, C.N. (1994). Modification of a hydrogen bond to a bacteriochlorophyll a molecule in the light-harvesting 1 antenna of *Rhodobacter sphaeroides*. *Proc Natl Acad Sci U S A* 91, 7124–7128.
- Olsen, J.D., Sturgis, J.N., Westerhuis, W.H.J., Fowler, G.J.S., Hunter, C.N., and Robert, B. (1997). Site-Directed Modification of the Ligands to the Bacteriochlorophylls of the Light-Harvesting LH1 and LH2 Complexes of *Rhodobacter sphaeroides*. *Biochemistry* 36, 12625–12632.
- Olson, J.M. (1998). Chlorophyll Organization and Function in Green Photosynthetic Bacteria. *Photochemistry and Photobiology* 67, 61–75.
- Overmann, J. (1997). Mahoney Lake: A case study of the eco-logical significance of phototrophic sulfur bacteria. In *Advances in Microbial Ecology*, J. Jones, ed. (New York: Plenum Press), pp. 251–288.
- Overmann, J. (2008). Ecology of phototrophic sulfur bacteria. In *Sulfur metabolism in phototrophic organisms*, R. Hell, C. Dahl, D. Knaff, and T. Leustek, eds. (Dordrecht, The Netherlands: Springer), pp. 375–396.
- Overmann, J., and Garcia-Pichel, F. (2000). The phototrophic way of life. In *The Prokaryotes*, M. Dworkin, ed. (New York: Springer), pp. 32–85.
- Overmann, J., Coolen, M.J., and Tuschak, C. (1999). Specific detection of different phylogenetic groups of chemocline bacteria based on PCR and denaturing gradient gel electrophoresis of 16S rRNA gene fragments. *Arch. Microbiol* 172, 83–94.

- Overmann, J., Cypionka, H., and Pfennig, N. (1992a). An Extremely Low-Light-Adapted Phototrophic Sulfur Bacterium from the Black Sea. *Limnology and Oceanography* 37, 150–155.
- Overmann, J., Fischer, U., and Pfennig, N. (1992b). A new purple sulfur bacterium from saline littoral sediments, *Thiorhodovibrio winogradskyi* gen. nov. and sp. nov. *Archives of Microbiology* 157, 329–335.
- Pandhal, J., Wright, P.C., and Biggs, C.A. (2007). A quantitative proteomic analysis of light adaptation in a globally significant marine cyanobacterium *Prochlorococcus marinus* MED4. *J. Proteome Res* 6, 996–1005.
- Papiz, M.Z., Prince, S.M., Howard, T., Cogdell, R.J., and Isaacs, N.W. (2003). The structure and thermal motion of the B800-850 LH2 complex from *Rps.acidophila* at 2.0Å resolution and 100K: new structural features and functionally relevant motions. *J. Mol. Biol* 326, 1523–1538.
- Passier, H.F., Bosch, H.-J., Nijenhuis, I.A., Lourens, L.J., Bottcher, M.E., Leenders, A., Damste, J.S.S., de Lange, G.J., and Leeuw, J.W. (1999). Sulphidic Mediterranean surface waters during Pliocene sapropel formation. *Nature* 397, 146–149.
- Permentier, H.P., Neerken, S., Overmann, J., and Amesz, J. (2001). A bacteriochlorophyll a antenna complex from purple bacteria absorbing at 963 nm. *Biochemistry* 40, 5573–5578.
- Pfennig, N. (1978). General physiology and ecology of photosynthetic bacteria. In *The Photosynthetic Bacteria*, R. Clayton, and W. Sistrom, eds. (New York: Plenum Press), pp. 3–18.
- Pierson, B.K., Sands, V.M., and Frederick, J.L. (1990). Spectral Irradiance and Distribution of Pigments in a Highly Layered Marine Microbial Mat. *Appl Environ Microbiol* 56, 2327–2340.
- Rabold, S., Gorlenko, V.M., and Imhoff, J.F. (2006). *Thiorhodococcus mannitoliphagus* sp. nov., a purple sulfur bacterium from the White Sea. *International Journal of Systematic and Evolutionary Microbiology* 56, 1945–1951.
- Rey, F.E., Oda, Y., and Harwood, C.S. (2006). Regulation of Uptake Hydrogenase and Effects of Hydrogen Utilization on Gene Expression in *Rhodopseudomonas palustris*. *J. Bacteriol.* 188, 6143–6152.
- Roszak, A.W., Howard, T.D., Southall, J., Gardiner, A.T., Law, C.J., Isaacs, N.W., and Cogdell, R.J. (2003). Crystal Structure of the RC-LH1 Core Complex from *Rhodopseudomonas palustris*. *Science* 302, 1969–1972.
- Sambrook, J., and Russell, D.W. (2001). *Molecular cloning: a laboratory manual* (CSHL Press).

References

- Schmid, M., Schmitz-Esser, S., Jetten, M., and Wagner, M. (2001). 16S-23S rDNA intergenic spacer and 23S rDNA of anaerobic ammonium-oxidizing bacteria: implications for phylogeny and in situ detection. *Environ. Microbiol* 3, 450–459.
- Schmitz, R.A., Klopprogge, K., and Grabbe, R. (2002). Regulation of nitrogen fixation in *Klebsiella pneumoniae* and *Azotobacter vinelandii*: NifL, transducing two environmental signals to the nif transcriptional activator NifA. *J. Mol. Microbiol. Biotechnol* 4, 235–242.
- Schwarz, G., and Mendel, R.R. (2006). Molybdenum cofactor biosynthesis and molybdenum enzymes. *Annu Rev Plant Biol* 57, 623–647.
- Serrano, A., Pérez-Castiñeira, J.R., Baltscheffsky, M., and Baltscheffsky, H. (2007). H⁺-PPases: yesterday, today and tomorrow. *IUBMB Life* 59, 76–83.
- Sharma, U.K., and Chatterji, D. (2010). Transcriptional switching in *Escherichia coli* during stress and starvation by modulation of σ 70 activity. *FEMS Microbiology Reviews* 34, 646–657.
- Siefert, E., and Pfennig, N. (1984). Convenient method to prepare neutral sulfide solution for cultivation of phototrophic sulfur bacteria. *Archives of Microbiology* 139, 100–101.
- Sieker, L.C., Jensen, L.H., and LeGall, J. (1986). Preliminary X-ray studies of the tetra-heme cytochrome c3 and the octa-heme cytochrome c3 from *Desulfovibrio gigas*. *FEBS Letters* 209, 261–264.
- Sinninghe Damste, J.S., Wakeham, S.G., Kohlen, M.E.L., Hayes, J.M., and de Leeuw, J.W. (1993). A 6,000-year sedimentary molecular record of chemocline excursions in the Black Sea. *Nature* 362, 827–829.
- Sorokin, Y. (2002). *The Black Sea. Ecology and oceanography* (Leiden, The Netherlands: Backhuys).
- Stomp, M., Huisman, J., Stal, L.J., and Matthijs, H.C.P. (2007). Colorful niches of phototrophic microorganisms shaped by vibrations of the water molecule. *ISME J* 1, 271–282.
- Sturgis, J.N., Olsen, J.D., Robert, B., and Hunter, C.N. (1997). Functions of Conserved Tryptophan Residues of the Core Light-Harvesting Complex of *Rhodobacter sphaeroides*. *Biochemistry* 36, 2772–2778.
- Tsutakawa, S.E., Jingami, H., and Morikawa, K. (1999). Recognition of a TG Mismatch: The Crystal Structure of Very Short Patch Repair Endonuclease in Complex with a DNA Duplex. *Cell* 99, 615–623.
- Tuschak, C., Beatty, J., and Overmann, J. (2004). Photosynthesis Genes and LH1 Proteins of *Roseospirillum parvum* 930I, a Purple Non-Sulfur Bacterium with Unusual Spectral Properties. *Photosynthesis Research* 81, 181–199.

- Tuschak, C., Leung, M., Beatty, J., and Overmann, J. (2005). The *puf* operon of the purple sulfur bacterium *Amoebobacter purpureus*: structure, transcription and phylogenetic analysis. *Arch Microbiol* 183, 431–443.
- Voelker, U., Voelker, A., and Haldenwang, W.G. (1996). Reactivation of the *Bacillus subtilis* anti-sigma B antagonist, RsbV, by stress- or starvation-induced phosphatase activities. *J. Bacteriol* 178, 5456–5463.
- Wang, Z.-Y., Gokan, K., Kobayashi, M., and Nozawa, T. (2005). Solution structures of the core light-harvesting alpha and beta polypeptides from *Rhodospirillum rubrum*: implications for the pigment-protein and protein-protein interactions. *J. Mol. Biol* 347, 465–477.
- Widdel, F., Kohring, G.W., and Mayer, F. (1983). Studies on dissimilatory sulfate-reducing bacteria that decompose fatty acids. III. Characterisation of the filamentous gliding *Desulfonema Limicola* gen. nov., spec. nov., and *Desulfonema magnum* sp. nov. *Arch. Microbiol.* 134, 286–293.
- Wiessner, C., Dunger, I., and Michel, H. (1990). Structure and transcription of the genes encoding the B1015 light-harvesting complex beta and alpha subunits and the photosynthetic reaction center L, M, and cytochrome c subunits from *Rhodopseudomonas viridis*. *J. Bacteriol* 172, 2877–2887.
- Willison, J.C., Jouanneau, Y., Colbeau, A., and Vignais, P.M. (1983). H₂ metabolism in photosynthetic bacteria and relationship to N₂ fixation. *Ann. Microbiol. (Paris)* 134B, 115–135.
- Yutin, N., and Béjà, O. (2005). Putative novel photosynthetic reaction centre organizations in marine aerobic anoxygenic photosynthetic bacteria: insights from metagenomics and environmental genomics. *Environ. Microbiol* 7, 2027–2033.
- Zuber, H., and Brunisholz, R. (1991). Structure and function of antenna polypeptides and chlorophyll-protein complexes: Principles and variability. In *Chlorophylls*, H. Sheer, ed. (Boca Raton, FL: CRC Press), pp. 627–703.
- Zuber, H., and Cogdell, R. (1995). Structure and Organization of Purple Bacterial Antenna Complexes. In *Anoxygenic Photosynthetic Bacteria*, R. Blankenship, ed. (Springer Netherlands), pp. 315–348.
- Zuker, M. (2003). Mfold web server for nucleic acid folding and hybridization prediction. *Nucleic Acids Research* 31, 3406–3415.

Publications

Publications originating from this thesis

Rücker O, Köhler A, Behammer B, Sichau K, Overmann J. (2012). *Puf* operon sequences and inferred structures of light-harvesting complexes of three closely related *Chromatiaceae* exhibiting different absorption characteristics. Arch Microbiol, Vol. 194, Nr. 2, Page 123-134

Danksagung

Zuallererst möchte ich mich bei Herrn Prof. Dr. Jörg Overmann für die Bereitstellung dieses spannenden Themas und natürlich für die hervorragende wissenschaftliche Betreuung bedanken.

Mein Dank gilt Herrn Prof. Dr. Tomas Hanson, Prof. Tom Beatty und Dr. Alessandro Sacca für die professionelle und hilfreiche Zusammenarbeit bei diesen interessanten Projekten.

Großer Dank gilt der gesamten AGO für das freundschaftliche Arbeitsklima und die immerwährende Hilfsbereitschaft. Ein Extra-Dankeschön möchte ich meinen Kollegen Mareike Jogler und Johannes Müller für die gemeinsame WG-Zeit in Braunschweig, sowie Annemarie Hütz und Roland Wenter für die super Zusammenarbeit im Labor und die vielen schönen gemeinsamen Unternehmungen aussprechen.

Außerdem bedanke ich mich bei Carie Franz und Dr. Christian Jogler für den gemeinsamen Spaß an der Forschung sowie für die zahlreichen Diskussionen über Mikrobiologie und darüber hinaus.

Ganz besonders herzlich danke ich meiner Frau Ursula Rücker für ihre Geduld, ihr Verständnis und ihre Einfühlsamkeit, die mir immer wieder neue Kraft gegeben hat.

Abschließend bedanke ich mich bei Hannelore Rücker, meiner Familie und meinen Freunden für Ihre Unterstützung und dass sie an mich geglaubt haben.

Curriculum vitae

Name Ovidiu Ludwig Rücker

Date of birth 01.07.1978

Place of birth Timișoara, Romania

University education

since 09.2007 Ph.D thesis in the group of Prof. Dr. Jörg Overmann at the LMU Munich;

Professional experience

01.2006 – 10.2007 Scientific Assistant at the Center of Excellence for Fluorescent Bioanalytics (KFB), University of Regensburg

University education

10.2004 – 09.2005 Diploma Thesis at the University of Regensburg: „Characterisation of silencing-deficient mutants of the green alga *Chlamydomonas reinhardtii*“

10.2003 – 04.2004 Research Project at the University of Uppsala, Sweden

10.1999 – 09.2005 Study of biology at the University of Regensburg (Diploma)
Specialization: microbiology, cell biology, botany

School education

1996 – 1998 Abitur at the Sophien-Gymnasium in Weimar

1993 – 1996 Secondary School „Lenau Lyzeum“ in Timisoara

1984 – 1992 Primary school „Scoala Generala Nr. 3“ in Timisoara